Medizinische Universität Graz

Dissertation

HDL composition and function in atherosclerosis and chronic kidney diseases

submitted by

Mag. rer. nat.

Michael HOLZER

for the Academic Degree of

Doctor of Philosophy

(Ph.D.)

at the

Medical University of Graz

Institute of Experimental and Clinical Pharmacology

under supervision of

Assoc.-Prof. Dr. Gunther Marsche

2011

Declaration

I hereby declare that this thesis is my own original work and that I have fully acknowledged by name all of those individuals and organisations that have contributed to the research for this thesis. Due acknowledgement has been made in the text to all other material used. Throughout this thesis and in all related publications I followed the guidelines of “Good Scientific Practice”.

Graz, 21.09.2011 ----------

Summary

Epidemiological studies have shown that HDL-cholesterol levels are inversely correlated with the risk for cardiovascular diseases (CVD). HDL is thought to protect against atherosclerosis by mediating reverse cholesterol transport and potentially through anti-oxidative and anti-inflammatory activities. It recently emerged that HDL can loose its anti-atherogenic functions and may even become pro-atherogenic(1-3). The mechanisms underlying this transformation are not well understood.

Within the first project, we investigated whether HDL is post-translational modified by cyanate in atherosclerotic lesions. Proteins are carbamylated through cyanate (OCN^-), a reactive electrophile that irreversibly transforms lysine to homocitrulline (also known as carbamyllysine). Cyanate is formed from thiocyanate via myeloperoxidase (MPO) or by decomposition of urea. Myeloperoxidase (MPO) can binds to HDL within human atherosclerotic lesions and might therefore act in closest proximity to HDL.

We established a state of the art method to quantitatively assess homocitrulline and 3-chlorotyrosine (a specific MPO oxidation marker) via liquid chromatography tandem mass spectrometry. The mass spectrometry analysis revealed that carbamylation through OCN^- is a major modification of HDL in atherosclerotic lesions, which was more than 20-fold higher than the MPO oxidation product 3-chlorotyrosine. The comparison with total lesion protein and lesion derived low-density lipoprotein (LDL) indicates that HDL is a specific target for carbamylation.

We translated the mass spectrometry result to functional experiments by using a similar modification rate as observed in atherosclerotic lesion. The functional analysis revealed that protein carbamylation alters HDL structure and function. Carbamylation increased binding affinity of HDL to its physiological receptor scavenger receptor B-I (SR-BI), shifting the balance between scavenger receptor B-I (SR-BI) mediated cholesterol efflux and uptake towards cholesterol uptake, thereby causing intracellular cholesterol accumulation and lipid droplet formation.

In addition, our studies provide convincing evidence that the anti-oxidative capacity of HDL is reduced upon carbamylation. Moreover, the activity of the HDL-

associated anti-inflammatory enzyme paraoxonase 1 was strongly reduced, whereas lipoprotein-associated phospholipase A2 activity increased.
In summary, the present results provide evidence that protein carbamylation is an important modulator of HDL functions in atherosclerotic lesions, thereby rendering HDL dysfunctional.

In the second part, we investigated the effect of advanced renal disease on HDL composition and function. Functional impairment of HDL during renal disease may contribute to the excess cardiovascular mortality in these patients. The data available regarding the impact of advanced renal disease on HDL composition and functionality are limited. In particular, the effect of renal disease on the first step of reverse cholesterol transport, the efflux of cellular cholesterol from macrophages to HDL, has not been determined yet
We used mass spectrometry and biochemical analyses to show that HDL isolated from patients on maintenance hemodialysis (HD) has a considerable altered protein and lipid composition. Our studies revealed a significant increase in acute phase protein serum amyloid A1, albumin, lipoprotein-associated phospholipase A2 and apoC-III content of HD-HDL, whereas apoA-I and apoA-II levels were decreased. Proteomic alterations were accompanied by a decreased phospholipid and increased triglyceride and lyso-phospholipid content of HDL. In regard to function, HDL from hemodialysis patients was less potent in promoting cholesterol efflux from lipid-laden macrophages. Importantly, correlation analysis showed that functional changes are linked to compositional alterations.
In summary, HDL functionality and composition are significantly altered in renal diseases patients. Our results provide insights into mechanism leading to the functional impairment of HDL and raise the possibility to identify humans at increased risk of cardiovascular disease.

Zusammenfassung

Epidemilogische Studien haben gezeigt, dass high-density Lipoprotein (HDL) - Cholesterin ein unabhängiger Risikofaktor in der Entstehung von kardiovaskulären Krankheiten ist. Dabei kommt HDL eine zentrale Rolle beim reversen Cholesterintransport, der zum Abtransport von überschüssigem Cholesterin aus dem Gewebe führt, zu. Zusätzlich besitzt HDL anti-entzündliche und anti-oxidative Eigenschaften die aus heutiger Sicht zum Schutz gegen kardiovaskuläre Krankheiten beitragen.

Seit kurzem ist bekannt, dass die Funktionalität von HDL eingeschränkt sein kann. Dabei kann HDL seine schützende Wirkung verlieren, oder sogar atherogene Prozesse fördern. Wie es zu dieser Umwandlung kommt ist aus heutiger Sicht weitgehend unbekannt.

Während der ersten Projektphase haben wir HDL aus humanen atherosklerotischen Läsionen isoliert und auf post-translationale Modifikationen untersucht. Cyanate hat die Fähigkeit Proteine zu Carbamylieren und dadurch Lysin in Homocitrullin umzuwandeln. Cyanate entsteht durch Myeloperoxidase (MPO) vermittelte Oxidation von Thiocyanat oder durch den Zerfall von Harnstoff. Dadurch, dass MPO an HDL binden kann und beide in atherosklerotischen Läsionen vorkommen, kann man postulieren, dass MPO generierte Oxidantien, wie z.B. Cyanate, in direkter Nachbarschaft zu HDL gebildet werden.

Im Zuge dieser Dissertation wurde eine auf Massenspektrometrie basierende Methode zur Quantifizierung von Homocitrullin und 3-chlorotyrosin (ein MPO spezifisches Oxidationsprodukt) etabliert. Mit Hilfe dieser Analysenmethode war es uns möglich zu zeigen, dass HDL in atherosklerotischen Lesionen wesentlich höher carbamyliert als chloriert war, ein durchaus überraschendes Ergebnis. Durch den Vergleich von HDL mit low-density Lipoportein (LDL) und Gesamtprotein von atherosklerotischen Läsionen konnten wir zeigen, dass HDL ein selektives und spezifisches Angriffsziel für Cyanate ist.

Diese *in vivo* Ergebnisse wurden genutzt um in *in vitro* Experimenten den Effekt vergleichbarer Carbamylierungsgrade auf die Funktionalität von HDL zu überprüfen. Interessanterweise zeigte sich, dass carbamyliertes HDL eine erhöhte Affinität zu dem HDL Rezeptor “Scavenger Receptor B-I“ (SR-BI) besitzt. Dadurch

verschiebt sich das Gleichgewicht zwischen SR-BI vermittelter Cholesterinaufnahme und –abgabe, zu Gunsten der Cholesterinaufnahme. wodurch eine intrazelluläre Cholesterinakkumulation verursacht wird, ein sicherlich stark pro-atherogener Effekt. In weiteren Experimenten konnten wir zeigen, dass die anti-oxidative Eigenschaft und die Aktivität des anti-entzündlichen Enzyms Paraoxonase durch Carbamylierung stark eingeschränkt wird.
Zusammenfassend veranschaulichen diese Ergebnisse, das HDL ein spezifisches Angriffziel für Cyanate in atherosklerotischen Läsionen ist. Darüber hinausgehend konnten wir zeigen, dass die Carbamylierung die wichtigen athero-protektiven Eigenschaften von HDL reduziert und dadurch an der Bildung von funktionell eingeschränkten HDL beteiligt sein kann.

In der zweiten Projektphase haben wir eine detaillierte Studie über die Zusammensetzung und Funktion von HDL in Patienten mit Niereninsuffizienz (NI) auf Hämodialyse (HD) durchgeführt. Diese Patienten leiden unter einem stark erhöhten Risiko für kardiovaskuläre Krankheiten, wobei vermutet wird, dass funktionell eingeschränktes HDL daran beteiligt ist. Daten, die beschreiben, in wie fern sich NI und HD auf HDL vermittelten reversen Cholesterintransport auswirken, sind nicht verfügbar.
Wir haben mittels Massenspektrometrie und biochemischen Analysen wurde die Protein- und Lipidzusammensetzung von HDL von HD Patienten analysiert. Dabei konnten wir feststellen, dass HDL von HD Patienten erhöhte Proteinmengen an serum amyloid A1, albumin, lipoprotein-associated phospholipase A2 und apoC-III beinhaltet, wogegen apoA-I und apoA-II reduziert waren. Auf Lipidseite wies HDL von HD Patienten reduzierte Phospholipide und erhöhte Triglyceride und Lyso-Phospholipide im Vergleich zu HDL von Kontrollprobanden auf. Auf funktioneller Ebene konnten wir zeigen, dass HDL von HD Patienten weniger Cholesterin aus Lipid-beladenen Makrophagen mobilisieren kann ein deutlicher Hinweis darauf, dass HD-HDL dysfunktional ist. Mittels Korrelationsanalysen von Protein-, Lipid- und Cholesterineffluxwerten haben wir festgestellt, dass die Änderungen der HDL Zusammensetzung in direkten Zusammenhang mit einer funktionellen Einschränkung stehen.

Zusammenfassend lässt sich feststellen, dass HDL von HD Patienten eine signifikant veränderte Zusammensetzung aufweist, welche die Fähigkeit von HDL, Cholesterin aus Makrophagen zu mobilisieren, signifikant einschränkt.

Acknowledgement

Though the following dissertation is an individual work, the accomplishment would not have been possible without the support, hard work and efforts of many people and institutions.

A special thanks goes to my supervisor Dr. Gunther Marsche for his great support, guidance and continuous encouragement. Our stimulating discussions and his goal-orientated research approach essentially added to my scientific success.

With finishing this thesis, I worked three years at the Institute of Experimental and Clinical Pharmacology. Undoubtfully, I fell lucky that I had the possibility to join this Institute with its great people and inspiring atmosphere. It was and still is a great place for research with enthusiastic people looking forward to collaborate and to support. Therefore, I want to give special thank to all members of our institute. I want to point out the members of the Marsche group Sabine Dirnberger, Dalia El-Gamal and Veronika Binder, which helped me numerous times with analytical methods and scientific advices. I want to thank all collaborators from several institutes for their scientific and personal impact on my work.

Not to forget about the peer of colleagues within the PhD program “Molecular Medicine” who made every scientific or social meeting a good time.

A very special thanks goes to my family and friends. I want to thank my father, Paul, my mother Hilde, my brother Thomas, my sister Kathrin and my brother-in-law Patrick for their support and our time spent together which helped my to clear my mind and to return focused when it was necessary. I want to say big thank to all my friends which are making my life every day a bit better. Especially, I want to acknowledge Tina, Heimo, Gerald, Herwig, Sabrina, Nicki, Samra and Admir.

Finally, my biggest thank goes to my beloved Senka. She has always been a source of inspiration and motivation for me. I am every day grateful for our relationship and all the little and big things we share.

Index

List of Tables

I. Chapter: Introduction into the field

II. Chapter: Carbamylation renders HDL dysfunctional in atherosclerotic lesions

III. Chapter: Uremia alters HDL composition and function

List of Figures

I. Chapter: Introduction into the field

II. Chapter: Carbamylation renders HDL dysfunctional in atherosclerotic lesions

III. Chapter: Uremia alters HDL composition and function

List of abbreviations:

2-AAA	L-2-aminoadipic acid
3-CT	3-chloro-L-tyrosine
ABCA1	ATP-binding cassette, sub-family A, member 1
ABCG1	ATP-binding cassette, sub-family G, member 1
ABCG5	ATP-binding cassette, sub-family G, member 5
ABCG8	ATP-binding cassette, sub-family G, member 8
apo	apolipoprotein
ATP	adenosine triphosphate
BSA	bovine serum albumin
CAD	coronary artery disease
cAMP	cyclic adenosine monophosphate
CE	cholesteryl-ester
CETP	cholesteryl-ester transfer protein
CHO	chinese hamster ovary
CML	N(6)-carboxymethyl-L-lysine
CVD	cardiovascular disease
DTPA	diethylene triamine pentaacetic acid
EDTA	ethylenediaminetetraacetic acid
EL	endothelial lipase
ESRD	end-stage renal disease
FA	fatty acid
FBS	fetal bovine serum
FC	free cholesterol
FFA	free fatty acid
HBr	hydrobromic acid
HCit	homocitrulline
HCl	hydrochloric acid
HDL	high-density lipoprotein
HDL-C	HDL-cholesterol
HL	hepatic lipase
HOCl	hypochlorous acid
HOSCN	hypothiocyanic acid
HPLC	high performance liquid chromatography
ICAM-1	intercellular adhesion molecule 1
IDL	intermediate-density lipoprotein

KBr	potassium bromide
kDa	kilo Dalton
LCAT	lecithin-cholesterol acyltransferase
LC-MS/MS	liquid chromatography – tandem mass spectrometry
LDL	low-density lipoprotein
LDL-C	LDL-cholesterol
Lp-PLA2 / PAF-AH	lipoprotein-associated phospholipase A2 / platelet-activating factor acetylhydrolase
MCP-1	monocyte chemotactic protein 1
MPO	myeloperoxidase
$MPO/H_2O_2/Cl^-$	myeloperoxidase/hydrogen peroxide/chloride oxidation system
MRM	multiple reaction monitoring
NaCl	sodium chloride
NPC1	Niemann-Pick disease, type C1
OCN^-	cyanate
PAGE	polyacrylamide gel electrophoresis
PBS	phosphate buffered saline
PC	phosphatidylcholine
PDVF	polyvinylidene difluoride
PE	phosphatidylethanolamine
PL	phospholipide
PLA2	phospholipase A2
PLOH	phospholipid hydroxide
PLOOH	phospholipid hydroperoxide
PLTP	phospholipid transfer protein
PON	paraoxonase
RBP4	retinol binding protein 4
RCT	reverse cholesterol transport
rHDL	reconstituted high-density lipoprotein
RT	room terperature
SAA1	serum amyloid A1
SAA4	serum amyloid A4
SDS	sodium dodecyl sulfate
SMC	smooth muscle cell
SR-BI	scavenger receptor, class B, type 1
TG	triglyceride
VCAM-1	vascular cell adhesion molecule 1
VLDL	very low-density lipoprotein

I. Chapter:

Introduction into the field

1. Cardiovascular diseases are a global healthcare problem

Cardiovascular diseases (CVD) are the leading cause of death worldwide (4). The world health organisation (WHO) estimated that 17.1 million people died from CVDs in 2004, which accounts for 29% of all global deaths (Fig I-1). Of these deaths, about 7.2 million were due to coronary heart disease and 5.7 million due to stroke (4,5). The prevalence of death by CVDs is even higher in Austria, representing ~40% of all deaths (Fig I-1). The perspective for the year 2030 is that CVDs will remain the leading cause of death worldwide, with the most increases in the Eastern Mediterranean and South-East Asia Region (4).

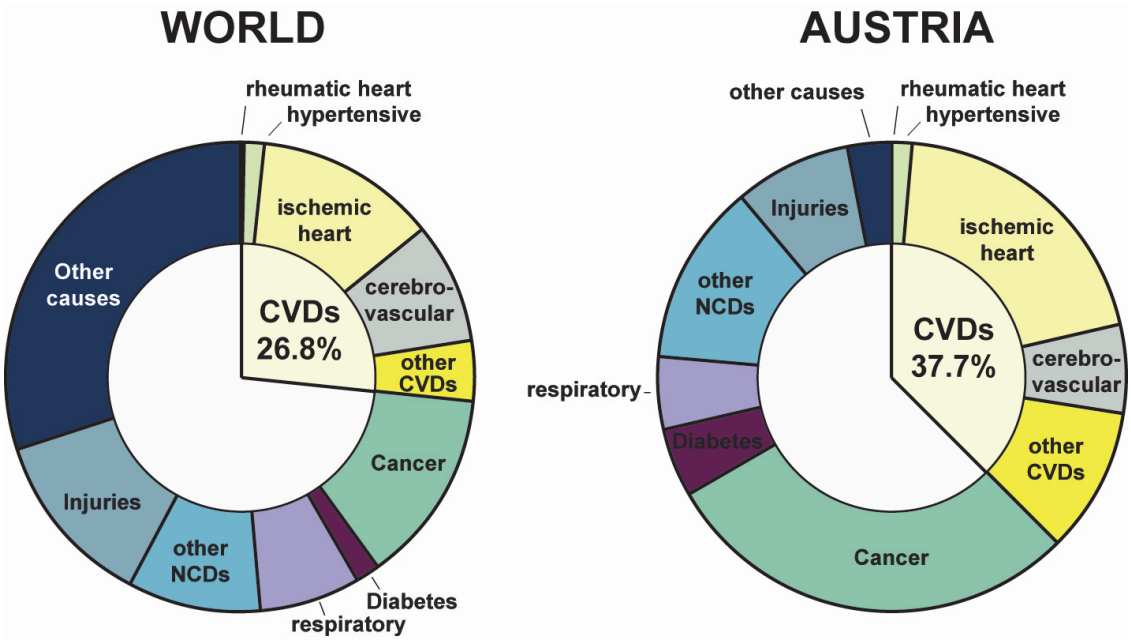

Figure I-1: Causes of deaths worldwide. A) Chart showing an estimate for global death dissected by causes. Cardiovascular diseases (CVDs) account for ~ 27 % of all deaths (4). B) Analysis of causes of death in Austria. Cardiovascular diseases account for more than 37 % of all deaths (4). NCD, non-communicable diseases.

This epidemiological data make CVDs to a global healthcare problem. CVDs were estimated to cost the European Union about € 167 Billion annually, with healthcare accounting for about 62% of costs (6).

Therefore, considerable effort is made to elucidate molecular mechanism behind disease initiation and progression, which should lead to improved diseases prevention and treatment strategies.

2. Pathogenesis of Atherosclerosis

The classical concept describes atherosclerosis as a disorder of lipid metabolism and lipid deposition in the arterial wall (7). The concept of low-density lipoprotein (LDL) as “bad cholesterol” and high-density lipoprotein (HDL) as “good cholesterol” has gained wide acceptance. However, a substantial body of evidence has shown that atherogenesis extends beyond lipid metabolism, and nowadays, atherosclerosis is seen as a multifactorial inflammatory disease.

Atherosclerotic lesions are local thickenings of arteries intima. The thickening progresses over time and can be asymptomatic for decades until vessel occlusion or plaque rupture occurs, which can lead to heart attack, stroke or death. The development of an atherosclerotic plaque is schematically shown in Figure I-2. Dependent on the morphology and severity, an atherosclerotic plaque can be classified into distinct stages (8,9).

Atherosclerosis is believed to start with the retention of lipoproteins in the vessel wall (Figure I-2A). LDL can infiltrate the arterial wall and is retained in the intima, particularly at sites of hemodynamic strain (10). Patterns of hemodynamic flow typically overlap with atherosclerosis-prone segments, especially where arteries branch and low average shear but high oscillatory shear stress occurs (11). LDL can bind to proteoglycans or lipoprotein lipase, both interactions are thought to contribute to retention LDL particles (12,13). The retained LDL might undergo oxidative and/or enzymatic damage, thereby releasing inflammatory lipid mediators, which can activate the endothelium. The retention of lipids, disturbed blood flow and/or injuries of the vessel wall are thought to initiate the inflammatory process leading to plaque formation.

The activated endothelium up-regulates the expression of leukocyte adhesion molecules, such as E-selectin, VCAM-1 and ICAM-1. Blood monocytes can bind and are retained at sites of activation. Once bound, they transmigrate into the subendothelial space (Figure I-2B). In experimental studies genetic abrogation and pharmacological blockade has proofed that inhibition/depletion of adhesion molecules restricted monocyte recruitment and atherosclerosis in mice (14).

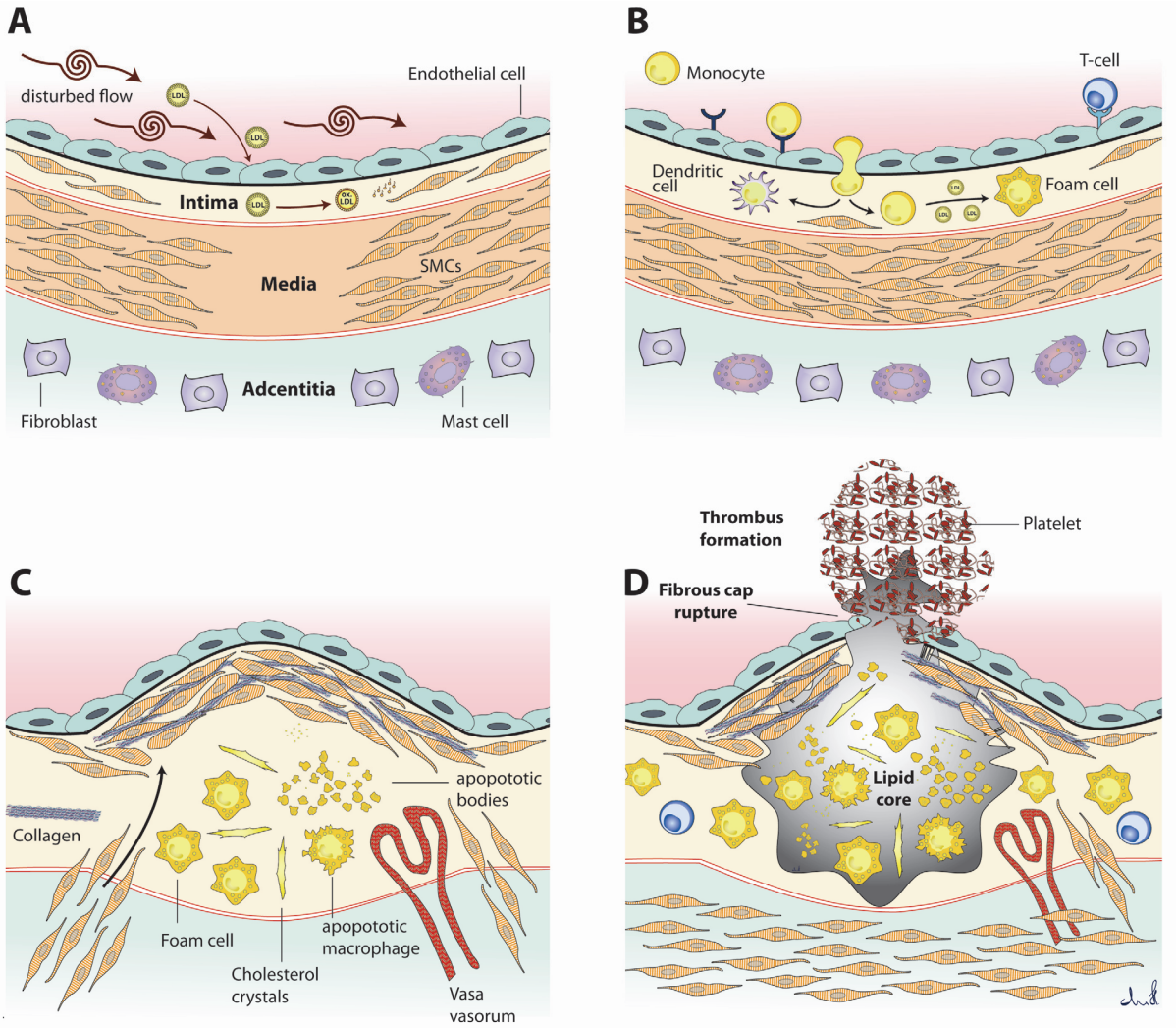

Figure I-2: Development of an atherosclerotic plaque. A) The arterial vessels consist of 3 layers. A layer of endothelial cells together with matrix proteins and connective tissue builds the tunica intima. The human tunica intima contains resident smooth muscle cells (SMC). The second layer, the tunica media, consist of elastic fibers, connective tissue, SMC and is separated from the third layer, the tunica adventitia, by the elastic band called external elastic lamina. The adventitia consists of mostly connective tissue with nerves. However, mast cells can be found in the adventitia. It is thought that the endothelium is activated due to injuries, disturbed flow or retained lipoproteins and subsequently releases inflammatory mediators. B) An initial step in plaque development is the adhesion of monocytes. The activated endothelium expresses adhesion molecules, which tether monocytes from the circulation, allowing them to transmigrate into the intima, where they differentiate into macrophages. Excessive lipid uptake subsequently leads to foam cell formation. C) Foam cells eventually die and release lipids/cholesterol extracellular, which act as inflammatory stimuli. As plaque progression continues, SMC migrate from the media into the intima. Proliferation of SMC together with an increased synthesis of matrix proteins, such as collagen, leads to the formation of a fibrous cap. D) In late stages, the excessive deposit of lipids/cholesterol forms a lipid rich core which is often associated with necrosis. Once the plaque ruptures, thrombogenic material is exposed, which leads to thrombus formation in the lumen, which can cause flow-limiting stenoses and tissue ischemia. Released thrombi can lead to myocardial infarction or stroke (15).

Monocytes in the intimal space differentiate into macrophage and/or dendritic cell-like cells (16,17), e.g. in response to macrophage colony-stimulating factor (mCSF) (18). Differentiated cells express scavenger receptors, such as scavenger

receptor A (SR-A) and scavenger receptor class B type 1 (SR-BI) (19), which are able to internalize a broad range of molecules, including bacterial endotoxins, apoptotic cell fragments, and oxidized LDL particles (20). If cholesterol is taken up by macrophages and cannot be mobilized again, foam cells are formed. The term foam cell reflect the microscopic appearance of these lipid-laden macrophages (15), which are the prototypical cells of the atherosclerotic plaque. The accumulation of foam cells leads to fatty streak formation, which is prevalent in young people, never cause symptoms, and may progress to atheroma or eventually disappear. Especially during this early stages HDL might act beneficial by removing excess lipids from initial lesions.

In atherosclerotic lesions the most abundant cells are macrophages, followed by resident smooth muscle cells (SMC), mast cells and T-cells. SMC are recruited from the tunica media into the tunica intima, where they proliferate, in response to mediators, such as platelet derived growth factor. Their proliferation and the synthesis of high amounts of matrix proteins (such as collagen) form a fibrous cap, which covers the plaque (Figure I-2C) (15). However, T-cells can also be found in atherosclerotic plaques, although their relative number is very low, they have been suggested to regulate inflammation within the vessel wall (15).
As monocytes continue to enter, lesion size and lipid accumulation increases. High local concentrations of cholesterol can lead to apoptosis of foam cells (21). When the removal of apoptotic bodies is insufficient, lipids/cholesterol can accumulate extracellular, which forms a lipid-rich core beneath the fibrous cap (Figure I-2D) (22). This extracellular disposal releases inflammatory mediators together with photolytic substances, which is thought to destabilize the plaque.

Sites of plaque rupture are mostly located on the shoulder region, nearby the lipid-rich core, where the fibrous cap is thin, and commonly high concentration of macrophages can be found (15). Once the plaque ruptures, thrombogenic material leads to thrombus formation in the lumen causing flow-limiting stenoses and tissue ischemia (Figure I-2d). Released thrombi can lead to myocardial infarction or stroke (15).

3. HDL as a novel drug target in the treatment of atherosclerosis

Cardiovascular diseases correlate with increased LDL and decreased HDL levels (23). Statins are widely used inhibitors of HMG-CoA reductase, the enzyme synthesizing endogenous cholesterol. Statin therapy reduces cardiovascular events and mortality in several patient cohorts at increased risk (24-26). Although statins effectively lower LDL cholesterol, the decrease in cardiovascular events in statin treated patients is modest (20-30%).

Therefore, additional therapeutic strategies are necessary for the treatment of cardiovascular disease. While the use of statins is effective against high levels of LDL cholesterol, it has little or no effect in raising HDL cholesterol. Therefore, HDL raising therapies might offer a novel treatment option.

A series of studies in small animal models could provide evidence that raising or administration of HDL is beneficial against cardiovascular diseases (27,28). Elevated levels of HDL have been found to slow progression and stabilize plaques in humans (29). Inhibition of cholesteryl ester transfer protein (CETP) leads to a substantial increase in plasma HDL and is therefore hypothesized to decrease cardiovascular events. However, the CETP inhibitor torcetrapib was tested in a large clinical trial, but failed due to an increase in cardiovascular events (30,31). Nevertheless, HDL plasma levels (+50%) and HDL functionality (measured as cholesterol efflux capacity) were increased in treated patients (32). Post-hoc analysis suggested that the failure of torcetrapib was probably caused by off-targets effects, most likely by an increase in blood pressure.
Two new CETP inhibitors (dalcetrapib, anacetrapib) are currently under investigation. Anacetrapib (high affinity CETP inhibitor) has already proven to be safe and effective (LDL - 40%, HDL +150%) (33), and an endpoint trial will finish in 2014. Dalcetrapib (low-affinity CETP inhibitor) has also been evaluated to be safe and to increase HDL (+40%) (34). A large clinical endpoint trial testing the hypothesis that CETP inhibition with dalcetrapib reduces cardiovascular morbidity and mortality in patients with recent acute coronary syndrome is ongoing and results are expected at the end of 2012 (35). The results of these trials will shed light on the hypothesis whether raising HDL through CETP inhibition is beneficial.

Increasing evidence suggest that the relationship between HDL and cardiovascular diseases extends beyond HDL levels. The prevalence of low HDL in patients with established cardiovascular diseases is only about 20 – 60% (36,37). A meta-analysis of clinical trials investigated the association between treatment-induced changes in HDL-cholesterol and CVD events, adjusted for changes in LDL-cholesterol (38). This analysis could not strengthen the theory that simply raising HDL would be beneficial. Furthermore, subjects with apolipoprotein A-I_{Milano} (major apolipoprotein of HDL) (which contains an Arg173→Cys mutation) have very low levels of HDL (less than 50 %), but no increase in atherosclerosis (39). Low levels of HDL are also present in subjects with heterozygosis for loss-of-function mutations in ATP-binding cassette, sub-family A, member 1 (ABCA1), which are not at increased risk for ischemic heart disease (40). ABCA1 mediates the efflux of cholesterol and phospholipids to lipid-poor apolipoproteins (apoA-I and apoE) generating nascent high-density lipoproteins (HDL).
These observations suggest a divergence between HDL quantity and quality. The determination of parameters describing the functional state of HDL is therefore of particular relevance. Evidence supporting these theory came from a recent clinical study, showing that HDL functionality (measured as cholesterol efflux capacity) was a better predictor of CAD than HDL-cholesterol and LDL-cholesterol levels (41).

In summary, there is a substantial need to understand and evaluate HDL functionality and its relationship to HDL quantity, which could provide new mechanistical insights as well as new therapeutic options.

4. Lipid metabolism

4.1. Structure and properties of lipoproteins

Lipoproteins are macromolecular complexes composed of proteins and lipids. They are classified into the following 4 major classes according to there density. chylomicrons, very-low density lipoprotein (VLDL), low-density lipoprotein (LDL) and high-density lipoprotein (HDL) (Table I-1).

Table I-1: characteristics of lipoproteins

		Chylomicrons	VLDL	LDL	HDL
TG	% by weight	80 - 95	45 - 65	4 - 8	2 - 7
PL		3 - 6	15 - 20	18 - 24	26 - 32
FC		1 - 3	4 - 8	6 - 8	3 - 5
CE		2 - 4	16 - 22	45 - 50	15 - 20
Protein		1 - 2	6 - 10	18 - 22	45 - 65
apoproteins		A-I, A-IV, A-V, B-48, C-I, C-II, C-III, E	B-100, E, C-I, C-II, C-III	B-100	A-I, A-II, E
MW (kDA)		400000	10000 - 80000	2300	170 - 360
size (nm)		75 - 1200	30 - 80	18 - 25	5 - 12
density (g/ml)		0.95	0.95 - 1.006	1.019 - 1.063	1.063 - 1.21

The lipoprotein classes are morphological and compositional distinct. Chylomicrons and VLDL are very large particles, which carry mostly triglycerides, whereas LDL is smaller in size and carries mostly cholesterol. HDL is the smallest subgroup (5 – 12nm), is phospholipid- and protein-rich, and contains only small amounts of triglyceride. The apoprotein composition is specific for each subclass, and each class has a distinct apoprotein profile supporting the biological functions (Table I-1).

4.2. Lipid metabolism

Metabolism of lipids can be divided into the exogenous pathway, which refers to the metabolism of intestinally derived lipids, and the endogenous pathway, which refers to hepatic-derived lipids. In case of cholesterol about 10 - 20 % is derived from the diet and 75 % is endogenously synthesized (42).

Dietary fats are emulsified with bile acid in the intestine to form mixed micelles, which contain triglycerides (TG), phospholipids (PL), cholesterol and bile salts. Pancreatic lipases bind to micelles and digest TG to yield fatty acids (FA) and 2-monoglyceride (2-MG). FA and 2-MG are taken up by fatty acid transporters, whereas cholesterol is shuttled by NPCL1 (Figure I-3). Short chain FA and cholesterol are also taken up via passive diffusion. Once inside the enterocytes, free cholesterol and fatty acids are re- esterified, packaged with triglyceride, phospholipids and apolipoprotein B-48 into chylomicrons (43). After secretion, chylomicrons enter the circulation via the lymph. In the circulation, chylomicrons acquire apoC-II, which activates lipoprotein lipase (LPL) to hydrolyse TG from chylomicrons. The released fatty acids are taken up by the adjacent tissue or cells

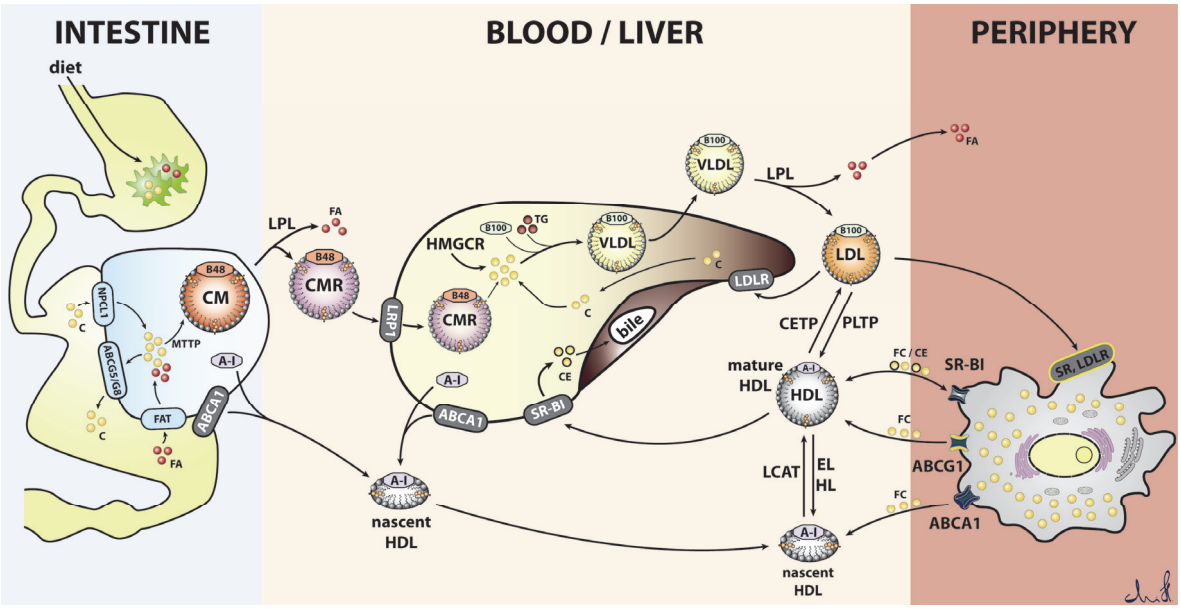

Figure I-3: Schematic overview on lipid metabolism. Lipid and cholesterol derived from the diet are emulsified with bile salts, taken up as fatty acids (FA) and free cholesterol (C) via FA-transporters or Niemann Pick diseases type 1 protein, respectively. Cholesterol together with phospholipids and re-synthesized triglyceride is packed with apoB48 by microsomal TG-transfer protein (MTTP) into chylomicrons. Cylomicrons are released into the circulation and hydrolyzed by lipoprotein lipase (LPL) to form chylomicron remnants (CMR), which are taken up by the liver via the LDL-receptor-related protein 1 (LRP1). Endogenous cholesterol is synthesized primarily in the liver by 3-hydroxy-3-methyl-glutaryl-CoA reductase (HMGCR). Endogenous and and/or dietary cholesterol are packed with TG into VLDL, which upon release is converted to LDL by LPL and hepatic lipase (HL). LDL transports cholesterol in form of cholesteryl-ester into the periphery or back to the liver via the LDL receptor (LDLR).
Reverse cholesterol transport (RCT) starts with the secretion of apoA-I from the liver/intestine, where it is immediately lipidated by ATP-binding cassette transporter A1 (ABCA1). In the periphery, nascent HDL acquires free cholesterol and phospholipids via ABCA1. Free cholesterol is esterified by lecithin-cholesterol acyltransferase (LCAT) to form mature HDL. Endothelial lipase (EL) has high phospholipase A1 activity and remodels HDL into small particles, whereas hepatic lipase (HL) is more effectively in hydrolysing triglycerides, causing shrinking of HDL and loss of lipid-poor apoA-I.
The mature particle can accept further cholesterol via ATP-binding cassette transporter G1 (ABCG1) and scavenger receptor B-I (SR-BI). Mature HDL undergoes remodeled by the plasma factors cholesteryl-ester transfer protein (CETP) and phospholipid transfer protein (PLTP). CETP transfers cholesteryl-esters to LDL, whereas PLTP transfers phospholipids onto HDL. RCT closes when HDL transports cholesteryl-ester (CE) back to liver via SR-BI. Excess cholesterol is excreted via the bile.

for utilization or storage. The chylomicron remnants are internalized by the liver via LDL- or LRP-receptor (Figure I-3). In liver cells (hepatocytes), cholesterol derives from the diet or is synthesized *de novo*, via 3-hydroxy-3-methylglutaryl coenzyme A reductase (HMGCR). Cholesterol is packed together with TG and apoB100 into very low-density lipoprotein (VLDL). VLDL is secreted and LPL hydrolyzes TG to generate VLDL remnants (IDL), which is further hydrolysed by hepatic lipase (HL) to yield cholesterol-rich LDL (44). LDL transports cholesterol from the liver to the periphery, where it is endocytosed by peripheral cells via LDL receptor, assisted by an adaptor protein (AP) (Figure I-3) (44).

5. HDL metabolism

5.1. HDL structure and diversity

HDL particles compromise a very heterogeneous population ranging from discoidal to spherical particles (Figure I-4), which differ in their density, size, shape, protein components and electrophobic mobility (45). HDL is protein-rich and the major protein constituents are apoA-I (~60%) and apoA-II (~10%). In addition, a substantial list of additional HDL-associated proteins (>70) has been identified recently (46-48). These HDL-associated proteins have been implicated in lipid metabolism, complement activation, growth-factors regulation and proteolysis regulation, indicating that HDL exerts multiple biological activities.

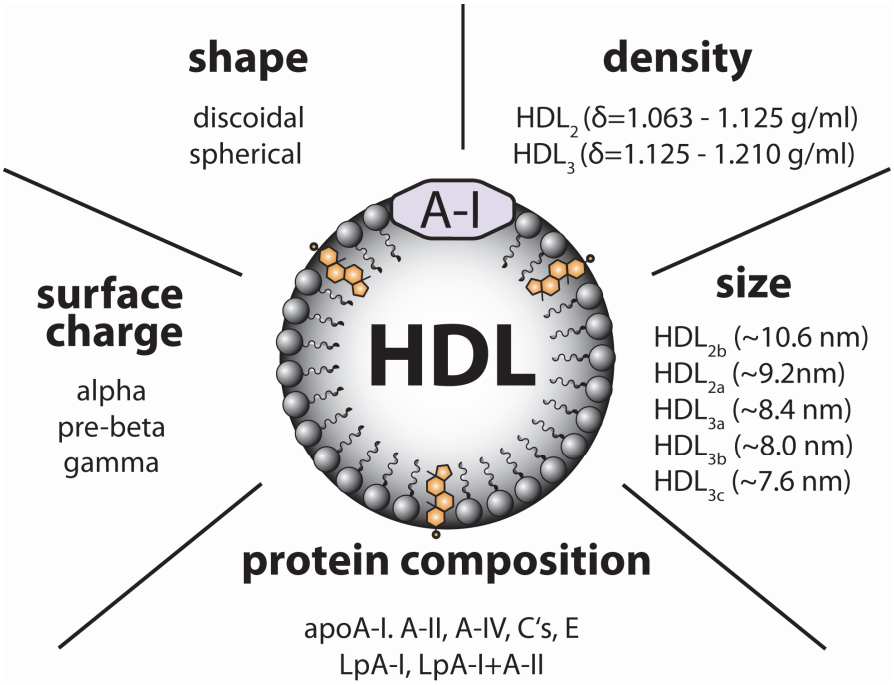

Figure I-4: Heterogeneity of HDL. HDL particles can be classified into distinct classes according to their physiochemical properties. Ultracentrifugation separates HDL according to density into HDL_2 and HDL_3. Isopycnic density centrifugation of fast performance liquid chromatography can separate HDL according to size in 5 subclasses. Electrophobic mobility on during gel electrophoresis separates HDL depending on its surface charge into alpha, pre-beta and gamma. The shape of HDL can be very distinct and particles are therefore classified as discoidal (nascent) and spherical (mature) HDL. In addition, classification depending on the presence or absence of protein yields different HDL subfractions (45).

HDL can be separated based on its density into two subclasses, the less dense HDL_2 (1.063–1.125 g/ml) and the denser HDL_3 (1.125–1.21 g/ml) (Figure I-4) (45). Separation of HDL with isopycnic density centrifugation or non-denaturating gel-electrophoresis yields five subclasses according to size: $HDL2_b$ (~10.6 nm), $HDL2_a$

(~9.2nm), $HDL3_a$ (~8.4 nm), $HDL3_b$ (~8.0 nm) and $HDL3_c$ (~7.6 nm). (45,49) In addition, HDL has been classified depending on its protein composition (presence of apoA-I or apoA-I and apoA-II) or its surface charge (Figure I-4) (49).

Accumulating evidence suggests that HDL functionality varies between subclasses (45,50,51). The current knowledge of subclass specificity has been reviewed recently (51). Nevertheless, the relationship of HDL subclass quantity and quality to CVD is not fully understood.

5.2. HDL biosynthesis and reverse cholesterol transport

ApoA-I, the main protein constituent of HDL, is mainly synthesized by the liver and partially derives from the intestine. Lipid-poor apoA-I is a cholesterol acceptor via the ATP-binding cassette transporter A1 (ABCA1) pathway, which is located on liver and peripheral cells (macrophages, SMC) (Figure I-3). In an ATP-dependent step, ABCA1 can transfer cholesterol together with phospholipids onto lipid-poor apoA-I, thereby forming nascent HDL (also called “discoidal” HDL). These particles consist of about two apoA-I molecules, phospholipids and free (un-esterified) cholesterol. Lecithin-cholesterol acyltransferase (LCAT) converts the hydrophilic free cholesterol into more hydrophobic cholesteryl-ester, which is immediately sequestered into the core of the HDL particle (52). As a result, mature HDL (also called spherical HDL) is generated, which is the major form of HDL in the circulation. The reaction between HDL and LCAT generates a cholesterol gradient from the core to the surface, which ensures that cholesterol moves into HDL.

Mature HDL is a ligand for ATP-binding cassette transporter G1 (ABCG1) and SR-BI. HDL does not bind directly to ABCG1, instead ABCG1 increases and reorganizes the pool of plasma membrane free cholesterol that it can be more readily absorbed by cholesterol acceptors (53). Nascent and mature HDL are equally effective acceptors for ABCG1, as expected for an aqueous diffusion pathway (45). SR-BI binds larger spherical HDL and forms a complex, probably containing a hydrophobic channel, which allows cholesterol efflux onto HDL (54,55). This process is bi-directional and also allows cholesterol to enter via SR-BI. In circulating monocytes, expression of SR-BI is undetectable, but increases highly upon differentiation into macrophages (56,57). The fourth cholesterol efflux

pathway is passive diffusion, which is driven by the cholesterol gradient between cell membrane and acceptors. It is thought that this pathway alone is insufficient, but further studies are necessary to clarify its role in RCT.

Besides LCAT, several other plasma factors are involved in remodelling of HDL (Figure I-3). Mature HDL is a substrate for cholesteryl-ester transfer protein (CETP), a lipid transfer protein that transfers cholesteryl-esters, triglycerides and, to a lesser extent phospholipids, between HDL, VLDL, and LDL (58). This transfer leads to an equilibration between the cholesteryl-ester pools, but in dyslipidemia this can cause net movement of cholesterol from HDL into VLDL/LDL, which has been proposed to contribute to cardiovascular diseases (59). Phospholipid transfer protein (PLTP) is a plasma factor that transfers phospholipids between VLDL and HDL. Lipid-poor apoA-I is shed from the particle and particle fusion generates large HDL.

Two lipases, endothelial lipase (EL) and hepatic lipase are important in HDL metabolism. Although both belong to the triglyceride lipase family, they have distinct activities. EL is secreted from endothelial cells and acts at site of secretion bound to proteoglycans of the glycocalix (60). EL has high phospholipase A1 activity and remodels HDL into small particles. In contrasts to EL, HL is produced by the liver and is more effectively in hydrolysing triglycerides. It also causes the remodelling of HDL into smaller particles, but additionally causes the release of lipid-poor apoA-I (60).

The important role of CETP, PLTP, EL and HL in lipid metabolism was further strengthened as genome-wide association studies identified genomic loci in these genes to be causally related to its plasma lipid levels (61-63).

The mature particle can deliver cholesterol via hepatic SR-BI to the liver or indirectly via CETP mediated CE-transfer to LDL/VLDL followed by subsequent liver uptake, where it can be excreted in form of bile acids. Besides clearance through the liver, a non-biliary RCT pathway has emerged, where HDL-cholesterol can be released into the intestine via the enterocytes with the help of ABCG5 and ABCG8 (64,65).

In summary, the net effect of reverse cholesterol transport is the removal of excess cholesterol from the peripheral tissue and its excretion. Recently, it was shown that the capacity of HDL to promote cholesterol efflux is associated with the risk for coronary artery diseases, pointing out its physiological importance (41).

5.3. Non-reverse cholesterol transport functions of HDL

Promoting cholesterol efflux form peripheral tissue and especially from lipid-laden macrophages is still considered to be the main function of HDL. However, several other functions of HDL have been described, which might contribute to the atheroprotective effects (Figure I-5). These non-classical functions of HDL have been recently reviewed in detail (50,58,66,67). Nevertheless, the anit-oxidant and anti-inflammatory properties of HDL will be discussed in the following.

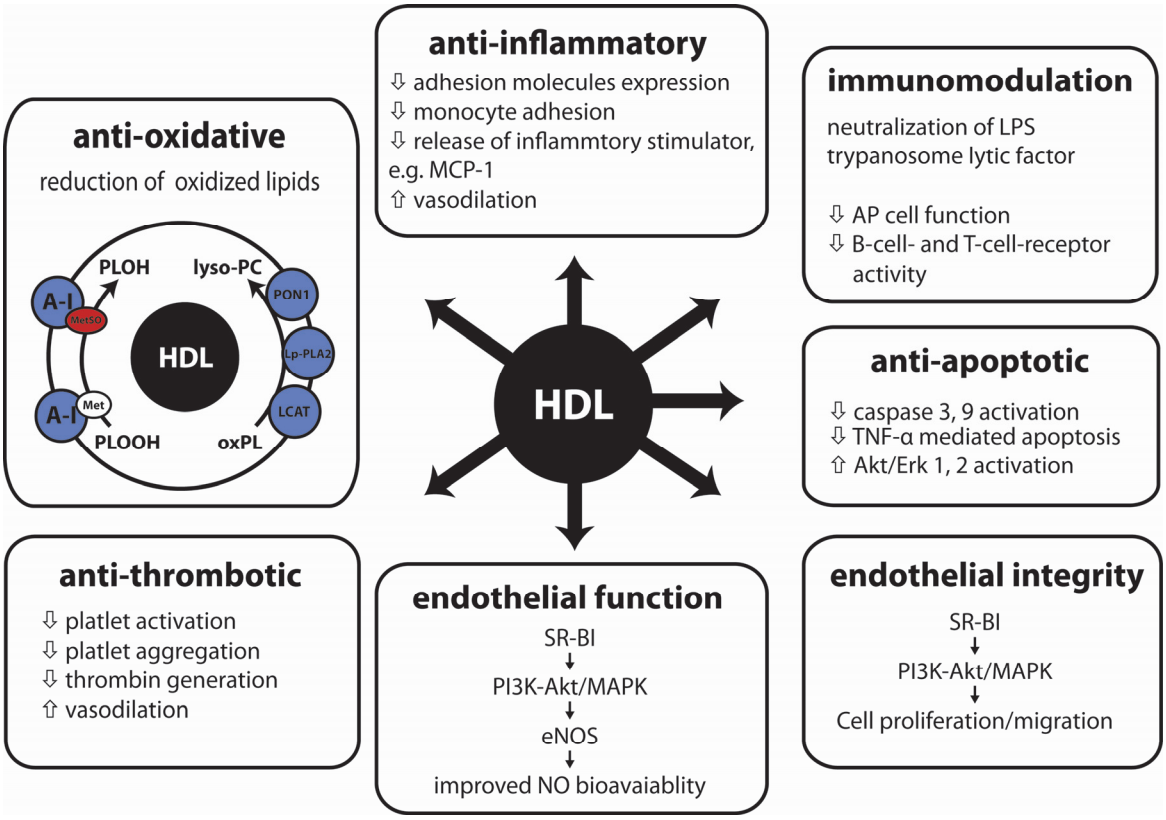

Figure I-5: Overview of non-cholesterol efflux functions of HDL. The figure summarizes described functions of HDL, which have been recently reviewed in detail (50,66-68).

5.3.1. Antioxidant properties of HDL

Already in 1990, it was recognized that HDL possesses anti-oxidative properties. HDL was found to be able to inhibit LDL oxidation induced by transition metals (69). Subsequently, it was found that HDL is the major carrier of lipid hydroperoxides in human plasma, (70) and that lipid hydroperoxides are faster taken up by the liver than non-oxidized lipids (71). This early results suggested an important role of HDL in conquering oxidative stress.

In recent years, it evolved that the anti-oxidative role of HDL critically involves HDL-associated enzymes, such as paraoxonase 1 (PON1), lipoprotein-associated phospholipase A2 (Lp-PLA2) and LCAT, which were reported to hydrolyse oxidized phospholipids into lyso-phosphatidylcholine (Figure I-5) (50,72-75). In addition, methionine residues on HDL can detoxify redox-active phospholipid hydroperoxides (PLOOH) in redox-inactive phospholipid hydroxides (PLOH), thereby forming methionine-sulfoxides (Figure I-5) (76).

5.3.2. Anti-inflammatory properties of HDL

One of the initial steps in atherogenesis is the activation of the vascular endothelium, leading to up-regulation of adhesion molecules (such as E-selectin, ICAM-1, VCAM-1) and to the secretion of pro-inflammatory mediators (such as monocyte chemoattractant 1, (MCP-1)) (Figure I-2b).

Several groups have shown that HDL has anti-inflammatory effects (77), which it mostly exerts on the vascular endothelium and on macrophages. HDL can inhibit cytokine-induced expression of VCAM-1, ICAM-1, and E-selectin on human umbilical vein endothelial cells, thereby reducing adhesion and transmigration of monocytes (78,79). Contrary, HDL did not inhibit cytokine-induced expression of VCAM-1 and ICAM-1 on human aortic endothelial cells, which represents a physiological more relevant model (80). Nevertheless, administration of apoA-I or HDL reduced adhesion molecule expression and monocyte infiltration in small animal models (27,81). In addition, HDL has the ability to change the secretion of mediators from endothelial cells. Secretion of MCP-1, a chemokine, which causes infiltration of blood monocytes into inflammatory sites, can be inhibited by HDL (82).

In summary, the non-cholesterol efflux properties of HDL are thought to contribute to HDLs atheroprotective role and open new avenue for research and treatment options.

5.4. HDL dysfunction

It recently emerged that HDL can loose its anti-atherogenic functions and may even become pro-atherogenic (1-3). The mechanisms underlying this transformation are not well understood.

The first observations that HDL functionality can be altered came from studies investigated HDL during the acute phase response or influenza A infection (83,84). Inflammation caused dramatic changes in HDL composition with incorporation of inflammatory cargo, such as serum amyloid A1 (SAA1). Acute phase HDL lost its ability to protect LDL against oxidation and to inhibit cytokine-induced adhesion molecule expression (84). The ability of HDL to promote cholesterol efflux was also markedly reduced (85).
The hypothesis that HDL can become dysfunctional was further supported by the observation that coronary artery diseases (CAD) patients, despite high levels of HDL, had less anti-inflammatory activity (as measured by inhibition of PL oxidation) (86,87). In a series of studies, several patient cohorts (systemic lupus, end-stage renal diseases and metabolic syndrome) showed pro-inflammatory HDL (2). Although, these results are very intriguing, there is still a need for better and more physiological assay to assess functional properties of HDL.

HDL particles are very heterogeneous in composition and particle size or density might have direct effects on its properties. In recent years, it was revealed that HDL has a substantial list of HDL-associated proteins (>70) (46-48). These associated proteins are involved in lipid metabolism, complement activation, growth-factors regulation and proteolysis regulation, reflecting that HDL exerts multiple biological activities. The impact of HDL protein cargo is evident as HDL from CAD patients had an altered proteome (46,88). Importantly, these changes could be reversed by a combined treatment of CAD patients with statins and niacin (89). These exchangeable proteins could be one of the key to the functional alterations of HDL. Especially, impairment of HDL-associated enzymes is thought to play a role in rendering HDL dysfunctional. For example, decreased PON1 activity was observed under chronic inflammatory conditions, such as in CAD and ESRD (90,91).

Myeloperoxidase (MPO) is a hem-containing protein, which resides within the azidic granula of neutrophils. Upon activation, neutrophils release MPO during the oxidative burst, to generate various reactive oxidants and diffusible radical species (92,93). These reactive compounds are key feature of the innate immunity. Besides the un-doubtful important role of MPO in host defence, excessive activity

of MPO is thought to contribute to oxidative damage of proteins, dysfunctional HDL formation and subsequently to CVD.

The MPO/Cl^-/H_2O_2 system of neutrophils produces hypochlorous acid (HOCl), a potent oxidizing agent. Oxidation reactions of HOCl can be measured specifically by determination of 3-chlorotyrosine (Figure I-6B) (94). High levels of MPO have been reported in atherosclerotic lesions (95), where it resides in close proximity to apoA-I and macrophages (96). Importantly, HDL isolated from atherosclerotic plaques was shown to co-immunoprecipitate with MPO (97) and to be enriched in 3-chlorotyrosine (98,99). The effect of HOCl oxidation on apoA-I was investigated intensively and can be summarized in the following (3).

- apoA-I is a selective target for MPO in atherosclerotic plaques
- 3-chlorotyrosine and 3-nitrotyrosine content is higher in patients with CAD
- apoA-I tyrosine chlorination causes specific loss of ABCA1-mediated cholesterol acceptor activity

Besides HOCl, MPO can produce further reactive nucleophils and oxidants. The preferred substrate of MPO is thiocyanate, which upon oxidation is transformed in hypothiocyanic acid (HOSCN) and cyanate (OCN^-) (100). HOSCN is cell membrane permeable and preferentially oxidises sulfhydryl groups, thereby leading to the activation of intracellular signalling pathways and/or to apoptosis (101,102).

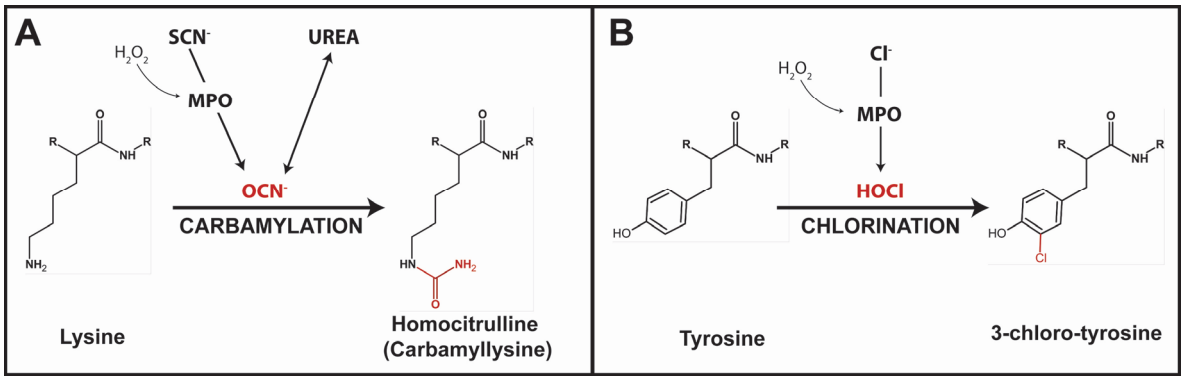

Figure I-6: Formation of homocitrulline and 3-chlorotyrosine. A) Cyanate (OCN) is a reactive electrophile, which transforms lysine into homocitrulline (also known as carbamyllysine). Cyanate is produced by the oxidation of thiocyanate (SCN^-) by myeloperoxidase (MPO), which requires hydrogen peroxide (H_2O_2) as cofactor. A second source for cyanate is urea, which slowly decomposes into cyanate. B) 3-chlorotyrosine is a marker of hypochlorite (HOCl) induced oxidation. HOCl is formed through MPO mediated oxidation of Cl^- in the presence of H_2O_2.

However, the reactive electrophile OCN^- causes protein carbamylation, thereby transforming lysine into homocitrulline (Figure I-6A). In a recent publication the content of plasma homocitrulline was found to correlate with the degree of CVD, raising the possibility that protein carbamylation contributes to the development of CVD (103).

The oxidation of thiocyanate by MPO might be of particular relevance in smokers with high levels of thiocyanate. It is thought that the MPO-thiocyanate axis contributes to the high burden of CVD in smokers. Nevertheless, carbamylation can also occur without the action of MPO. Urea slowly decomposes to cyanate, which in turn can cause protein carbamylation (Figure I-6A). This pathway might be especially important in patients with chronic kidney diseases, where urea levels are very high.

In summary, the discovery that atheroprotective HDL may be rendered dysfunctional or even pro-atherogenic is of major importance for understanding CVD development. Nevertheless, the pathophysiological pathways leading to the formation of dysfunctional HDL are poorly understood and warrant further studies.

6. Aim and description of the thesis projects

The present doctoral thesis aimed to elucidate possible compositional and functional alteration of HDL in patients with atherosclerosis and in patients with chronic kidney disease (CKD).

The aim of the first project was to establish a mass spectrometry (MS) method to assess post-translational modifications of HDL. The general requirements for this method were a fast protein hydrolysis method combined with simple sample preparation and quantification of homocitrulline and 3-chlorotyrosine as well as its parent amino acids lysine and tyrosine.
With the established MS method, we quantified homocitrulline and 3-chlorotyrosine levels of lesion-derived HDL, LDL and total lesion protein. The analysis revealed that HDL is a specific target for carbamylation, reflected by the high content of homocitrulline.
We translated the MS-result to functional *in vitro* experiments by using a similar modification rate as observed in atherosclerotic lesion. Functional assays were performed to determine the impact of carbamylation on HDL cholesterol efflux, anti-oxidative, anti-inflammatory functions.

The aim of the second project was to perform a detailed analysis of compositional and functional alterations of HDL from patients with CKD on maintenance hemodialysis, a patients group with high risk for CVDs..
We made use of a state-of-the-art MS method to quantify HDL-associated proteins and biochemical analysis to quantify major lipid species on HDL. The result indicated specific changes in the protein and lipid cargo of HDL from CKD patients.
In regard to function, we investigated the ability of HDL to promote cholesterol efflux and observed that HDL from CKD patients was functionally impaired. The combination of compositional and functional data indicated that the functional impairment was linked to specific compositional alterations.

II. Chapter:

Carbamylation renders HDL dysfunctional in atherosclerotic lesions

1. Abstract:

Aim: Protein carbamylation by the reactive electrophile cyanate is associated with increased cardiovascular risk. Cyanate is formed *in vivo* through oxidation of thiocyanate by the phagocyte enzyme myeloperoxidase or by break-down of urea. Myeloperoxidase binds to HDL within human atherosclerotic lesions and might therefore act in closest proximity to HDL. Therefore, we investigated in the present study whether cyanate specifically targets HDL for carbamylation and whether cyanate alters HDL function.

Results: We established a rapid method to quantitatively assess homocitrulline and 3-chlorotyrosine via LC-MS/MS. We were successful to reduce the extensive protein-hydrolysis time (110°C for 24 hours) to (160°C, 5 minutes) by implementing a rapid-low volume hydrolysis method. With this method, we were able to show that carbamylation of HDL through OCN^- is a major modification of HDL in atherosclerotic lesions, which was more than 20-fold higher in comparison to 3-chlorotyrosine levels, a specific oxidation product of MPO. Notable, the homocitrulline content of lesion-derived HDL was 5 to 8-fold higher when compared to lesion-derived low-density lipoprotein (LDL) or total lesion protein and increased with lesion severity. Functional analysis of carbamylated HDL revealed that carbamylation shifts the balance between SR-BI mediated cholesterol efflux and uptake towards cholesterol uptake, thereby causing intracellular cholesterol accumulation and lipid droplet formation. Moreover, carbamylation of HDL impaired the lipoproteins ability to activate LCAT, thereby presumably inhibiting particle maturation.

Concerning, non-classical functions, carbamylated HDL was less potent in inhibiting LDL oxidation compared to native HDL. The activity of the HDL-associated enzyme paraoxonase was dramatically reduced already at low levels of carbamylation. In striking contrast, the activity of Lp-PLA2 was increased, revealing another potential pro-atherogenic feature of protein carbamylation.

Conclusion: The present results provide convincing evidence that protein carbamylation is an important modulator of HDL function in atherosclerotic lesions.

2. Introduction

There is a consensus that atherosclerosis represents a state of heightened oxidative stress characterized by lipid and protein modifications in the vascular wall (104). LDL and HDL are prone to be modified in atherosclerotic lesions, but there is considerably less known about the role of HDL modifications in atherogenesis. Increasing evidence suggests that endogenously generated aldehydes are involved in pathophysiologies associated with cardiovascular diseases such as atherosclerosis (104,105). Recent observations demonstrated that HDL isolated from subjects with cardiovascular disease is dysfunctional and shows pro-inflammatory activities (2,77), indicating that dysfunctional HDL is involved in the pathogenesis of atherosclerosis.

Functional impairment of proteins through carbamylation is of particular relevance as clinical studies have shown that carbamylated proteins (measured as plasma levels of protein-bound homocitrulline) are independent risk factors for development of coronary artery disease, future myocardial infarction and stroke (103). Proteins are carbamylated through cyanate (OCN^-), a reactive electrophile that irreversibly transforms lysine to homocitrulline (also known as carbamyllysine). One potential major enzymatic source for OCN^- generation within human atheroma is the heme protein MPO (103). MPO utilizes hydrogen peroxide in the presence of the preferred substrate thiocyanate to generate OCN^-. In line with this observation previous immunohistochemical data showed that polymorphonuclear neutrophils and monocytes, MPO-rich cells, are markedly enriched with carbamylated proteins (106).

OCN^- is also a decomposition product of urea. This is particularly relevant in renal disease, where plasma concentrations of urea and carbamylated proteins increase (107). Notably, carbamylated LDL was shown to be the most abundant LDL modification found in human plasma (108). Moreover, in a mouse model of renal disease, the oral administration of urea increased carbamylated LDL significantly resulting in more severe atherosclerosis (109). However, there is very little information available about the vulnerability of HDL to carbamylation: with only one study reporting that carbamylation decreases anti-apoptotic activities of HDL (103).

We could previously demonstrate that proteins oxidized by hypochlorous acid (specific oxidation products of the MPO/H_2O_2/Cl^- system) localize with apoA-I in the human atheroma (110). Subsequently, it was found that 3-chlorotyrosine (a specific fingerprint of the MPO/H_2O_2/Cl^- system) is enriched on lesion-derived HDL indicating that MPO selectively targets HDL for oxidative modification in atherosclerotic lesions (97,98). We therefore hypothesized that MPO/H_2O_2/thiocyanate derived OCN^- specifically targets HDL in atherosclerotic lesions, thereby modulating the functional properties of HDL. This could be of particular importance, since thiocyanate, even at low physiologic concentrations, is reported to be the preferred substrate for MPO (100).

In this study, we developed a mass spectrometry method to analyse post-translational modifications on HDL. The LC-MS/MS analysis demonstrated that homocitrulline levels were markedly elevated in HDL isolated from human atherosclerotic tissue. We observed that less than one homocitrulline residue per HDL-associated apoA-I was sufficient to induce cholesterol accumulation in macrophages through a pathway involving scavenger receptor class B, type 1 (SR-BI). Overall, our observations raise the possibility that OCN^- promotes human atherogenesis by promoting macrophage cholesterol accumulation.

3. Material and Methods

3.1. Materials

Table II-1: List of materials

NAME	Pr.Nr.:	COMPANY
[^{3}H]-cholesterol	118303	Hartman Analytic
^{125}I-sodium iodide	141571	Hartman Analytic
$^{13}C_6$-3-chlorotyrosine	CLM-7103	EUROISO-TOP
$^{13}C_6$-homocitrulline	custom-made	Ascent Scientific
$^{13}C_6$-lysine	CLM-2247	EUROISO-TOP
$^{13}C_6$-tyrosine	CLM-1542	EUROISO-TOP
2,2′-Azobis(2-methylpropionamidine) dihydrochloride (AAPH)	44,091-4	SIGMA
3-chloro-L-tyrosine	512443	SIGMA
Ammonium formiate (for HPLC)	17843	SIGMA
Butylated hydroxyl toluene (BHT)	W218405	SIGMA
chloroform	2445	Merck
Cholesterol FS Kit	1 1300	Diasys
deoxycholate	D6750	SIGMA
Diethylenetriaminepentaacetic acid (DTPA)	32319	SIGMA
Dynabeads Protein G	10003D	Invitrogen
EZ:faast amino acid analysis	KHO-7339	Phenomenex
Free cholesterol	C3045	SIGMA
Free cholesterol FS Kit	1 1360	Diasys
hexane	4273.1	Roth
Homocitrulline	F2995	Bachem
Hydrobromic acid	18730	SIGMA
isopropyl alcohol	I9516	SIGMA
KH_2PO_4	P5655	SIGMA
LCAT assay Kit	428900	Merck
L-glycine	50046	SIGMA
Lithium-Citrat buffer	80-2038-10	Biochrom
L-lysine	L5501	SIGMA
L-methionine	64319	SIGMA
Lp-PLA2 assay Kit	760901	Cayman Europe
L-tyrosine	91515	SIGMA
lyso- phosphatidylcholine	97281-36-2	Avanti Pol. Lipids
Lyso-phosphatidylcholine (LPC) assay Kit	325779-2	ALFRESA
L-α-phosphatidylcholine	840053P	Avanti Pol. Lipids
Methanol Chromasolv (for HPLC)	34860	SIGMA
Na_3PO_4	342483	SIGMA
NaCl	3957.1	ROTH
NEFA (Non-Esterified Fatty Acid) Kit	434-91795	Wako Chemicals
Paraoxon	PS-610	Supelco
PD Minitrap G-25	28-9180-07	GE Healthcare
PD Spintrap G-25	28-9180-04	GE Healthcare
PD-10 columns	17-0851-01	GE Healthcare

Phenol	328111	SIGMA
Phenylacetate	108723	SIGMA
Phorbol 12-myristate 13-acetate (PMA)	P1585	SIGMA
phospholipase A2	60500	Cayman Europe
Phospholipids FS Kit	1 5741	Diasys
Potassiumbromide	60093	SIGMA
Potassiumcyanate	60160	SIGMA
Protease inhibitor cocktail	P8340	SIGMA
Qsert vials	186001130DV	Waters
Sodium hypochlorite (HOCl)	239305	SIGMA
Sodiumcholate	C6445	SIGMA
Sydrogen peroxide	34,998-7	SIGMA
T0901317	T2320	SIGMA
Thiocyanate	467871	SIGMA
Triglycerides FS Kit	1 5710	Diasys
Triton X-100	BP151	Fisher Scientific
Ultra Clear centrifuge tubes (16x76 mm)	344322	Beckman Instr.
Urea	5378	SIGMA
Water (for HPLC)	95304	SIGMA

Table II-2: List of antibodies

NAME	dilution	Pr.Nr.:	COMPANY
apoA-I, mouse monoclonal	1:1000	NB100-65491	NOVUS Bio.
paraoxonase 1, mouse monoclonal	1:1000	ab24261	Abcam
SR-BI, rabbit polyclonal	1:1000	ab24603	Abcam

3.2. Sources of human tissue and plasma

Atherosclerotic tissue was collected by the Division of Transplantation Surgery at the Medical University of Graz.

Aorta abdominalis of 15 subjects, who died of cerebral haemorrhage during multi-organ procurement, was harvested according to a protocol approved by the Ethics Committee of the Medical University of Graz. The harvested arteries were snap-frozen and stored in liquid nitrogen for further analysis. Blood was obtained from the investigated subjects in parallel for plasma analysis and HDL/LDL isolation. The subjects were 61.4 +/- 15.2 years old with normal total cholesterol (< 180 mg/dl) and no increase in plasma urea (< 45 mg/dl). The morphology of the aortas investigated ranged from thickened intima up to pronounced atheroma containing calcium inclusions. The morphology of the aortas was classified according to previously described methodology (8,9).

3.3. Isolation of HDL-like particles from atherosclerotic lesions

HDL- or LDL-like particles were isolated from human atherosclerotic tissue as previously described with minor modifications (98).

The atherosclerotic tissue was snap-frozen in liquid nitrogen and pulverized. As extraction buffer 10 mmol/L Na_3PO_4, pH 7.4 containing 15 mol/L NaCl, 100 µmol/L DTPA, 100 µmol/L butylated hydroxyl toluene and protease inhibitor cocktail was used. The pulverized tissue powder was suspended in 2 ml extraction buffer and incubated overnight with gently shaking. The tissue was pelleted by centrifugation and the supernatant collected. The tissue pellet was extracted a second time with 1 ml extraction buffer for 1 hour. The supernatants were pooled and used for isolation of lipoprotein-like particles (HDL, LDL) by sequential density gradient ultracentrifugation as described above. Following centrifugation, HDL was isolated and purified with a polyclonal anti-apoA-I and LDL with a polyclonal anti-apoB antibody bound to magnetic beads (Dynabeads Protein G) according to the manufacturers instructions.

The main components of the isolates were identified by LC-MS/MS analysis (performed by Dr. Birner-Gruenberger, Core Facility Proteomics, Center for Medical Research, Medical University of Graz) and by immunoblotting.

3.4. Isolation of HDL and apoA-I

HDL was isolated by a rapid one-step density gradient ultracentrifugation method, with minor modifications (111). Plasma or serum was isolated by centrifugation at 400 g for 15 minutes at 8°C. Serum density was adjusted to 1.24 g/l with potassium bromide (KBr). To improve the separation capacity of the published method, we used longer centrifuge tubes (16 x 76 mm, Beckman). A two-layer density gradient was produced by layering the density-adjusted plasma (1.24 g/ml) underneath a KBr-density solution (1.063 g/ml). Centrifugation tubes were sealed and centrifuged at 90.000g for 4 hours. After centrifugation, the HDL band was clearly separated from the serum and was isolated by puncturing the tube with a syringe. HDL was desalted by gel filtration on a PD-10 column and either directly used or stored at -70°C.

3.5. Preparation of reconstituted HDL

Discoidal reconstituted HDL (rHDL) containing L-α-phosphatidylcholine (PC), free cholesterol (FC) and apoA-I were prepared using the cholate dialysis method (112). PC was dissolved in chloroform to 10 mg/ml (13.2 µmol/L), FC to 1 mg/ml in chloroform (2.6 µmol/L) and apoA-I to 0.167 µg/ml (5.83 µmol/L) in 0.2 mol/L potassium phosphate buffer, pH 7.4. From these stock solutions, 250 µl (3.3 µmol) of PC was mixed with 5.6 µl (14.0 nmol) of FC and chloroform was evaporated under a stream of argon. Dried PC/FC was resuspendend during vortexing by drop wise addition of ~200 µl sodium-cholate (10% solution in 0.2 mol/L potassium phosphate buffer, pH 7.4) to achieve a clear solution. Afterwards, 560 µl apoA-I (3.27 nmol) was drop wise added and the solution was vortexed twice for 30 seconds. The resulting solution was extensively dialyzed against PBS. During preparation, lipids and apoA-I were kept under argon to prevent oxidation.

3.6. Carbamylation of HDL, rHDL and apoA-I

HDL (1 - 5 mg protein/ml) was incubated with potassium cyanate (100 µmol/L up to 250 mmol/L) in phosphate buffered saline (pH 7.4) containing 100 µmol/L DTPA for 4 hours at 37°C. Under these conditions, from ~0.5 to 50% of apolipoprotein lysine residues were carbamylated as estimated by mass spectrometry analysis. Modified HDL preparations were passed over a PD10 column to remove unreacted reagents and used immediately for experiments

3.7. Plasma parameter analysis

Plasma parameter analysis was performed by the Clinical Institute of Medical and Chemical Laboratory Diagnostics at the Medical University of Graz. Levels of total cholesterol, triglycerides, creatinine and urea and were measured enzymatically with commercially available kits (Diasys, Holzheim, Germany). LDL cholesterol was calculated according to the Friedewald equation described previously (113) using HDL cholesterol values measured in the supernatant of phosphotungstic precipitates.

3.8. Phospholipid analysis

Phospholipid analysis of HDL samples was performed by the Core Facility Lipidomics at the Medical University of Graz. The used methodology was as

follows. HDL-lipids were extracted with methyl-tert-butyl ether as previously published (114). The lipid extract was re-suspended in 100 µl $CHCl_3$ / MeOH (1:1, v/v) and 100 pmol 12:0/13:0 phosphatidylethanolamine (PE) was added as internal standard. Lipids were chromatographically separated with an Accela UHPLC (Thermo Scientific, Vienna, Austria) equipped with a Thermo Hypersil GOLD C18, 100 x 1 mm, 1.9 µm column.

The mobile phase A was water with 1% ammonia acetate and 0.1% formic acid, and mobile phase B was acetonitrile/2-propanol (5:2, v/v) with 1% ammonia acetate and 0.1% formic acid. Lipids were eluted with a discontinuous gradient ramping solvent B from 35 – 70 % in 4 minutes, followed by ramping solvent B to 100 % in 16 minutes. Elution was continued for 10 minutes at 100 % of solvent B. The flow rate was 250 µl/min. Phospholipids were determined by a TSQ Quantum Ultra (Thermo Scientific) in positive ESI mode. Total phosphatidylcholine was detected in a precursor ion scan on m/z 184 at 30 eV and PE was detected with a neutral loss scan on mass 141 at 25 eV.

3.9. Measurement of lipoprotein hydroperoxide content

Conjugated dienes develop in lipoproteins through the oxidation of polyunsaturated fatty acids with isolated double bonds to polyunsaturated fatty acid hydroperoxides with conjugated double bonds (= dienes). The formation of dienes can be monitored by an increase of UV-absorption maximum at 234 nm. Baseline absorption of native HDL was determined and compared to absorption of HDL after carbamylation.

3.10. Protein hydrolysis

A custom-made aluminium block with pore holes to support 20 vials with an aluminium cover plate was used to heat samples on a “IKAMAG RTC basic” hotplate to 160°C for 5 minutes. Initial experiments confirmed that 160°C interior temperature for 5 minutes is sufficient to hydrolyze samples comparable to the standard protocol, which features heating to 110°C for 24 hours. Due to the heat transfer time and capacity of the used apparatus, the hot plate was pre-heated to 203°C and the aluminium block was heated for 11 minutes to achieve 5 minutes of 160°C exposure.

Protein samples (3 to 20 µg) for hydrolysis were placed in Qsert vials and 10 µl internal standard containing 10 ng $^{13}C_6$-HCit, 10 ng $^{13}C_6$-3-CT, 0.3 µg $^{13}C_6$-tyrosine and 1 µg $^{13}C_6$-lysine was added. Hydrobromic acid containing 0.25% phenol (phenol was always dissolved freshly) was added to a final concentration of 6 N. Vials were flushed carefully with argon and sealed with screw caps. The vials were inserted in the aluminium block and incubated on the pre-heated hotplate (203°C) for 11 minutes. Afterwards, the aluminium block was cooled in ice-chilled water for 2 minutes. Hydrobromic acid was evaporated in a speed vac and sample stored afterwards at -20°C.

3.11. Homocitrulline, 3-chlorotyrosine and amino acid quantification

Protein hydrolysates were suspended in 100 µl 0.2 mol/L Li-Citrat buffer (pH 2.8) and derivatized with the EZ:faast Kit (Phenomenex, Aschaffenburg, Germany) according to the manufacturers instructions.

Electrospray ionization tandem mass spectrometry (LC-MS/MS) with online HPLC was used for quantification of HCit and lysine. Calibrations curves were prepared by using varying amino acids and HCit levels with fixed amounts of internal standards. The calibration curves had a linearity range from 100 pg – 50 ng for HCit and 3-CT (R^2: 0.9981 and R^2: 0.9990), 50 – 3000 ng for lysine (R^2: 0.9993) and 20 – 1200 ng for tyrosine (R^2: 0.9988).

The HPLC column (250x4 mm, AAA-MS HPLC column, Phenomenex, Aschaffenburg, Germany) was equilibrated for 15 minutes with 100% solvent A at 35°C. Solvent A was 10 mmol/L ammonium formiate in water and solvent B was 10 mmol/L ammounium formiate in methanol. After equilibration, the sample (10 µl) was injected onto the HPLC column at a flow rate of 0.25 ml/min. Compounds were eluted with a discontinuous gradient starting with 83% solvent B for 13 minutes followed by 68% of solvent B for 4 minutes. The HPLC column effluent was introduced into an API 200 triple quadrupole mass spectrometer. Ions were generated by electrospray ionization in the positive-ion mode with multiple reactions monitoring of parent and characteristic daughter ions. Following transitions were monitored indicated by their mass-to-charge ratio (m/z): m/z 318→127 for HCit; m/z 324→132 for $^{13}C_6$-HCit; m/z 430 →170 for 3-CT; m/z 436→176 for $^{13}C_6$-3-CT; m/z 361→170 for lysine; m/z 367→175 for $^{13}C_6$-lysine; m/z 396→136 for tyrosine; m/z 402→142 for $^{13}C_6$-tyrosine. Following mass

spectrometry analysis, the generated calibration curves were used to quantify HCit, 3-CT, tyrosine and lysine.

3.12. Cell culture

3.12.1. Cell culture materials

Table II-3: List of materials

NAME	Pr.Nr.:	COMPANY
DMEM	E15-883	PAA
RPMI 1640	E15-885	PAA
Ham's F-12	E15-890	PAA
FBS Gold	A11-151	PAA
Penicilin/Steptomycin 100x (PS)	P11-010	PAA
G-418	P11-012	PAA
Accutase	L11-007	PAA
Cryomaxx S	J05-013	PAA
BSA, fatty acid free	K31-502	PAA
BSA, fraction V	K41-001	PAA
PBS (1x) with Ca & Mg	H15-001	PAA
PBS (1x) without Ca & Mg	H15-002	PAA

3.12.2. Thawing, freezing and splitting of cells

Vials with cells frozen in CryoMaxx S were transferred from liquid nitrogen into a 37°C water bath. After thawing, cells were transferred into 10 ml media and centrifuged at 400g for 5 minutes. The cell pellet was re-suspended in media and transferred into a new cell culture flask.

Cells in culture were grown to confluency and splitted twice a week. Cells were detached with accutase for ~3 - 5 minutes at 37°C. After cells were detached, accutase was inactivated by adding fresh media containing 10% FBS. An appropriate aliquot of cells was transferred into a new cell culture flask containing 10 ml media.

For freezing, cells were detached, collected in falcon tube and spinned down at 400g for 5 minutes. The cells pellet was resuspendend in CryomaxxS to a cell density of about 1 – $5*10^6$/ml. Cells were transferred to -70°C for 24 hours and transferred afterwards into liquid nitrogen.

3.12.3. Culture of cell lines

THP-1: Human monocytic THP-1 cells were maintained in RPMI 1640 medium with stable glutamine supplemented with 1% PS (100 units/ml penicillin, 100 µg/ml streptomycin) and 10% FBS. To induce differentiation into macrophages, THP-1 cells were cultured for 48 hours in the presence of 100 nmol/L PMA.

RAW 264.7: Murine monocytic RAW 264.7 cells were maintained in DMEM medium with stable glutamine supplemented with 1% PS (100 units/ml penicillin, 100 µg/ml streptomycin) and 10% FBS.

CHO: Stable transfected murine Chinese hamster ovary (CHO) cells expressing SR-BI (LdlA7[SR-BI]) and control CHO cells (LdlA7) were cultured in Ham's F12 medium supplemented with 5% FBS and 100 units/ml penicillin, 100 µg/ml streptomycin. The medium for LdlA7[SR-BI] additionally contained 1% Geniticin (G-418) to assure continuation of receptor expression. Both cell lines were kindly provided by Dr. Monty Krieger (Massachusetts Institute of Technology, Boston).

HepG2: Human liver HepG2 cells were maintained in DMEM medium supplemented with 2 mmol/L glutamine, 1% PS (100 units/ml penicillin, 100 µg/ml streptomycin) and 10% FBS.

3.13. Cell culture experiments

3.13.1. Recombinant adenovirus preparation

Adenoviral vectors encoding for SR-Bi and lacZ were kindly provided by Dr. Sasa Frank (Medical University of Graz, Austria). Vectors were constructed as described previously (115,116).

3.13.2. Induction of SR-BI expression in THP-1 macrophages

THP-1 macrophages ($3*10^6$ cells) were plated on 6-well plates and differentiated with PMA (100 nM) for 48 hours. In initial experiments, cells were infected with adenoviral vectors encoding human SR-BI or LacZ with a multiplicity of infection (moi) ranging from 50 - 500 for 1 hour, inducing moderate (50 moi), moderate to high (100 moi) and very high (500 moi) SR-BI expression. Infections were

performed in serum-free media for 2 hours followed by a medium change (RPMI 1640, 10% FBS), without washing of cells. After infection, THP-1[Ad/SR-BI] or THP-1[Ad/LacZ] cells were cultured for two days in RPMI 1640 containing 10% FBS to allow SR-BI expression (115,117). SR-BI expression was verified by Western blotting. Cell surface expression of SR-BI was assessed by immunofluorescence staining using a primary polyclonal SR-BI antibody for 1 hour and secondary anti-rabbit AF488 antibody (Invitrogen) for 1 hour. Cells were imaged using the Olympus IX70 system. Cells infected with moi 100 were used for further experiments. No cell toxicity was observed under these experimental conditions.

3.13.3. Induction of ABCA1 expression in RAW 264.7 macrophages

RAW 264.7 macrophages were treated for 16 h in DMEM supplemented with 0.2% BSA in the presence or absence of 0.3 mM cAMP to induce ABCA1 activity as described (118).

3.13.4. Cholesterol efflux experiments

THP-1 macrophages were seeded in RPMI (10% FBS, 100nmol/L PMA) on 24- or 48-well plate, with $1.2*10^6$ cells or $3*10^5$ cells, respectively. Cells were allowed to differentiate for 48 hours. Adherent cells were labelled with 1 µCi/ml [^{3}H]cholesterol in the presence of 50µg/ml carbamylated LDL for 48 hours. After cholesterol loading, cells were rinsed twice with PBS containing 5 mg/ml BSA and equilibrated in serum-free RPMI media supplemented with 2 mg/ml BSA for 2 hours at 37°.

Cells were washed afterwards and cellular cholesterol efflux was initiated by addition of HDL/apoA-I, carbamylated HDL/carbamylated apoA-I in serum-free RPMI containing 2 mg/ml BSA. After 4 h, the medium was collected and centrifuged at 1000g for 5 minutes to remove cell depris. An aliquot was transferred into scintillation vial, scintillation cocktail was added and radioactivity (cpm) assessed. To estimate the total cell associated [^{3}H]cholesterol-label, cells were lysed with 0.1% SDS in 0.3N NaOH for 30 minutes on a shaker. The complete lysate was transferred into scintillation vials, scintillation cocktail added and radioactivity measured. Cholesterol efflux was calculated as follows:

$$\% \text{ Cholesterol efflux} = \frac{\text{cpm supernatant}}{\text{cpm supernatant + cpm cell lysate}} \times 100$$

To determine SR-BI specific efflux, [^{3}H]cholesterol-efflux of lacZ-transfected THP-1 cells were subtracted from efflux of SR-BI transfected THP-1 cells.

3.13.5. Cell association studies

Association studies with native or carbamylated HDL, rHDL and apoA-I to THP-1[Ad/SR-BI] or THP-1[Ad/LacZ] cells were performed for 1 hour at 37°C with increasing concentration of [125I]-labelled proteins. After the association period, cells were rinsed twice with PBS containing 5% (wt/vol) BSA and twice with PBS alone. Cells were lysed with 0.1% SDS in 0.3N NaOH for 30 minutes on a shaker. The radioactivity and protein content of the cell lysate were measured in the same aliquot. Specific association was calculated as the difference between the total and nonspecific association.

3.13.6. Total cholesterol accumulation of THP-1 macrophages

THP-1 macrophages were seeded on 6-well plates (3 - 5*10^6 cells/well) in RPMI (10% FBS, 100 nmol/L PMA). Cells were allowed to adhere and to differentiate for 48, where medium was changed again after 24 hours. After 2 days, THP-1 cells were transfected with MOI 100 of either adenoviral vectors encoding human SR-BI (THP-1[Ad/SR-BI]) or LacZ (THP-1[Ad/LacZ]) as described above. Additional 48 hour of incubation were allowed to assure high expression of SR-BI or lacZ in THP-1 cells.

To investigate, the effect of native or carbamylated HDL on cellular cholesterol accumulation in THP1 macrophages, cells were incubated in the presence or absence of native or carbamylated HDL (100 µg/ml in serum-free RPMI 1640) for 48 hours at 37°C. The medium was aspirated subsequently, and cells were rinsed twice with PBS containing 2 mg/ml BSA followed by two washes with PBS alone.

The cellular cholesterol content was determined with Cholesterol FS Kit (DiaSys; Holzheim, Germany). Therefore, 1 ml cholesterol-PAP solution was added to each well and incubated for 15 minutes at 37°C. The supernatant was transferred into eppendorf tubes and centrifuged at 13000 rpm for 5 minutes. An aliquot of the supernatant was transferred into cuvettes and absorbance measured at 500 nm.

To quantify cellular cholesterol, a standard curve with a standard solution was measured in parallel.
HDL induced cholesterol uptake was calculated by subtracting cholesterol content of cells grown in the absence of HDL from cells incubated with different HDL preparations. To determine the specific effect of SR-BI on cholesterol content of macrophages, THP-1[Ad/LacZ] cells were subtracted from THP-1[Ad/SR-BI] cells. Each condition was measured in triplicates in two independent experiments.

3.13.7. Bodipy staining of lipid droplets

To assess neutral lipid accumulation, THP-1 macrophages were differentiated for 72 hours in RPMI1640 containing 3% lipoprotein-deficient serum. Cells were incubated with 200 µg/ml lipoproteins for 48 hours and lipid droplets were stained in formaldehyde fixed cells with 1 µl/ml Bodipy.

3.14. Paraoxonase/Arylesterase assay

$Ca2^{+}$-dependent paraoxonase activity was determined as the rate of hydrolysis of paraoxon into 4-nitrophenol, which can be monitored by an increase in absorbance at 405 nm (119). Native or carbamylated HDL (10 µg protein) was placed into a 96-well and the reaction initiated by the addition of 200 µl buffer per well containing 100 mmol/L Tris, 2 mmol/L $CaCl_2$, 1 mmol/L paraoxon, pH 8.0. The assay was performed at 37°C and readings were taken every 5 minutes at 405 nm on a plate reader to generate a kinetic plot. Form the kinetic chart, the slope was used of the determine ΔAb_{405nm} / min. Enzymatic activity was calculated with the Beer-Lambert Law from the molar extinction coefficient of 17100 $mol*l^{-1}*cm^{-1}$. PON activities were expressed as formed 4-nitrophenol (nmol/L/min).
$Ca2^{+}$-dependent arylesterase activity was determined with a photometric assays using phenylacetate as substrate (119). Native or carbamylated HDL (2 µg protein) was added to 200 µl buffer containing 100 mmol/L Tris, 2 mmol/L $CaCl_2$ at pH 8.0, either containing 1 mmol/L phenylacetate. The rate of hydrolysis of phenylacetate was monitored in the increase of absorbance at 270 nm and readings were taken every 30 seconds to generate a kinetic plot. Form the kinetic chart, the slope was used of the determine ΔAb_{270nm} / min. Enzymatic activity was calculated with the Beer-Lambert Law from the molar extinction coefficient of 1310 $L*mol^{-1}*cm^{-1}$ for phenylacetate.

3.15. Substrate efficiency of HDL for LCAT

LCAT activity was measured using a commercial available kit (Merk, Darmstadt, Germany), which was adapted to measure substrate efficiency of HDL preparations. Therefore, native or carbamylated HDL was pre-incubated with LCAT substrate (Kit component No.KP23001) for 90 minutes at 37°C and unbound substrate was removed via gel-filtration. The binding efficiency was ~95% of the added substrate, determined by fluorescence measurement of the substrate at 470 nm after gel-filtration. The labelled HDL preparations were used to determine the substrate efficiency in response to LCAT enzymatic activity. LPDS was used as source for LCAT.
The experimental setting was as follows: 200 µl / well: 100 µg labelled HDL + 10 µl LPDS, completed with LCAT puffer to 200 µl. LCAT puffer contained 150 mmol/L NaCl, 10 mmol/L TRIS, 4 mmol/L mercaptoethanol and 1 mmol/L EDTA.

Endpoint readouts were obtained after incubation for 5 hours at 37°C. Results are expressed as percent of substrate hydrolysed.

3.16. Lp-PLA2 activity assay

Lp-PLA2 activity was measured with a commercially available photometric assay. The assay uses 2-thio platelet-activating factor (PAF) as substrate, which is hydrolysed by Lp-PLA2 and upon hydrolysis, free thiols are detected by 5,5`-dithio-bis-(2-nitrobenzoic acid) (DTNB). Reactions mixtures contained 0.40 – 0.75 mg/ml HDL in assay buffer (0.1 mol/L Tris-HCl, pH 7.2, containing 1 mmol/L EGTA) and 160 µmol/L 2-thio PAF. Measurements were performed on 384-well plates and measurements at 405 nm were taken every 5 minutes to generate a kinetic chart. Form the kinetic chart, the slope was used of the determine ΔAb_{405nm} / min. Enzymatic activity was calculated from the extinction coefficient of 12.8 $mmol*l^{-1}*cm^{-1}$ for DTNB.

3.17. Determination of the anti-oxidative capacity of HDL

The anti-oxidative activity of HDL was determined as described previously (69,120). LDL (100 µg/ml protein) was oxidized *in vitro* with the free radical initiator AAPH (1 mmol/L in PBS) in the presence or absence of HDL (100 µg/ml protein) at 37°C. The oxidation was monitored at 234 nm. One single time point in the

middle of the propagation phase was selected for quantification. Oxidation in presence of HDL was calculated as relative value to oxidation of LDL alone, which was set to 100 %.

3.18. SDS-PAGE and Western blotting

SDS-PAGE and subsequent Western blotting experiments of different HDL preparations were performed with 5-20% polyacrylamide gradient gels as described (96).

3.19. Statistical analysis

Statistical analyses were performed using PASW Software V.18 or GraphPad Prism. Mean values of 2 independent groups were compared with the Mann-Whitney U-test (for non-parametric data) or 2-tailed student's *t-test* (for parametric data). Comparisons of 2 dependent groups were performed using the Wilcoxon signed-rank test. Significances were accepted at * $p<0.05$, ** $p<0.01$ and *** $p<0.001$.

4. Results:

4.1. Development of an LC-MS/MS method for quantification of post-translational modified amino acids

In order to investigate and quantify post-translational modifications on HDL and other serum proteins, we developed an LC-MS/MS quantifications method within this doctoral thesis. The general requirements for this method were:

- fast protein hydrolysis with low sample volumes
- fast sample preparation for MS-detection
- quantification of the homocitrulline and 3-chlorotyrosine as well as its parent amino acids lysine and tyrosine

In order to meet the criteria of a fast an easy to handle protein hydrolysis method, we developed in collaboration with the group of Dr. Oliver Kappe (Christian Doppler Laboratory for Microwave Chemistry, University of Graz) a low-volume high-throughput hydrolysis method.
The conventional hydrolysis protocol requires a 24 hours heating period at 110°C with 6N HCl, whereas the new adapted method can be performed within 5 minutes of microwave-irradiation at 160°C with 6N HCl or HBr (121). To make this method even more feasible, we transferred the microwave-assisted irradiation protocol to a simple heating plate. Aluminium plates with 20 pore holes with the proper size to fit standard screw-cap HPLC vials were produced. The thermal properties and heating characteristics of the used Qsert HPLC vials inside the aluminium plate were analyzed with a thermal probe by our collaborators (Damm, M; Kappe, O). The thermal analysis shows that preheating of the heating plate to 202°C is required to achieve 160°C inside the vial. To compensate for pre-heating of the aluminium block, a total heating period of 11 minutes is sufficient to achieve a 5 minutes period of 160°C (Figure II-1). The thermal analysis also showed that 2 minutes of cooling in an ice-bath is enough to cool the HPLC vials inside the aluminium plate. In total, the time necessary for protein hydrolysis could be reduced from 24 hours to 11 minutes. Due to the low-volume used, evaporation of acid using a speed vac can be performed in approximately 60 minutes.

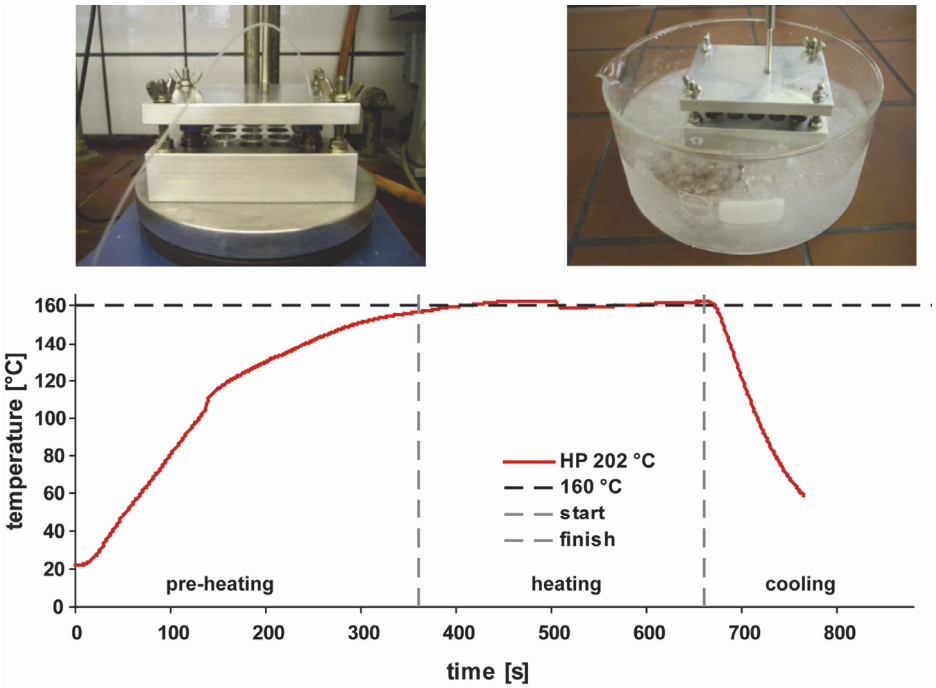

Figure II-1: Thermal analysis of aluminium plate. An aluminium plate was custom-made to support 20 standard HPLC vials. The vials are covered with a plate to counteract vapour pressure during heating. The aluminium block was placed onto the preheated hotplate and the temperature was measured inside the vial over time. After 6 minutes, 160°C were achieved inside the vial, which remained constant over the next 5 minutes. The plate was transferred into an ice-bath and cooled for 2 minutes, which was sufficient to reduce in-vial temperature for further handling.

The second criterion for the MS-based quantification method was a fast sample preparation. We choose to use a commercial available Kit for amino acid analysis from Phenomenex. The “EZ:faast amino acid kit for protein hydrolysates” is build for protein hydrolysates analysis and features a sample clean-up and a derivatisation step to improve MS-fragmentation. The used HPCL column also ensured that sufficient resolution of amino acids prior to detection, which allowed multiple reactions monitoring (MRM).

In the initial experiments, homocitrulline, 3-chlorotyrosine, lysine and tyrosine were derivatized with the EZ:faast kit for MS-detection on a API2000 system. The derivatized pure compounds were used to detect their mass to charge ratio (m/z) (Figure II-2). The molecules m/z, e.g. m/z = 327 for HCit, was selected in “Product Ion” scan mode and fragmented (Figure II-2). The most abundant daughter ion was selected and used in MRM scan mode to optimize the fragmentation process. The optimal settings for each single compound were determined and are summarized in Table II-4. The same procedure was performed for internal standards used ($^{13}C_6$-homocitrulline, $^{13}C_6$-chlorotyrosine, $^{13}C_6$-lysine, $^{13}C_6$-tyrosine).

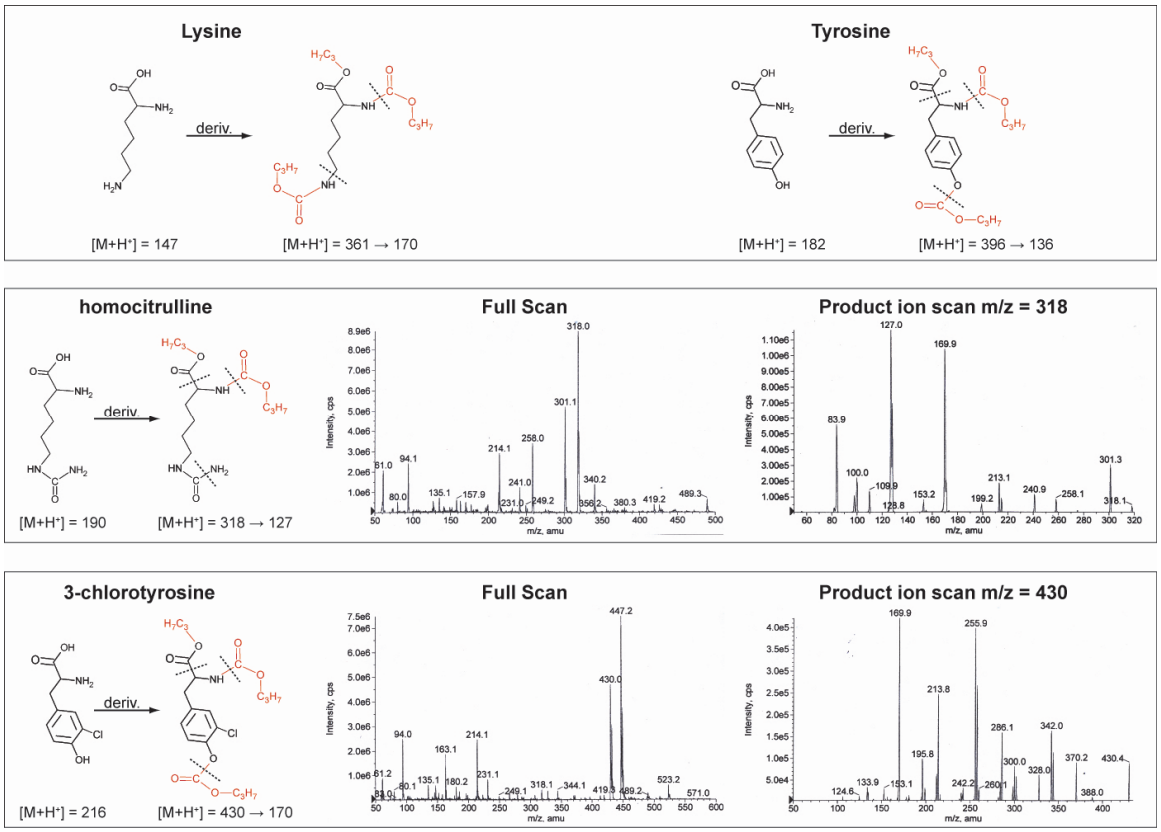

Figure II-2: Derivatisation and fragmentation strategy for MS-detection. Amino acids and derivatives were hydrolyzed with the EZ:faast Kit. Shown are the mass to charge (m/z) ratios detected for the non- and derivatized compounds. The derivatized compounds were analyzed in Full Scan mode to identity the corresponding molecule peak. The m/z for lysine was 361, for tyrosine 396, for homocitrulline 318 and for 3-chlorotyrosine 430. The molecule m/z was selected and fragmented in product ion scan mode. The daughter ions were selected and the most abundant further optimized, which were m/z 170 for lysine, m/z 136 for tyrosine, m/z 127 for homocitrulline and m/z 170 for 3-chlorotyrosine.

Table II-4: API 2000 settings

	HCit	3-CT	lysine	tyrosine
Declustering Potential (DP)	10	6	13	12
Focusing Potential (FP)	400	400	400	400
Entrance Potential (EP)	6	7	7	10
Collision Energy (CE)	32	44	26	42
Exit Potential (CXP)	6	3	7	6
Curtain Gas (CUR)	50	50	50	50
Collision Gas (CAD)	4	4	4	4
Ionspray Voltage (IS)	4500	4500	4500	4500
Temperature (TEM)	200	200	200	200
Ion Source GAS 1 (GS1)	55	55	55	55
Ion Source GAS 2 (GS2)	55	55	55	55

Calibration curves were established to allow quantification of amino acids and derivatives. They were prepared by varying amino acids or derivatives levels with fixed amounts of internal standards. To mimic the complexity of protein samples, unrelated amino acids were added to the calibrations solution as matrix (Table II-5). The following concentrations were used for calibration of homocitrulline and 3-chlorotyrosine.

Table II-5: Calibration solutions for HCit and 3-CT

	1	2	3	4	5	6	7
HCit (pg)	100	250	500	1500	5000	15000	50000
3-CT (pg)	100	250	500	1500	5000	15000	50000
$^{13}C_6$-HCit (pg)	10000	10000	10000	10000	10000	10000	10000
$^{13}C_6$-3-CT (pg)	10000	10000	10000	10000	10000	10000	10000
lysine (ng)	1000	1000	1000	1000	1000	1000	1000
tyrosine (ng)	300	300	300	300	300	300	300
methionine (ng)	100	100	100	100	100	100	100
glycine (ng)	1000	1000	1000	1000	1000	1000	1000

Due to the high concentrations differences between the analytes (e.g. HCit in pg range, lysine in µg range), a separate calibration was performed for lysine and tyrosine with the following calibration solution (Table II-6):

Table II-6: Calibration solutions for lysine and tyrosine

	1	2	3	4	5	6
lysine (ng)	50	100	200	500	1000	3000
tyrosine (ng)	20	40	80	200	400	1200
$^{13}C_6$-lysine (ng)	1000	1000	1000	1000	1000	1000
$^{13}C_6$-tyrosine (ng)	300	300	300	300	300	300
methionine (ng)	100	100	100	100	100	100
glycine (ng)	1000	1000	1000	1000	1000	1000

Samples for calibration went through the complete sample preparation including acid hydrolysis and derivatisation prior to MS-measurement. The ratio between the peak areas of internal standard and analyte were blotted to generate standard curves. The calibrations curves had a linearity range from 100 pg – 50 ng for homocitrulline ($r = 0.9981$) and 3-chlorotyrosine ($r = 0.9990$). Lysine had a linearity

range from 50 – 3000 ng (r = 0.9993) and tyrosine from 20 – 1200 ng (r = 0.9988). The workflow of the established method is summarized in Figure II-3.

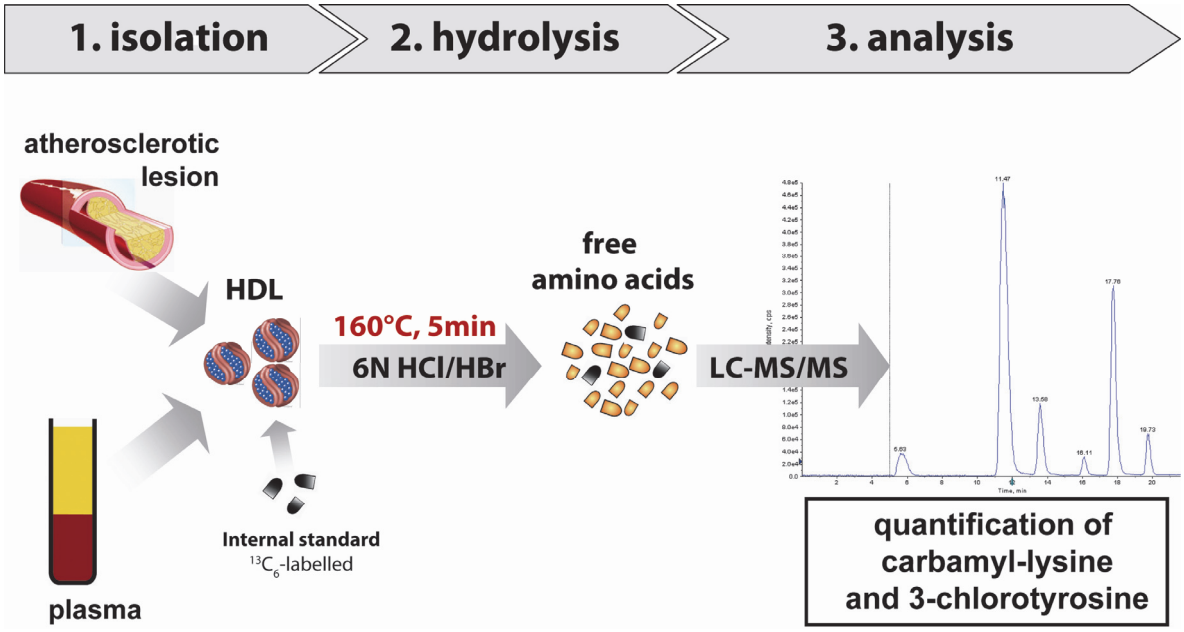

Figure II-3: Workflow of LC-MS analysis of post-translational modifications. The protein of interest is isolated from tissue or plasma and subjected to acid hydrolysis to generate free amino acids. The hydrolysis can be performed rapidly in 11 minutes using the new established hydrolysis protocol as described. Free amino acids are derivatized and subjected to mass spectrometry analysis. The amino acids are separated on a HPLC column prior to MS-detection to allow multiple reaction monitoring.

4.2. Quantification of the homocitrulline and 3-chlorotyrosine content of HDL isolated from plasma and lesions

The MPO/H_2O_2/SCN^- system of activated phagocytes is a dominant mechanism for cyanate formation and protein carbamylation at sites of inflammation (103). Since MPO is a component of HDL in the human atherosclerotic intima, we investigated whether carbamylated HDL accumulates in the artery wall.

In this study, we used tissue and plasma from patients with atherosclerosis and healthy controls. The atherosclerotic plaques were classified based on their histological composition and structure (by Dr. Martin Gauster, Medical University of Graz) (8,9). The morphology of the lesions ranged from initial lesion of type I with thickened intima until advanced lesions of type V with fibrous connective tissue and lipid cores. Concerning the blood lipid parameters, both, control and atherosclerotic subjects had normal total cholesterol and no increase in plasma urea (Table II-7).

Table II-7: Clinical characteristics of study subjects

	atherosclerosis	control
n	15	5
Age	61.4 ± 15.2	54.9 ± 10.3
Creatinine (mg/dL)	1.0 ± 0.4	0.9 ± 0.2
Urea (mg/dL)	36.9 ± 13.9	28.9 ± 7.0
Total cholesterol (mg/dL)	129.6 ± 52.1	146.1 ± 47.0
Triglycerides (mg/dL)	103.2 ± 67.1	94.0 ± 36.0
LDL-cholesterol (mg/dL)	78.3 ± 28.4	89.0 ± 26.2
HDL-cholesterol (mg/dL)	41.1 ± 38.1	44.6 ± 13.3
VLDL-cholesterol (mg/dL)	10.2 ± 6.7	12.5 ± 5.5

Results are given as means ± SD. Significances were accepted at the level of *p<0.05

The atherosclerotic tissue and the corresponding plasma were used to isolate HDL by density gradient ultracentrifugation. HDL recovered from atherosclerotic tissue was further purified with a monoclonal apoA-I antibody bound to magnetic bead reagent. The purity of the isolated HDL was determined with two different approaches. First, isolated proteins were blotted and visualization via silver staining. Second, recovered HDL was enzymatically digested and peptides mass was identified by mass spectrometry. The corresponding protein was determined by homology search in the SpectruMill database.

From these analyses, we concluded that the preparations mainly contained apoA-I, lower amounts of apoA-II and albumin followed by low levels of apoE and antitrypsin (Figure II-4).

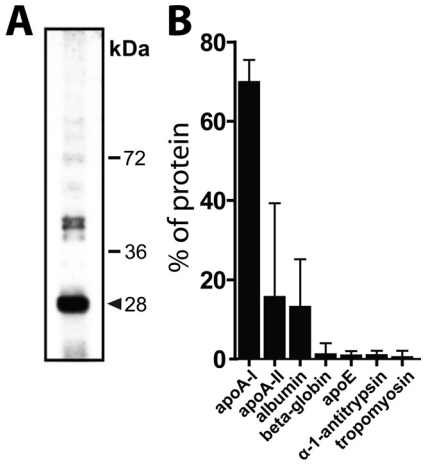

Figure II-4: Protein composition of lesion-derived HDL. HDL was isolated from atherosclerotic plaques by ultracentrifugation and further purified with a monoclonal anti-apoA-I antibody bound to magnetic beads. (A) Proteins were separated by SDS-PAGE (5–20% gradient gels) and visualized by silver staining. (B) In addition, lesion-derived HDL was analyzed by LC-MS/MS. The data were analyzed by searching the human NCBI nonredundant public database with Spectrum mill Rev. A.03.03.078 (Agilent) and Mascot 2.2 (MatrixScience).

Next, mass spectrometry analysis was performed to quantitatively assess the homocitrulline content of HDL isolated from plasma and atherosclerotic lesions. To test whether MPO contributes to HDL carbamylation in vivo, the specific MPO oxidation product 3-chlorotyrosine was determined in parallel (94). Measurement of 3-chlorotyrosine levels is currently the best method available for probing the MPO-mediated oxidation in the pathology of inflammatory diseases (122). Mass spectrometry analysis showed that both, control and atherosclerotic subjects had comparable homocitrulline levels in plasma HDL (Figure II-5A). Remarkably, the homocitrulline content of lesion-derived HDL was significantly higher in comparison with total lesion tissue or lesion-derived LDL (isolated from the same atherosclerotic tissue) (Figure II-5B). The homocitrulline levels of lesion-derived HDL were dependent on lesion severity and increased significantly from initial or moderate lesions (type I – type III) to advanced lesions (type IV-V) (Figure II-5B). The 3-chlorotyrosine content of lesion-derived HDL followed the trend observed for homocitrulline (Figure II-5C). However, 3-chlorotyrosine levels of lesion-derived HDL were more than 20-fold lower when compared to the homocitrulline content. This clearly indicates that protein carbamylation is a major post-translational modification of HDL in the vessel wall.

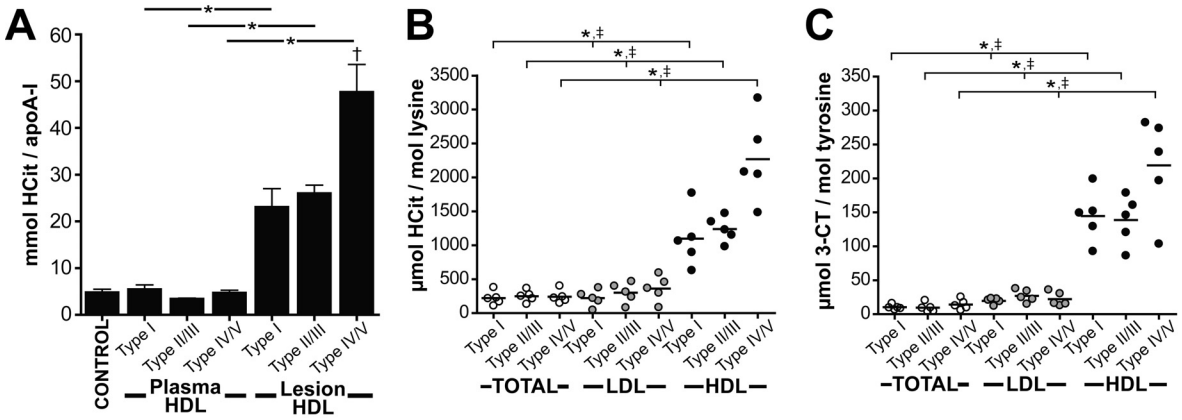

Figure II-5: Homocitrulline content is increased in lesion-derived HDL. (A) LC-MS/MS quantification of homocitrulline (HCit) in plasma HDL and lesion-derived HDL from subjects with atherosclerotic lesions, classified as type I (initial lesion, n=5), type II-III (intermediate, n=5) and type IV-V (complicated lesion, n=5). Quantification of HCit (B) and 3-chlorotyrosine (3-CT) (C) levels in total atherosclerotic tissue protein (TOTAL), lesion-derived LDL and lesion-derived HDL isolated from type I (n=5), type II-III (n=5) and type V (n=5) lesions.
* *p<0.05*; total tissue protein vs. lesion-derived HDL.
† *p<0.05*; lesion-derived HDL (type I) vs. lesion-derived HDL (type IV/V).
‡ *p<0.05*; lesion-derived LDL vs. lesion-derived HDL.

4.3. Correlation between homocitrulline content of lesion-derived HDL and 3-chlorotyrosine levels

Both, homocitrulline and 3-chlorotyrosine levels were increased in lesion-derived HDL. Further data analysis revealed a positive correlation between homocitrulline and 3-chlorotyrosine levels in lesion-derived HDL (Figure II-6A), whereas the homocitrulline content of LDL or total lesion tissue did not correlate with 3-chlorotyrosine levels (Figure II-6B, C). Importantly, neither plasma urea concentration (Figure II-6D) nor plasma lipid levels correlated with the homocitrulline content of lesion derived HDL (Table II-8). These results implicate that MPO significantly contributes to HDL carbamylation in atherosclerotic lesions.

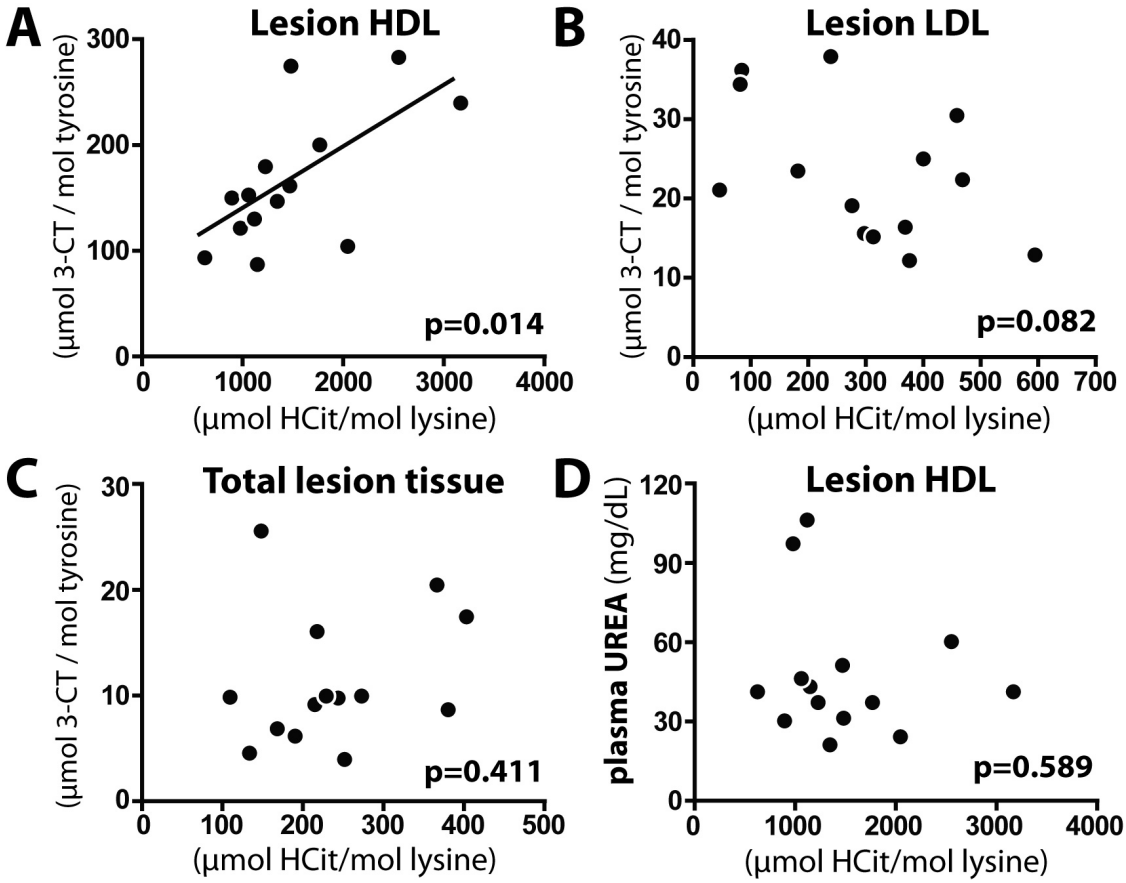

Figure II-6: Correlation between HCit and 3-CT of lesion-derived HDL indicate a possible role of MPO in carbamylation. (A) Blot between HCit and 3-CT levels in lesion-derived HDL (A), LDL (B) and total lesion tissue (C) (n=15). The correlation between HCit and 3-CT in lesion-derived HDL was significant, while no significance was observed in lesion LDL and total lesion tissue. (D) Plasma urea levels blotted against the HCit level of lesion-derived HDL. The significance level of Pearson's correlation is noted for each plot.

Table II-8: Correlation between HCit and plasma parameters of patients with atherosclerosis

HCit		CREA	UREA	TC	TRIG	LDL-C	HDL-C	VLDL-C
total lesion protein	Pearson's r	-.053	-.078	-.236	**.756****	-.244	-.251	.576
	p	*.858*	*.791*	*.438*	***.003***	*.445*	*.431*	*.064*
lesion HDL	Pearson's r	-.423	-.158	.403	.040	.338	.268	.400
	p	*.132*	*.589*	*.172*	*.898*	*.282*	*.400*	*.223*
lesion LDL	Pearson's r	.449	.126	-.557	.166	-.437	-.545	-.119
	p	*.107*	*.667*	*.048*	*.587*	*.155*	*.067*	*.728*
total plasma protein	Pearson's r	**.535**	**.756****	.034	.071	.259	-.218	.365
	p	***.049***	***.002***	*.912*	*.818*	*.416*	*.496*	*.270*
plasma HDL	Pearson's r	-.310	.100	.503	-.189	.508	.235	.609
	p	*.302*	*.745*	*.096*	*.556*	*.111*	*.488*	*.062*
plasma LDL	Pearson's r	**.712**	**.801****	-.039	.209	-.176	.027	-.033
	p	***.006***	***.001***	*.899*	*.494*	*.584*	*.933*	*.922*

Pearson's correlation coefficients (Pearson's r) are shown. Significances were accepted at the level of **p<0.01. CREA, creatinine; TC, total cholesterol; LDL-C, LDL-cholesterol; HDL-C, HDL-cholesterol; VLDL-C, VLDL-cholesterol.

4.4. Carbamylation increased binding affinity of HDL to the HDL receptor SR-BI

In line with our observation that MPO mediates carbamylation of HDL in the vessel wall, a previous study had demonstrated that carbamylated epitopes co-localize with MPO in human atherosclerotic lesions (103). These findings suggest that macrophage associated MPO generates OCN^-, which subsequently reacts with HDL-associated apolipoproteins to generate homocitrulline. Given that macrophages express high levels of the HDL receptor SR-BI in human atherosclerotic lesions (56,57,123), we hypothesized that carbamylation of apoA-I in the artery wall might modulate binding of HDL to SR-BI in macrophages.

To test this hypothesis, HDL was carbamylated with OCN^- and the homocitrulline content was assessed by LC-MS/MS, which confirmed that a relevant degree of protein carbamylation was present (0.57 and 5.25 HCit/apoA-I). Carbamylated HDL was separated by SDS-PAGE and visualized by silver staining, revealing that OCN^- treatment did not induce crosslinking or degradation of apoA-I (Figure II-7). We also tested whether HDL associated phospholipids were modified upon OCN^- treatment, since the primary amino group of phosphatidylethanolamine (PE), a minor fraction of HDL associated phospholipids (about 3 % of total HDL phospholipids, 1-2 molecules PE per HDL) (124), is prone to be modified by reactive aldehydes (125). As seen in Figure II-7B, total phospholipid content was

not significantly altered in carbamylated HDL, whereas the PE content was significantly decreased. Importantly, OCN^- treatment did not induce hydroperoxide formation (Figure II-7C).

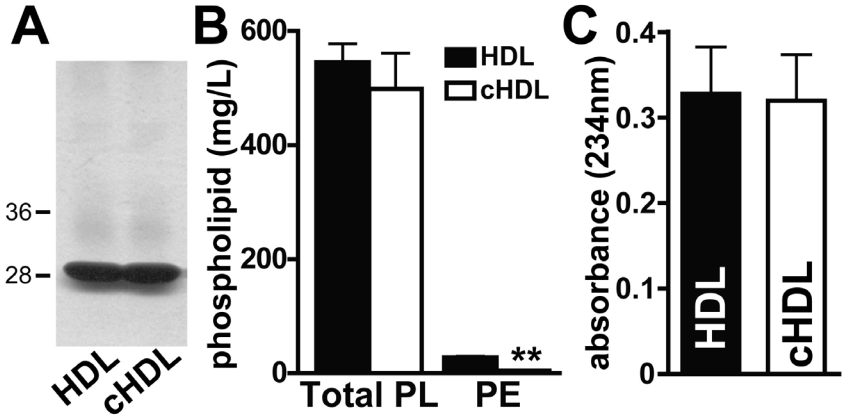

Figure II-7: Carbamylation does not alter HDL integrity. HDL and carbamylated HDL (cHDL, 5.25 HCit/apoA-I) was analyzed for (A) protein integrity by silver staining; (B) for changes in phospholipid (PL) and phosphatidylethanolamine (PE) composition and (C) for changes in the hydroperoxide content (formation of dienes). Results shown in B and C represent the mean of triplicate determinations ± SD of a representative experiment performed at least two times. ***p<0.01*

In contrast to macrophages in atherosclerotic lesions, cultured macrophages generally express low levels of SR-BI (56,126). Therefore, we used a human monocytic cell line (THP-1), that can be infected by adenoviral vectors to induce SR-BI expression (Figure II-9A).

We first investigated whether OCN^- induced HDL carbamylation could affect the binding properties of HDL to SR-BI expressing THP-1 cells. As seen in Figure II-8A, SR-BI specifically mediated the binding of ^{125}I-labeled carbamylated HDL and ^{125}I-labeled native HDL. Carbamylation of HDL increased the binding affinity and capacity to SR-BI (Table II-9), whereas binding of HDL to control macrophages was unaltered (Figure II-8A).

To directly demonstrate that homocitrulline formation in HDL associated apoA-I increases binding affinity to SR-BI, we prepared reconstituted HDL (rHDL) using human apoA-I and 1-palmitoyl-2-oleoyl-sn-glycero-3-phosphocholine (POPC), an inert phospholipid. As seen in Figure II-8B and Table II-9, binding affinity and capacity of rHDL to SR-BI increased after OCN^- treatment. Moreover, already 2 homocitrulline residues present on lipid-free apoA-I increased binding affinity to SR-BI more than 5-fold (Table II-9).

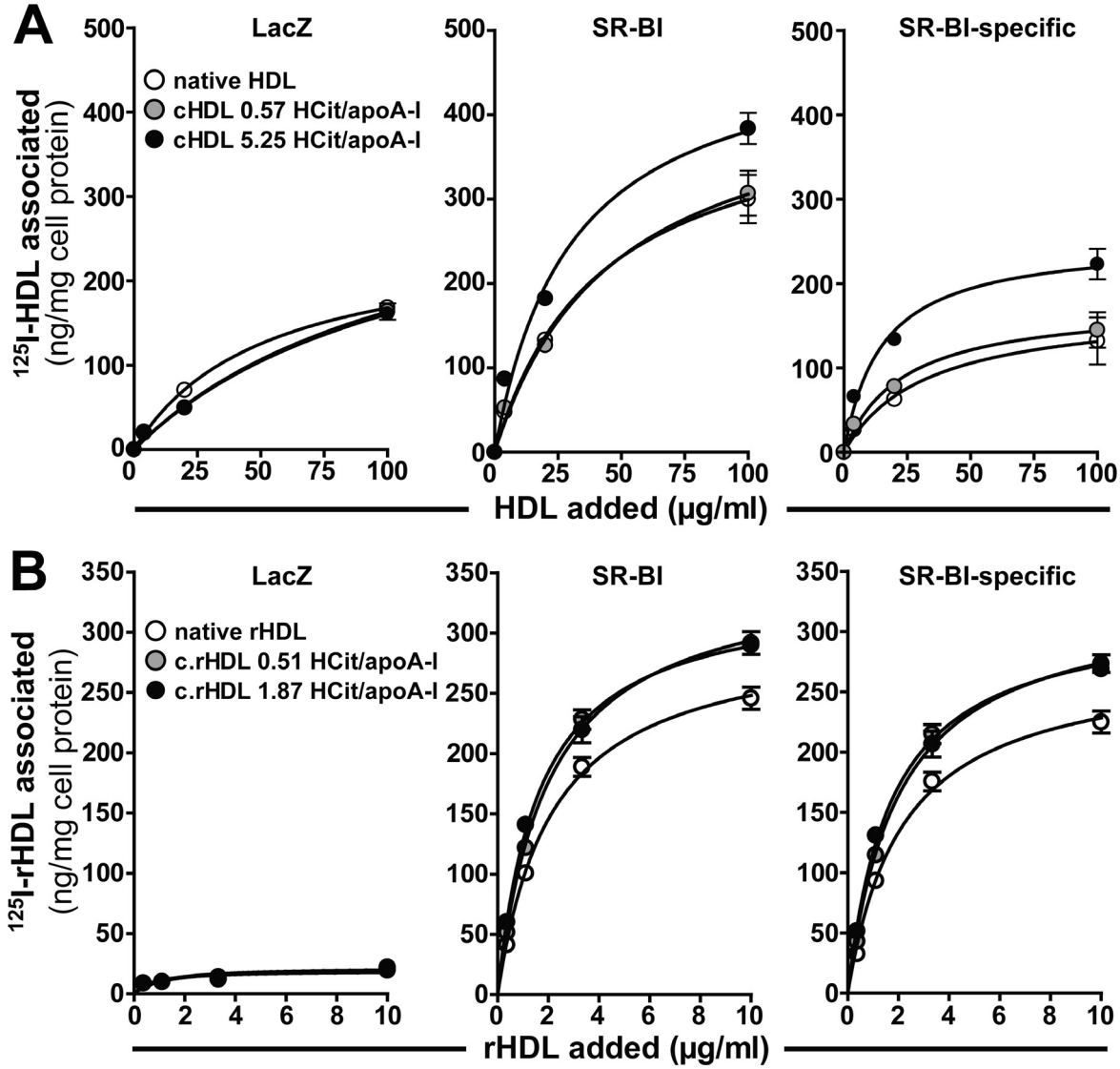

Figure II-8: Carbamylation of HDL increases binding affinity to SR-BI. THP-1 macrophages infected with adenoviral vectors encoding SR-BI or LacZ (control) were incubated for 2 hours at 4 °C in the presence of increasing concentrations of (A) ^{125}I-labeled native HDL or ^{125}I-labeled carbamylated HDL (cHDL) or (B) ^{125}I-labeled reconstituted HDL (rHDL) or ^{125}I-labeled carbamylated rHDL. Values obtained with LacZ expressing cells were subtracted from SR-BI expressing cells to calculate SR-BI specific binding. Results represent the mean of triplicate determinations ± SD of a representative experiment performed at least two times.

Table II-9: Binding properties of different ligands to SR-BI

	HCit / apoA-I	K_d [µg/ml]	B_{max} [ng/mg]
HDL	<0.01	32 ± 7.9	173 ± 15
cHDL	0.57	23 ± 4.9	175 ± 12
cHDL	5.25	15 ± 3.9	251 ± 19
rHDL	<0.01	2.2 ± 0.2	248 ± 13
c.rHDL	0.51	2.0 ± 0.2	299 ± 10
c.rHDL	1.87	1.7 ± 0.2	289 ± 11
apoA-I	<0.01	293 ± 53	205 ± 28
c.apoA-I	0.58	138 ± 27	171 ± 21
c.apoA-I	2.04	57 ± 35	93 ± 14

Calculated *K*d and *B*max values for binding of ^{125} I-labeled HDL, rHDL and apoA-I to SR-BI. Calculations were performed by nonlinear regression analysis (GraphPad Prism).

4.5. Carbamylated HDL-induced cholesterol accumulation in macrophages is SR-BI dependent

SR-BI mediates selective HDL cholesteryl-ester uptake by formation of a productive lipoprotein/receptor complex, which requires specific structural domains and conformation states of apoA-I (127). We hypothesized that increased binding of HDL through carbamylation might confer pro-atherosclerotic properties by inducing SR-BI dependent cholesterol accumulation in macrophages. Remarkably, HDL exposed to OCN^- induced marked total cholesterol accumulation in SR-BI expressing THP-1 cells, but not in control cells (Figure II-9B). A recent study demonstrated that cholesterol efflux of human macrophages is dependent on SR-BI and ABCA1, but independent of ABCG1 (128). Therefore, we tested whether OCN^- modulates the ability of HDL to induce SR-BI and ABCA1 mediated cholesterol efflux from macrophages. Interestingly, carbamylation moderately, but significantly reduced the ability of HDL to promote SR-BI dependent cholesterol efflux (Figure II-9C), whereas cholesterol efflux of control cells was not altered. Lipid-poor apoA-I removes cellular cholesterol from macrophages exclusively by an active transport process mediated by ABCA1. The process appears to involve the amphipathic α-helical domains of apoA-I. Modification of lysine residues may alter the ability of lipid poor apoA-I to remove ABCA1 dependent cholesterol from lipid-laden macrophages (129). However, carbamylation of apoA-I did not decrease ABCA1 mediated cholesterol efflux (Figure II-9D).

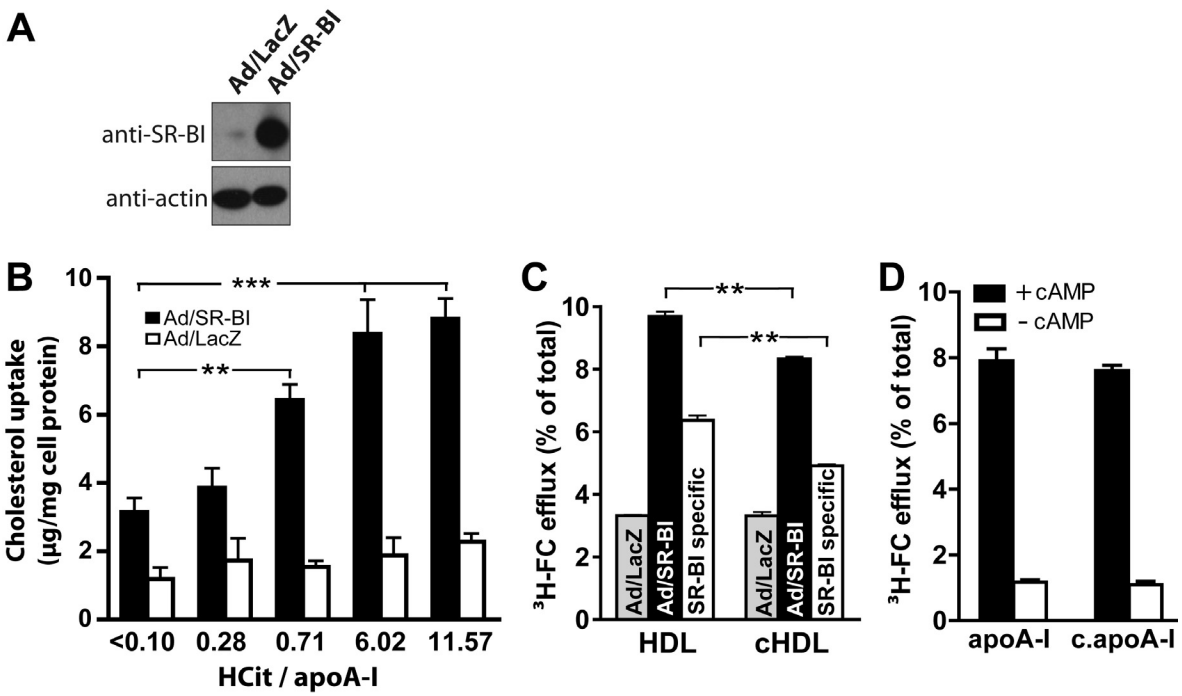

Figure II-9: Carbamylated HDL induces cholesterol accumulation in THP-1 macrophages via SR-BI. (A) Western-blot analysis of SR-BI and β-actin (loading control) expression of differentiated THP-1 macrophages infected with adenoviral vectors encoding SR-BI (Ad/SR-BI) or LacZ (Ad/LacZ) (B) SR-BI or LacZ (control) expressing THP-1 macrophages were incubated with 100 µg/ml native HDL or carbamylated HDL (with increasing amounts of homocitrulline (HCit) per apoA-I) for 24 hours at 37°C. Subsequently, cells were rinsed and total cellular cholesterol was estimated. HDL-induced cholesterol-uptake was calculated by subtracting cholesterol content of cells grown in the absence of HDL (16.1 ± 2 µg/mg cell protein) from cells grown in presence of HDL. (C) To measure SR-BI dependent cellular cholesterol efflux, THP-1 cells expressing SR-BI or LacZ were labeled with [^{3}H]-cholesterol. Subsequently, cells were incubated with 100 µg/ml native HDL or carbamylated HDL (0.57 HCit/apoA-I) as cholesterol acceptors for 2 hours at 37°C. At the end of the experiment, media and cells were separately collected to determine cholesterol efflux. To calculate SR-BI specific [^{3}H]-cholesterol (FC)-efflux, values obtained with LacZ expressing cells were subtracted from SR-BI expressing cells. (D) RAW264.7 cells were [^{3}H]-cholesterol-labeled and incubated in the presence or absence of cAMP to induce ABCA1 expression. Cells were incubated with 10 µg/ml native or carbamylated apoA-I (5.62 HCit / apoA-I) for 2 hours at 37°C. Media and cells were collected separately to determine cholesterol efflux. Specific cholesterol efflux was calculated by subtracting efflux in the absence of acceptors from efflux in the presence of acceptors. Results represent the mean of triplicate determinations ± SD of a representative experiment performed at least three times. ***p<0.01; ***p<0.001*

4.6. Carbamylated HDL induces SR-BI dependent lipid droplet formation in macrophages

The cholesterol uptake and efflux experiments indicate that carbamylation of HDL destabilizes the HDL/SR-BI mediated balance between cholesterol-uptake versus efflux, indicating that net cholesterol content of macrophages increases. Therefore, further assessment whether carbamylated HDL could induce lipid-droplet formation in macrophages was performed. Transfection of THP-1 cells with adenovirus was used to induce SR-BI expression in differentiated macrophages (Figure II-10A) Incubation of SR-BI expressing macrophages with HDL led to a

significant increase in lipid-droplet formation, which was dependent on the degree of carbamylation. Only minor lipid droplet accumulation was observed in control cells (Figure II-10B).

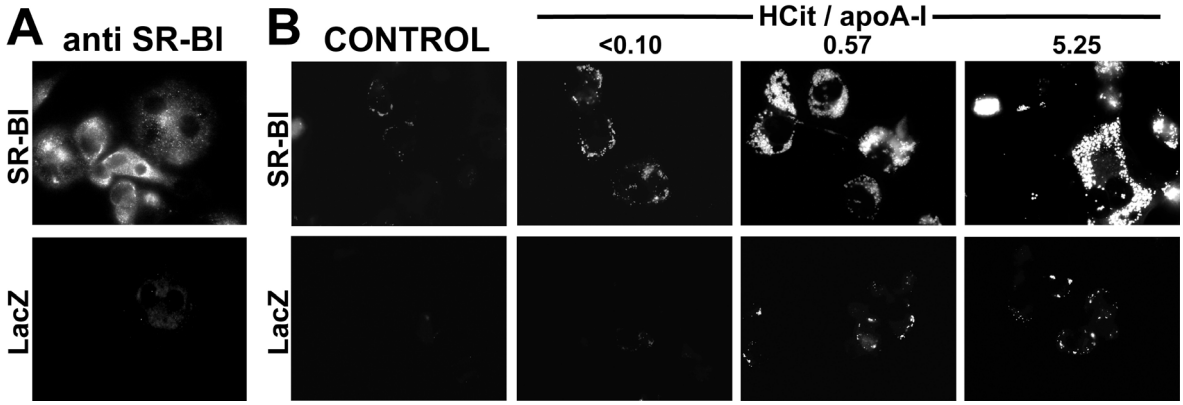

Figure II-10: Carbamylated HDL induces SR-BI dependent lipid droplet formation. (A) SR-BI or LacZ (control) expression was induced in THP-1 macrophages by infection with adenoviral vectors encoding SR-BI or LacZ. Cell surface expression of SR-BI was visualized by immunofluorescence staining with an anti-SR-BI antibody of non-permeabilized cells. (B) SR-BI and LacZ expressing macrophages were incubated with 200 µg/ml native HDL (control) or carbamylated HDL (0.57 or 5.25 HCit/apoA-I) for 48 hours at 37°C. The intracellular uptake of neutral lipid was visualized by Bodipy staining

4.7. Carbamylated HDL is a less potent substrate for LCAT

HDL plays a central role in lipid metabolism and especially in the reverse cholesterol transport pathway (described in Chapter I). HDL effluxes free cholesterol from peripheral cells, which is converted into cholesteryl-ester by LCAT. The esterified cholesterol is sequestrated into the core of HDL. This step drives the maturation of nascent HDL into spherical HDL, an essential step in RCT.

LCAT activation was found to be dependent on stoichiometry, structure and conformation of apoA-I, and on the sequence of apoA-I that includes amino acids 140–163 (130-132). Since this amino acid sequence includes a lysine residue, which might be targeted by cyanate, we investigated the impact of carbamylation on HDL-mediated LCAT activation.

To assess this question, we adopted a commercial available assay for serum/plasmaLCAT activity to measure the efficiency of different HDL preparation to activate LCAT. Therefore, HDL was labeled with a fluorescent LCAT substrate, which upon LCAT activity changes its fluorescent emission wavelength from 390 nm to 460 nm. The labeled substrate was rapidly incorporated into HDL (Figure

II-11A). Afterwards, the labeled HDL preparations were incubated with the same amount of LCAT to determine their activation capacity. Interestingly, carbamylation caused a dose-dependent decrease in LCAT activation (Figure II-11B).

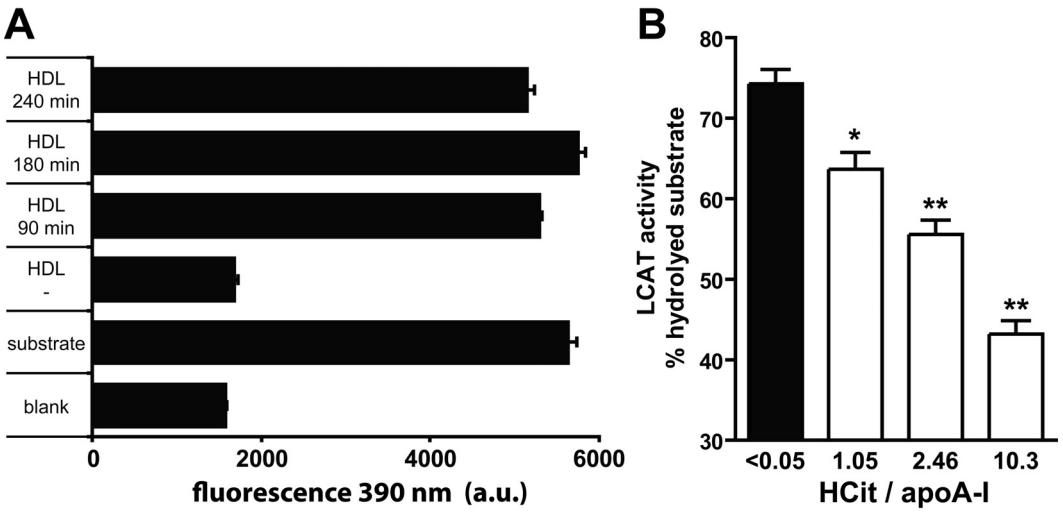

Figure II-11: Carbamylation decreases HDL ability to activate LCAT. (A) A fluorescent lipid substrate for LCAT was incubated with HDL for 90, 180 or 240 minutes. After filtration of HDL, the total fluorescence was found in the HDL fraction indicating that the fluorescent substrate was incorporated. Blank sample confirmed the sufficient removel of unbound substrate by gelfiltration. (B) Labeled HDL (100 µg/ml) was incubated with lipoprotein-deficient serum as LCAT source. Upon LCAT activity the substrates fluorescence emission changes from 390 nm to 460 nm, which can be monitored over time and used for quantification. Results represent the mean of duplicate determinations ± SEM of three independent experiments. **p<0.05; **p<0.01*

4.8. HDL-mediated protection of LDL oxidation is impaired by carbamylation

Besides HDL's important role in lipid metabolism, HDL has anti-oxidative capacity. We investigated the ability of HDL to inhibit radical-induced LDL oxidation. LDL was incubated with AAPH (a radical inducer) and a characteristic oxidation curve with lag time and propagation phase was obtained (Figure II-12A). The oxidation could be markedly reduced by the addition of native HDL. However, the ability of HDL to inhibit radical-induced oxidation was decreased by increasing amounts of homocitrulline on HDL (Figure II-12B), which indicates that carbamylation impairs HDL anti-oxidative capability.

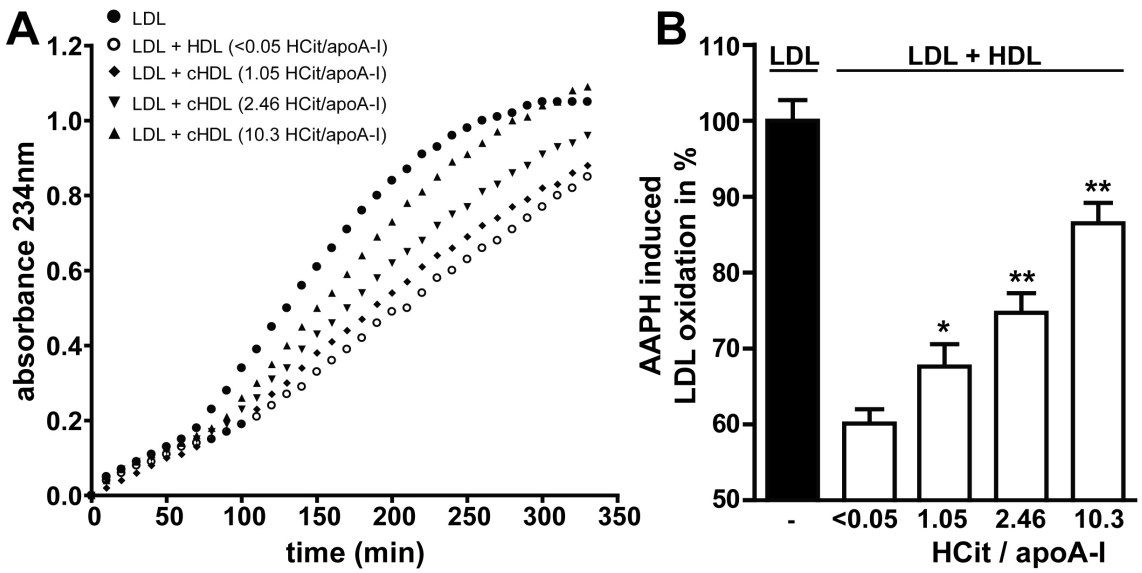

Figure II-12: Carbamylated HDL fails to prevent LDL oxidation. LDL (100 µg/ml) was incubated with AAPH (free radical inducer) in the presence or absence of HDL (100 µg/ml). (A) A representative time course of an AAPH-induced oxidation process is shown, which was monitored at 234 nm for 350 minutes. (B) One time point in the middle of the propagation phase was selected for quantification. Oxidation in presence of HDL was calculated as relative value to oxidation of LDL alone, which was set to 100 %. Results represent the mean of triplicate determinations ± SEM of three independent experiments.

4.9. Carbamylation decreases activity of HDL-associated paraoxonase

Paraoxonase (PON), a HDL-associated enzyme has been demonstrated to be an important contributor to the antioxidant capacity of HDL (75). Increased expression of PON has been reported in human atherosclerotic lesions (133). Interestingly, HDL from CAD patients has decreased PON activity, which was linked to an impaired ability of HDL to stimulate endothelial eNOS-activating pathways and NO production (134). PON has at least three enzymatic activities (135), namely paraoxonase activity, arylesterase activity and lactonase activity. Importantly, the activity of PON is regulated by its interaction with apoA-I (136). We addressed whether carbamylation of HDL influences HDL-associated paraoxonase and arylesterase activity. Strikingly, we observed that already a minimal carbamylation of HDL significantly reduced paraoxonase and arylesterase activity (Figure II-13A, B).

We investigated whether a loss or deactivation of paraoxonase from HDL was responsible for the decreased enzymatic activity. We subjected carbamylated HDL to native non-denaturating gel electrophoresis and observed that increased carbamylation caused PON (~ 45kDa) to dissociate from HDL (Fig II-13C).

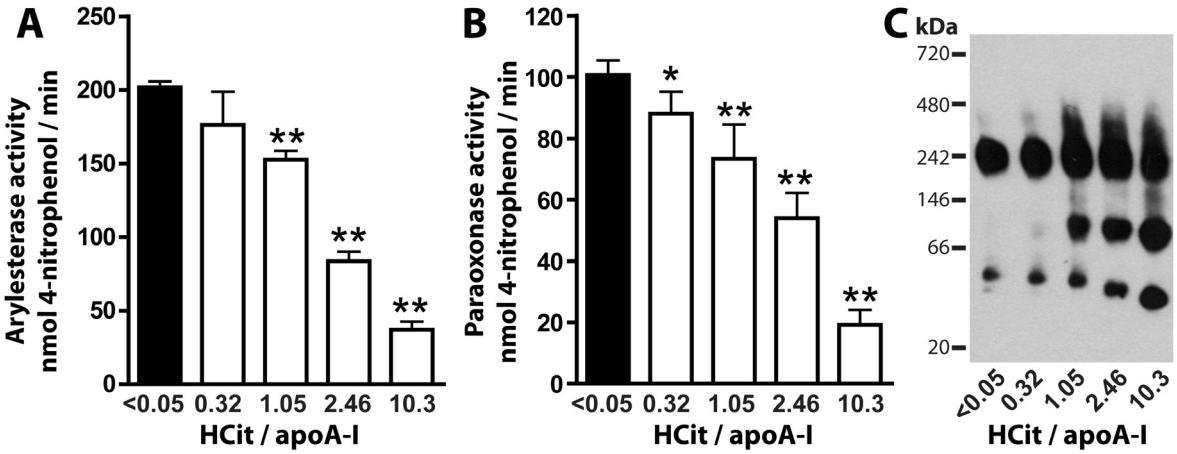

Figure II-13: Carbamylation decreases activity of HDL-associated paraoxonase. (A) Arylesterase activity of HDL-associated paraoxonase (PON) was measured with phenylacetate as substrate (HDL, 20 µg/ml). (B) Paraoxonase activity of HDL-associated PON was measured with paraoxon as substrate (HDL, 50 µg/ml). Paraoxonase and arylesterase activity were calculated from the slopes of three independent experiments and are expressed as means ± SEM. .**p<0.05; **p<0.01* (C) Native gel of HDL was blotted and probed for PON. Free paraoxonase is visible at ~45kDa.

4.10. Lp-PLA2 activity increases upon carbamylation of HDL

Lp-PLA2 is a lipoprotein associated enzyme which partially resides on HDL (~20%) (137).It hydrolyses platelet activating factor (PAF) and its activity is associated with CVD (138). We addressed whether carbamylation of HDL influences Lp-PLA2 activity. In striking contrast to PON activity, Lp-PLA2 activity trended to increase upon HDL carbamylation (Fig II-14). The changes were moderate, but significant.

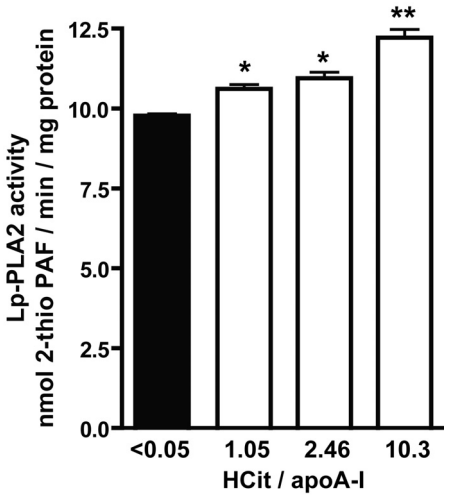

Figure II-14: Lp-PLA2 activity after carbamylation of HDL. Lipoprotein-associated phospholipiase A2 (Lp-PLA2) activity was measured with 2-thio PAF as substrate. Kinetics of 2-thio PAF turnover can be monitored at 405 nm and used to calculate the enzymes activity. Results represent the mean of triplicate determinations ± SEM of two independent experiments. **p<0.05; **p<0.01*

5. Discussion

A clinical study demonstrated that plasma levels of protein-bound homocitrulline independently predict an increased risk of coronary artery disease (35).

In the present study, we established a state of the art method to quantitatively assess modified amino acids with mass spectrometry. We could substantially reduce the extensive hydrolysis time (from 24 hours to 11 minutes) of amino acid analysis by implementing a rapid-low volume hydrolysis method. With this method, we were able to provide evidence that post-translational modification of HDL through OCN^- is a major modification of HDL in atherosclerotic lesions. Compared to other atherosclerotic tissue derived fraction (LDL, total protein), the HDL fraction contained the highest amount of homocitrulline, suggesting that HDL is a specific target for carbamylation. The high homocitrulline content was accompanied by an increase in 3-chlorotyrosine. MPO has been found bound to HDL recovered from atherosclerotic lesions and immunohistochemical analysis showed that MPO and apoA-I colocalizes in atherosclerotic lesions (96-98). It suggests that MPO-derived oxidants will be generated in closest proximity to HDL. This is in good agreement with our observation that HDL was much higher carbamylated and oxidized as other lesion proteins. Interestingly, carbamyllysine content of HDL was about 30-times higher than the oxidation marker 3-chlorotyrosine (Figure II-5). Importantly, homocitrulline and 3-chlorotyrosine did correlate with each other, indicating that MPO is involved in both reactions (Figure II-6A). We suggest that under conditions found in atherosclerotic lesions the MPO/SCN^-/H_2O_2 carbamylation-pathway is dominant over the MPO/Cl^-/H_2O_2 chlorination pathway. SCN is the preferred target of MPO and as long as SCN is present, cyanate and hypothiocyanate will be the major products (100).

A recent report demonstrated that carbamylated LDL is the most abundant LDL modification found in human plasma (108). We observed that the homocitrulline content of plasma proteins and HDL is high (about 60-fold higher than 3-chlorotyrosine) (Figure II-5). The homocitrulline content of plasma proteins did not correlate with 3-chlorotyrosine, suggesting that plasma proteins are mainly

carbamylated by urea derived cyanate. This pathway may be of particular importance in renal patients where urea concentrations are high (106,139).

Prompted by the observation that high levels of carbamylated HDL are present in atherosclerotic lesions, we investigated the effect of carbamylation on HDL atheroprotective functions. We observed that carbamylated HDL induced cholesterol accumulation in macrophages via a SR-BI dependent pathway. Macrophages in human atherosclerotic lesions express high levels of SR-BI (56,57). The multiligand receptor SR-BI has been described to mediate (i) selective HDL cholesteryl-ester uptake, (ii) uptake of oxidized lipoproteins as well as (iii) the secretion of cholesterol to high-density lipoprotein (140). On the one hand, macrophage SR-BI is thought to play an atheroprotective role, because of its ability to mediate cholesterol efflux from macrophages. On the other hand, macrophage SR-BI in early stage lesions was shown to induce cholesterol accumulation, thereby triggering fatty streak development (141). The binding affinity of HDL to SR-BI increased dependent on the degree of carbamylation (Figure II-8). Several modified proteins that are being recognized by the multiligand receptor SR-BI hold in common a negative charge, suggesting that SR-BI recognizes the negative charge of proteins. Our findings indicate that modification of HDL-lysine residues by OCN^- (leading to a decrease of positive charge) affects the interaction of HDL with SR-BI, consistent with the observation that oxidation of (lipo)proteins with hypochlorous acid, resulting in the oxidation of lysine residues, show increased binding affinity to SR-BI (96,142).

Taken together, our results support the hypothesis that carbamylation shifts the balance – between SR-BI mediated cholesterol efflux and uptake – towards cholesterol uptake, thereby causing intracellular cholesterol and lipid droplet accumulation (Figure II-10B).

HDL maturation during the RCT pathway is an important step, which is partially mediated by LCAT. Interestingly, we found that HDLs ability to activate LCAT was reduced when HDL was carbamylated (Figure II-11B). LCAT activation is dependent on stoichiometry, structure and parts of the apoA-I sequence (131). It was observed that, the apoA-I sequence between amino acid residue 140 - 150 is essential for LCAT activation (130). Interestingly, this sequence part of apoA-I harbors a lysine residue, which could be targeted by carbamylation. This could in

turn interfere with structural or charge requirements of LCAT activation. Interestingly, previous reports from uremic patients with high levels of urea (source for cyanate) showed that LCAT activity was low and particle maturation was perturbed (143,144), raising the possibility that protein carbamylation contributes to the observed effects.

Non-classical HDL function has been intensively studied over the last decade (51,77). HDL was found to possess anti-oxidative, anti-inflammatory and anti-thrombotic activity which might contribute to its atheroprotective effects. In our study, the ability of carbamylated HDL to inhibit radical-induced LDL oxidation was significantly decreased (Figure II-12). Cyanate targets mainly lysine residues, but can also react with cysteine to form carbamylcysteine (145). Cysteine has antioxidant properties and the sulfhydryl groups of cysteine have been found to be important for the enzymatic functions of PON or LCAT (146,147). Therefore, the loss of anti-oxidative function of HDL might be due to the loss of lysine and/or cysteine residues. It will need further studies to elucidate the molecular mechanism, how carbamylation causes a loss of anti-oxidative capacity of HDL.

The anti-oxidant ability of HDL depends on the apoprotein moiety and on the presence of associated enzymes. HDL-associated paraoxonase has been demonstrated to be an important contributor to the anti-oxidant capacity of HDL (75,148). Experimental studies indicated that impaired paraoxonase activity leads to dysfunctional HDL and diet-induced atherosclerosis in mice (149,150). A very intriguing finding of the present study was that already minimal modification of one homocitrulline per apoA-I was sufficient to significantly decrease of HDL-associated paraoxonase and arylesterase activity (Figure II-13A, B). By native gel-electrophoresis, we observed that carbamylation caused paraoxonase to dissociate from HDL (Figure II-13C). Since PON activity is dependent upon binding to apoA-I (136), the observed dissociation might be the major trigger in reducing PON activity.

Lp-PLA2 has been recently associated with enhanced risk of coronary artery disease (138) and inhibitors are currently undergoing clinical trials (151,152). An interesting finding in our study was that Lp-PLA2 activity trended to increase upon HDL carbamylation. A Previous study suggested that Lp-PLA2 bound to HDL is less active than LDL bound Lp-PLA2, which was suggested to be dependent on the lipid environment (137). The changes in our study were moderate, but

significant (Figure II-14). This unexpected result might be related to conformational changes in apoA-I, the enzyme itself or to the release of the enzyme and its presumably higher activity in free form.

In summary, the present study provide evidence that carbamylation is a physiological relevant modification of HDL in atherosclerotic lesions. Carbamylation might critically impair anti-atherogenic properties of HDL in the atherosclerotic intima, thereby destabilizing the cellular balance between macrophage mediated cholesterol-uptake versus efflux, a critical step in the development of atherosclerosis. Carbamylated HDL showed impaired anti-oxidative and anti-inflammatory functions. Taken together, carbamylation counteracts HDL athero-protective function and might be causally involved in atherogenesis.

III. Chapter:

Uremia alters HDL composition and function

1. Abstract:

Aim: Functional impairment of high-density lipoprotein (HDL) during renal disease may contribute to the excess cardiovascular mortality in these patients. However, the data available regarding the impact of advanced renal disease on HDL composition and functionality are limited. In particular, the effect of renal disease on the first step of reverse cholesterol transport, the efflux of cellular cholesterol from macrophages to HDL, has not been determined yet.

Results: Mass spectrometry and biochemical analyses showed that HDL isolated from patients on maintenance hemodialysis (HD) depicts considerable alterations in the protein and lipid composition. Our studies revealed a significant increase in acute phase protein serum amyloid A1, albumin, lipoprotein-associated phospholipase A2 and apoC-III content of uremic HDL, whereas apoA-I and apoA-II were decreased. Proteomic alterations were accompanied by a decreased phospholipid and increased triglyceride and lyso-phospholipid content of HDL. In regard to function, HDL from hemodialysis patients was less potent in promoting cholesterol efflux from lipid-laden macrophages. Exposure of lipid-laden macrophages to control and HD-HDL did decrease intracellular cholesterol stores, but uremic HDL was significantly less potent. Importantly, correlation analysis could show that functional changes are linked to compositional alterations.

Conclusion: HDL functionality and composition is significantly altered in renal failure patients on hemodialysis. Our results provide insights into mechanism leading to the functional impairment of HDL and raise the possibility to identify humans at increased risk of cardiovascular disease.

2. Introduction:

Cardiovascular disease, stroke and peripheral vascular disease are notorious problems in patients with chronic kidney disease (153). Cardiac mortality in dialysis patients aged 45 years or younger is more than 100-fold increased in comparison to the general population (154). Accelerated atherosclerosis is thought to be a consequence of increased inflammation, oxidative stress and impaired triglyceride and HDL metabolisms (155,156). HDL is thought to protect against atherosclerosis by promoting reverse cholesterol transport and potentially through anti-oxidative and anti-inflammatory activities (77,157,158). More recent studies suggest that the HDL proteome is implicated in HDL functionality; identifying HDL-associated proteins involved in lipid metabolism, complement activation, growth-factor and proteolysis regulation (46-48). These multiple mechanisms of action make HDL a therapeutic target with great potential for the treatment of patients with atherosclerosis.

Low levels of HDL, such as found in renal patients, correlate with an increased risk of atherosclerotic vascular disease (159). However, more recent findings have suggested that the relationship between HDL and cardiovascular risk is more complex and extends beyond the levels of HDL in plasma (160). Notable, it was found that HDL particles may become dysfunctional or even pro-inflammatory in chronic and inflammatory diseases (161). Recent studies focused on the loss of antioxidant and anti-inflammatory effects of HDL in dialysis patients (162-164). The loss of anti-inflammatory properties in HDL of renal patients was shown to correlate with a higher 30-month adjusted hazard ratio for death in uremic patients (162). Moreover, oxidized plasma proteins in end-stage renal disease patients were shown to interfere with HDL clearance, thereby potentially contributing to the abnormal composition of HDL (117). However, the data available regarding the effect of advanced renal disease on HDL functionality are limited and the effects of renal disease on the first step of reverse cholesterol transport, the efflux of cellular cholesterol from macrophages to HDL, has not been established yet. This is of particular interest, since cholesterol efflux capacity from macrophages, has a strong inverse association the likelihood of coronary artery disease, independently of the HDL cholesterol level (41). Accordingly, to understand the role of HDL in

chronic and inflammatory diseases, such as end stage renal disease, it is essential to analyze the protein and lipid composition of HDL, reflecting its functional state. Therefore, the current study was designed to test the hypothesis that renal disease modifies HDL composition, thereby altering anti-atherogenic properties of HDL.

In this explorative study, LC-MS/MS analysis was used to investigate the proteomic profile of HDL from 27 hemodialysis patients and 19 control subjects. The analysis revealed that HDL from hemodialysis patients carries a distinct protein and lipid cargo that is linked to decreased cholesterol efflux properties.

3. Materials and Methods:

Isolation of HDL, culture of cell lines and Lp-PLA2 activity assay are described in Chapter II in the section Materials and Methods.

3.1. List of Materials:

Sources of materials are described in Chapter II section 3.1.

Table III-1 antibodies

name	dilution	Nr.:	company
apoA-I, mouse monoclonal	1:1000	NB100-65491	NOVUS Biol.
apoC-II, rabbit polyclonal	1:1000	ab76452	Abcam
apoA-IV, rabbit polyclonal	1:100	ab72395	Abcam
Lp-PLA2, rabbit polyclonal	1:250	160603	Cayman Europe
albumin, rabbit polyclonal	1:1000	ab83465	Abcam
antitrypsin, mouse monoclonal	1:1000	ab90158	Abcam
transthyretin, rabbit polyclonal	1:4000	ab16006	Abcam
SAA 1, mouse monoclonal	1:1000	ab81483	Abcam
RBP4, rabbit polyclonal	1:1500	ab64194	Abcam

3.2. Blood collection

Blood was taken from hemodialysis patients prior to the dialysis session and age matched control subjects at the time of routine laboratory investigations in agreement with the Ethical Committee of the Medical University of Graz. Blood (5 ml) was collected in standard sterile polystyrene vacuum tubes containing 5 mmol/L EDTA.

3.3. Plasma parameter and HDL lipid analysis

Plasma parameter analyses were performed by the Clinical Institute of Medical and Chemical Laboratory Diagnostics at the Medical University of Graz. Levels of total cholesterol, non-esterified cholesterol, triglycerides, phospholipids, creatinine, urea, (Diasys, Holzheim, Germany), lysophosphatidylcholine (Cosmo Bio Co. LTD., Tokyo, Japan) and non-esterified fatty acids (Wako Chemicals, Neuss, Germany) were measured enzymatically with commercially available kits. LDL cholesterol was calculated according to the Friedewald equation described

previously (113) using HDL cholesterol values measured in the supernatant of phosphotungstic precipitates.

3.4. Apolipoprotein determination by immunoturbidimetry

Apolipoprotein quantification was performed by the Clinical Institute of Medical and Chemical Laboratory Diagnostics at the Medical University of Graz. The following methodology was used: ApoA-I, apoA-II, apoB, apoC-II, apoC-III, apoE (Greiner, Flacht, Germany) and lipoprotein(a) (Wako Chemicals, Neuss, Germany) were determined by immunoturbidimetry. All analyses were performed on an Olympus AU640 analyser (Olypmpus Diagnostika, Hamburg, Germany).

3.5. Lipid extraction from cells

Cells were washed twice with PBS (0.5 % BSA) and once with PBS. Lipids were extracted from 6-well plates with 2 ml hexane/isopropyl alcohol (3:2, v/v) for 1 hour at 4°C. Lipids were dried under nitrogen and re-suspended in 200 µl 0.5 % Triton X-100 in chloroform. Chloroform was evaporated under nitrogen and lipids re-suspended in 100 µl PBS for 15 minutes at 37°C. Aliquots were used to quantify lipid species.
Cellular proteins were extracted with 0.3N NaOH overnight at RT. The protein solution was frozen and incubated for additional 2-3 h at RT. Protein content was determined with the Lowry protein assay.

3.6. Protein isolation for SDS-PAGE

Cells were washed twice with PBS. Ice-cold RIPA buffer (50 mmol/L KH_2PO_4, 150 mmol/L NaCl, 1% Triton X-100, 0.5% deoxycholate, 1:1000 protease inhibitor cocktail (before use)) was added to the cells and incubated for 10 minutes at 4°C on a shaker. Cells were scraped down, the solution carefully re-suspended and transferred into a sterile 1.5 ml eppendorf tube and stored at -20°C.

3.7. SDS-PAGE and Western blotting

SDS-PAGE and subsequent Western blotting experiments of different HDL preparations were performed with 5-20% polyacrylamide gradient gels as described (96).

ApoA-IV, albumin, antitrypsin, transthyretin, SAA1, RBP4 and Lp-PLA2 were immunodetected by, separating HDL (1 µg for apoA-I, 2.5 µg for albumin, 5 µg for antitrypsin, RBP4, SAA1, 10 µg for transthyretin, apoA-VI) SDS-Page. Gels were blotted onto PDVF membranes and probed using specific antibodies (see list of materials).

3.8. Cellular cholesterol efflux assays:

Cholesterol efflux assay: RAW264.7 macrophages were plated on 24-well plates (~$7.5*10^5$ cells) and grown overnight. Cells were labelled for 24 hours with 1 µCi/ml [^{3}H]cholesterol in medium supplemented with 5% FBS and 50 µg/ml carbamylated LDL. In addition, cells were stimulated with the LXR agonist TO-901317 (2 µmol/L). After labelling, cells were washed with PBS, equilibrated in serum free media with 0.2% BSA for 2 hours, washed again with PBS, and incubated with 50 µg/ml HDL for 2 or 20 hours at 37°C to determine [^{3}H]cholesterol efflux.

SR-BI specific cholesterol efflux: ldlA7 or ldlA7[SR-BI] cells were plated on 24-well plates and grown overnight. Cells were loaded with 1 µCi/ml [^{3}H]cholesterol for 24 hours, washed once with PBS, equilibrated in serum free media with 0.2% BSA for 2 hours and washed once with PBS again. The cellular cholesterol efflux was assessed in response to 100 µg/ml HDL for 2 hours at 37°C. SR-BI specific efflux was calculated by subtracting the efflux of ldlA7 cells from ldlA7[SR-BI] cells.

ABCA1 specific cholesterol efflux: RAW264.7 macrophages were plated on 24-well plates (~$7.5*10^5$ cells) and grown overnight. Cells were labelled for 24 hours with 1 µCi/ml [^{3}H]cholesterol and stimulated with 300 µmol/L cAMP in medium containing 5% FBS and 50 µg/ml carbamylated LDL. Cells were equilibrated in serum free media with 0.2% BSA for 2 hours in the absence or presence of 20 µmol/L probucol. To initiate efflux, cells were incubated with 20 µg/ml HDL or apoA-I. ABCA1-specific efflux was determined by subtracting efflux of probucol-treated cells from efflux of untreated cells.

For all efflux experiments, supernatants and cells were separately collected. Supernatants were transferred into eppendorf tubes and centrifuged for 5 minutes at 5000 rpm to remove cells and cell debris. An aliquot was used to determine the radioactivity through scintillation counting.

Cells were lysed with 0.3 N NaOH containing 0.1 % SDS for 2 hours. Cells were suspended carefully and transferred into scintillation vials to estimate the cell-associated radioactivity.

[^{3}H]cholesterol efflux is expressed as the radioactivity in the supernatant relative to total radioactivity in the supernatant and cells. HDL-specific cholesterol efflux was calculated by subtracting cholesterol efflux in the absence of HDL from efflux in the presence of HDL.

3.9. PLA2-treatment and lyso-phospholipid enrichment of HDL

HDL was incubated in the presence of 500 ng/ml phospholipase A2 for 16 hours to hydrolyse HDL associated phospholipids. After incubation, phospholipase A2 was removed by density gradient ultracentrifugation of HDL as described above. To generate lyso-PC-enriched HDL, 0.65 mmol 1-palmitoyl-2-hydroxy-sn-glycero-3-phosphocholine (lyso-PC) dissolved in chloroform/methanol (1:1, v/v) was placed in a glass tube and the solvent was evaporated under a stream of nitrogen. Dried lyso-PC were re-suspended in PBS by vortexing for 3 minutes, drop wise added to 1 mg/ml HDL, and incubated for 2 hours at 37°C. Unbound lyso-PC was removed by gel filtration and lyso-PC content analyzed as described above.

3.10. Net cholesterol efflux from lipid-laden macrophages

RAW264.7 macrophages were plated on 6-well plates (3-4*10^6) and grown overnight. Cells were cholesterol-loaded by incubating with 100 µg/ml aggregated LDL in DMEM plus 5% FBS in the presence of 100 nmol/L PMA for 48 hours. The cellular cholesterol mass of untreated control cells was 11.4 ± 2.3 µg total cholesterol / mg cell protein and 53.9 ± 2.0 µg total cholesterol / mg cell protein for cholesterol-loaded cells. After cholesterol loading, cells were washed twice with PBS and equilibrated in serum free media with 0.2% BSA for 8 hours. Media was removed and cholesterol efflux was initiated by addition of 100 µg/ml HDL for 14 hours. At the end of the experiment, the cells were washed twice with PBS, containing 0.2% BSA and once with PBS. Lipids were extracted as described in section 3.5. To adjust for cell density, total cellular proteins were determined in parallel (see section 3.6).

3.11. LC-MS/MS analysis and homology search

Proteomic analysis of HDL was performed by the Core Facility Mass Spectrometry at the Medical University of Graz by Dr. Birner-Gruenberger. The used methodology was as follows.

For tryptic digest, 50 µg protein of HDL preparations were precipitated with 3 volumes of acetone at -20°C overnight, solubilised in 30 µl (6 mol/L) ammonium guanidinium hydrochloride, reduced with 34 µl of (10 mmol/L) DTT for 20 minutes by shaking at 550 rpm at 56°C and alkylated with 8 µl of (55 mmol/L) iodoacetamide for 15 minutes by shaking at 550 rpm at room temperature. Protein was digested by adding 1 µg of modified trypsin (Promega, Mannheim, Germany) and left for overnight shaking at 550 rpm at 37°C. Completeness of digests was controlled by analyzing 5 µg aliquots by SDS-PAGE. The resulting peptide solution was acidified by adding 1.6 µl of 5% formic acid and diluted in solvent A (see below) to a theoretical final concentration of 50 ng/µl. Samples (40 µl) were separated by nano-HPLC on an Agilent 1200 system equipped with a Zorbax enrichment column (300SB-C18, 5 µm, 5 x 0.3 mm) and a Zorbax nanocolumn (300SB-C18, 3.5 µm, 150 x 0.075 mm). The samples were injected and concentrated on the enrichment column for 6 minutes using 0.1% formic acid as an isocratic solvent at a flow rate of 20 µl/min. The column was then switched into the nanoflow circuit, where the sample was loaded for 6 minutes on the nanocolumn at a flow rate of 300 nl/min and separated using the following gradient: solvent A: water, 0.3% formic acid; solvent B: acetonitril/water 80/20, 0.3% formic acid; 0-10 minutes: 10% solvent B; 10-120 minutes 10-60% solvent B, 120-122 minutes 60-95% solvent B, 122-130 minutes 95% solvent B, 130-132 minutes 95-10% solvent B, 132-140 minutes re-equilibration at 10% B. The sample was ionized in the nanospray source equipped with nanospray tips (PicoTipTM Stock# FS360-75-15-D-20, Coating: 1P-4P, 15+/- 1µm Emitter, New Objective) and analyzed in a LTQ-FT mass spectrometer (Thermo Scientific, Waltham, US) in positive ion mode by alternating full scan MS (m/z 200 to 2000) in the ion cyclotron resonance cell and MS/MS by collision-induced dissociation of the 5 most intense peaks in the ion trap with dynamic exclusion enabled.

LC-MS/MS data were analyzed by searching the human NCBI nonredundant public database with Spectrum mill Rev. A.03.03.078 (Agilent, Vienna, Austria)

and Mascot 2.2 (MatrixScience, London, UK). Detailed settings: Enzyme: trypsin, max. missed cleavage sides: 2, N-terminus: hydrogen, C-terminus: free acid, search mode: homology search, possible multiple oxidised methionine and carbamylated lysine, maximum precursor charge 3; precursor mass tolerance +/- 0.05 Da, product mass tolerance +/- 0.7 Da; acceptance parameters were 2 or more identified peptides after automatic validation (Mascot: $p<0.05$, FDR < 5 %; Spectrum Mill: for precursor charge of 2: score threshold is 6.0, %SPI threshold is 60.0, Fwd-Rev score threshold is 2.0 and rank 1-2 score threshold is 2.0, for precursor charge of 1: score threshold is 6.0, %SPI threshold is 70.0, Fwd-Rev score threshold is 2.0 and rank 1-2 score threshold is 2.0, for precursor charge of 3: score threshold is 8.0, %SPI threshold is 70.0, Fwd-Rev score threshold is 2.0 and rank 1-2 score threshold is 2.0).

3.12. Statistical analysis

Differences in plasma and HDL parameters between hemodialysis and control group were analyzed using Mann-Whitney-U-test. Two-way ANOVA was used to assess for differences in plasma- and HDL parameters between the control group and four hemodialysis subgroups (with/without diabetes mellitus, with/without lipid lowering therapy).

Changes in HDL-associated proteins were evaluated from spectral counts (e.g. the number of MS/MS spectra assigned to a protein) of automatically validated proteins. The standard deviation of spectral counts was below 10% between duplicates. The Shapiro–Wilk test (at the level of 10%) was used to assess data normality. Because proteomic data markedly violate the assumption of normality, the Mann-Whitney-U-test was used for analysis of differences.

Correlations between HDL mediated [^{3}H]cholesterol efflux, HDL-phospholipids, HDL-triglycerides, HDL-Lp-PLA2 and proteomic data were determined using Pearson product–moment estimates.

Significances were accepted at probability level of $*P<0.05$ and $**P<0.01$. Statistical analyses were performed with PASW Statistics, version 18.

4. Results:

4.1. Characteristics of study subjects

HDL was isolated from end-stage renal disease patients on maintenance hemodialysis (n = 27) and healthy subjects (n = 19). The hemodialysis patient group consisted of both, diabetic and non-diabetic individuals with and without lipid-lowering therapy. The control subjects showed no sign of renal insufficiency, were neither hyperlipidemic nor diabetic, and did not receive any lipid-lowering therapy. The clinical characteristics of the study groups are given in Table III-2A. The hemodialysis group showed significantly elevated plasma concentrations of creatinine, urea and CRP, whereas plasma hemoglobin was reduced. Plasma lipids of hemodialysis patients displayed characteristics of renal dyslipidemia, with significantly increased triglyceride and free-cholesterol levels. Triglyceride/HDL-C ratios were increased in hemodialysis patients whereas the apoA-I/apoC-III ratios were decreased.

Table III-2A: Clinical characteristics of study subjects

	CONTROL	**HD**
n	19	27
mean age (yr)	52.9±12.3	61.9±17.2
male/female	9/11	15/12
statins	0/19	6/27
diabetes mellitus	0/19	10/27
plasma parameter	**CONTROL**	**HD**
creatinine (mg/dL)	0.9 (0.9-1.1)	6.9 (6.3-10.0)**
urea (mg/dL)	28 (25-34)	116 (97-143)**
hemoglobin (mg/dL)	13.8 (13.1-14.1)	11.5 (10.5-12.4)**
CRP (mg/dL)	1 (0-2)	9 (3-19)**
fibrinogen (mg/dL)	307 (235-396)	490 (411-618)**
total cholesterol (mg/dL)	182 (176-224)	164 (126-199)
free cholesterol (mg/dL)	54 (49-62)	54 (38-67)
cholesterolester (mg/dL)	101 (99-119)	115 (88-134)*
triglycerides (mg/dL)	112 (83-169)	147 (97-202)
HDL-cholesterol (mg/dL)	61 (45-72)	43 (37-47)*
LDL-cholesterol (mg/dL)	109 (87-123)	87 (62-127)
phospholipids (mg/dL)	270 (221-314)	201 (185-239)*
free fatty acids (µmol/L)	310 (300-440)	370 (240-560)
TG / HDL-C ratio	2.5 (1.3-3.2)	3.4 (2.3-5.0)*
apoA-I / apoC-III ratio	19.5 (16.3-25.7)	12.8 (8.4-20.3)*

Results are given as medians with the inter-quartile range. Significances were accepted at the level of *0.01 and **0.001 TG, triglycerides; HDL-C, HDL-cholesterol

In addition, we quantified the major lipid classes of HDL. HDL from hemodialysis patients had significant lower levels of phospholipid and free cholesterol, whereas triglycerides and lyso-PC were increased (Table III-2B)

Table III-2B: HDL lipid composition

	CONTROL	HD
total cholesterol (µg/mg protein)	260 (235-295)	228 (181-260)*
triglycerides (µg/mg protein)	37 (23-47)	74 (52-123)**
cholesterylester (µg/mg protein)	196 (175-223)	183 (160-214)
free cholesterol (µg/mg protein)	62 (50-71)	37 (28-56)*
phospholipids (µg/mg protein)	442 (420-482)	297 (235-371)**
lyso-PC (nmol/mg protein)	8.8 (8.2-9.1)	13.5 (11.6-20.9)**

Results are given as medians with the interquartile range. Significances were accepted at the level of *0.01 and **0.001 (Mann Whitney U test). lyso-PC, lysophosphatidylcholine.

We assessed the impact of diabetes and lipid-lowering therapy on plasma and HDL parameters. In the hemodialysis patient group, only plasma triglyceride levels of individuals receiving statin therapy was significantly decreased, all other parameters were not altered (Table III-3A, 3B).

Table III-3A: Impact of diabetes and lipid therapy on plasma parameters

plasma parameter		HD patients, n=27			
		non-diabetic n=17	diabetic n=10	without lipid therapy n=20	lipid lowering therapy n=7
TC	[mg/dL]	181.9 ± 57.6	159.7 ± 46.4	178.2 ± 55.6	159.9 ± 49.2
FC	[mg/dL]	58.2 ± 19.6	48.7 ± 15.2	56.5 ± 19.3	49.0 ± 15.3
CE	[mg/dL]	123.7 ± 41.1	111.0 ± 31.7	121.7 ± 39.2	110.9 ± 34.0
TG	[mg/dL]	171.1 ± 100.1	160.0 ± 76.7	181.5 ± 100.5	128.6 ± 36.7*
HDL-C	[mg/dL]	45.6 ± 12.6	41.2 ± 11.0	44.0 ± 13.0	43.4 ± 9.6
LDL-C	[mg/dL]	102.0 ± 44.7	86.5 ± 35.9	97.8 ± 42.8	90.7 ± 40.3
PL	[mg/dL]	219.8 ± 49.3	201.0 ± 46.9	221.1 ± 48.0	189.7 ± 44.3
FFA	[mmol/L]	0.4 ± 0.3	0.5 ± 0.1	0.4 ± 0.2	0.5 ± 0.3
apoA-I	[mg/dL]	128.0 ± 24.6	121.3 ± 23.9	126.3 ± 24.7	122.9 ± 24.2
apoA-II	[mg/dL]	27.1 ± 6.7	22.8 ± 6.4	25.9 ± 7.4	24.0 ± 5.1
apoB	[mg/dL]	89.3 ± 27.3	79.4 ± 28.1	88.1 ± 28.1	78.3 ± 26.3
apoC-II	[mg/dL]	4.7 ± 2.7	3.1 ± 2.4	4.5 ± 2.8	2.8 ± 1.5
apoC-III	[mg/dL]	11.7 ± 6.3	9.0 ± 5.4	11.7 ± 6.4	7.7 ± 3.5
apoE	[mg/dL]	9.0 ± 4.8	7.3 ± 5.2	8.6 ± 5.2	7.8 ± 3.6
lp(a)	[mg/dL]	15.6 ± 18.9	25.7 ± 13.4	17.4 ± 19.0	26.2 ± 7.5

Data are given as mean ± SD. Statistical analysis was performed by two-way ANOVA. *p<0.05; HD patients without lipid therapy vs. HD patients with lipid therapy. TC, total cholesterol; FC, free cholesterol; CE, cholesteryl ester; TG, triglycerides; HDL-C, HDL-cholesterol, LDL-C, LDL-cholesterol; PL, phospholipids; FFA, free fatty acids; lyso-PC, lysophophatidylcholine; lp(a), lipoprotein a.

Table III-3B: Impact of diabetes and lipid therapy on HDL lipid parameters

HDL lipid parameter		HD patients, n=27			
		non-diabetic n=17	diabetic n=10	without lipid therapy n=20	lipid lowering therapy n=7
TC	[mg/dL]	238.8 ± 62.8	216.7 ± 40.7	234.5 ± 60.4	222.6 ± 43.1
FC	[mg/dL]	41.2 ± 18.7	41.3 ± 14.2	41.5 ± 17.5	40.4 ± 16.2
CE	[mg/dL]	197.7 ± 46.5	175.4 ± 30.3	192.0 ± 45.8	182.1 ± 30.5
TG	[mg/dL]	85.5 ± 45.8	91.2 ± 45.2	90.2 ± 48.1	80.3 ± 35.9
PL	[mg/dL]	320.7 ± 132.6	277.9 ± 77.0	315.5 ± 125.2	274.6 ± 81.4
lyso-PC	[nmol/mg]	9.8 ± 2.7	9.9 ± 3.9	9.8 ± 3.0	9.9 ± 3.4

Data are given as mean ± SD. Statistical analysis was performed by two-way ANOVA. TC, total cholesterol; FC, free cholesterol; CE, cholesteryl ester; TG, triglycerides; PL, phospholipids; lyso-PC, lysophophatidylcholine.

4.2. HDL from HD patients carries a unique protein cargo

Over the past years, proteomic studies have markedly extended the list of HDL-associated proteins (46-48). We sought to investigate possible alterations in the HDL proteome of end-stage renal disease patients undergoing regular hemodialysis. HDL was proteolytically digested, and the resulting peptides were analyzed by tandem mass spectrometry.

LC-MS/MS analysis identified 35 proteins to be associated with HDL (Table III-4A). As expected, we found that the major protein components of HDL, from the hemodialysis group and the control group, were apolipoprotein (apo)A-I and apoA-II, accounting for about 50% and 10% of all detected peptides, respectively. Most of the major apolipoproteins (apoA-I, apoA-II, apoC-III, apoE, apoC-I, apoD, apoC-II, apoM) as well as SAA1, SAA4 and albumin were detected in all samples from hemodialysis patients and controls, whereas antitrypsin, retinol-binding protein 4 (RBP4), transthyretin, apoA-VI and further minor proteins were only detected in uremic HDL. ApoB was detected in four samples in trace amounts, always accompanied by apo(a) indicating the presence of lipoprotein(a), whose hydrated density overlaps with HDL (Table III-4A).

Quantification of proteomic data is still a substantial challenge, but many lines of evidence suggest that spectral counting is a valid tool for assessing overall protein abundance (165,166). After statistical analysis, we identified 9 proteins to be significantly altered in hemodialysis patients ($p<0.001$). Strikingly, we observed on average a 3 and 8-fold increase in albumin and SAA1 content of uremic HDL, respectively, making them major HDL-associated proteins (Table III-4A).

Table III-4: Identification of proteins in HDL isolated from hemodialysis (HD) patients or control subjects (control)

(A)		HD		CONTROL			
accession nr.	protein name	HDL derived peptides per subject				*p*	ratio
178775	**apoA-I**	**331.3**	**(27/27)**	**416.2**	**(19/19)**	***<0.001***	**0.8**
4502149	**apoA-II**	**60.9**	**(27/27)**	**72.3**	**(19/19)**	***<0.001***	**0.8**
167887493	**apoC-III**	**46.5**	**(27/27)**	**33.5**	**(19/19)**	***<0.001***	**1.4**
119588814	**SAA1**	**45.6**	**(27/27)**	**5.6**	**(17/19)**	***<0.001***	**8.2**
10835095	SAA4	44.9	(27/27)	37.9	(19/19)	*0.001*	1.2
4557325	apoE	42.9	(27/27)	45.0	(19/19)	*0.671*	1.0
4502027	**albumin**	**40.8**	**(27/27)**	**13.5**	**(19/19)**	***<0.001***	**3.0**
4502157	apoC-I	25.4	(27/27)	30.2	(19/19)	*0.001*	0.8
4502163	apoD	17.2	(27/27)	16.2	(19/19)	*0.300*	1.1
32130518	apoC-II	13.9	(27/27)	8.5	(19/19)	*0.001*	1.6
22091452	apoM	8.0	(27/27)	11.8	(19/19)	*0.002*	0.7
105990532	apoB	4.0	(4/27)	-	(0/19)	*0.067*	-
114062	apo(a)	3.2	(5/27)	0.4	(3/19)	*0.778*	-
93163358	**apoA-IV**	**2.9**	**(27/27)**	**-**	**(0/19)**	***<0.001***	-
15080499	**antitrypsin**	**2.9**	**(11/27)**	**-**	**(0/19)**	***<0.001***	-
18088326	**RBP4**	**2.0**	**(17/27)**	**-**	**(0/19)**	***<0.001***	-
114318993	**transthyretin**	**1.0**	**(14/27)**	**-**	**(0/19)**	***<0.001***	-
6960317	α-2 catenin	1.0	(14/27)	0.6	(3/19)	*0.002*	-
298532	paraoxonase 1	0.8	(8/27)	0.4	(3/19)	*0.329*	-
34364645	Ig alpha	0.7	(5/27)	-	(0/19)	*0.067*	-
45643462	GIP 12	0.3	(1/27)	-	(0/19)	-	-
4557894	lysozyme	0.3	(1/27)	-	(0/19)	-	-
194386720	KIAA0590	0.3	(4/27)	-	(0/19)	-	-
7020972	PHIP	0.3	(7/27)	-	(0/19)	-	-
4503107	cystatin C	0.3	(5/27)	-	(0/19)	-	-
194386720	unknown protein	0.3	(4/27)	-	(0/19)	-	-
4505733	unknown protein	0.3	(7/27)	-	(0/19)	-	-
146424184	apoC-IV	0.2	(5/27)	-	(0/19)	-	-
179665	complement C3	0.1	(1/27)	-	(0/19)	-	-
4885179	defensin alpha 3	0.1	(1/27)	-	(0/19)	-	-
119579599	haptoglobin	0.1	(1/27)	-	(0/19)	-	-
181482	Vit.D-BP	0.1	(2/27)	-	(0/19)	-	-
4507261	statherin	0.1	(1/27)	-	(0/19)	-	-
4505733	platelet factor 4	-	(0/27)	0.6	(8/19)	-	-
148745121	apoL-I	-	(0/27)	0.2	(1/19)	-	-
Mean total peptides / subject		**698 ± 61**		**693 ± 79**			

(B)			
Lp-PLA2 mass (densitometry units)	**2.70 ± 1.3**	**1.00 ± 0.8**	**<0.001**

(A) HDL was isolated from 27 HD patients and 19 control subjects by one-step-ultracentrifugation. The HDL proteome was analyzed on a LC-MS/MS system. The data were analyzed by searching the human NCBI nonredundant public database with Spectrum mill Rev. A.03.03.078 (Agilent) and Mascot 2.2 (MatrixScience). Values shown represent the mean peptide count per analyzed subject with the corresponding number of patients where the protein was identified. Statistical significances were calculated with the Mann-Whitney U-test. (B) Lp-PLA2 mass associated with HDL was determined by western blot and densitometric quantification. The Lp-PLA2 activity was determined using 2-thio PAF as substrate. Activity is shown as nmols hydrolysed 2-thio PAF per min per mg HDL protein. RBP4, retinol-binding protein 4; GIP12 growth-inhibiting protein 12; Vit.D-BP, Vitamin D-binding protein; PHIP, PH interacting protein.

We were not able to assess the content of lipoprotein-associated phospholipase A2 (Lp-PLA2) (alternatively named platelet-activating factor acetylhydrolase *or* PAF-AH) with LC-MS/MS. Lp-PLA2 is an important phospholipase that has been recently associated with an enhanced risk of coronary artery disease, stroke, and mortality (138). Therefore, we performed immunoblot analysis, revealing a 2.8-fold increased Lp-PLA2 content in uremic HDL (Table III-4B).

To validate the proteomic results, further immunoblot analysis was performed choosing significantly enriched proteins (Table III-4A). Protein enrichment could be confirmed by appearance of specific bands at 67 kDa for albumin, 48 kDa for Lp-PLA2, 47 kDa for antitrypsin, 45 kDa for apoA-VI, 23 kDa for RBP4, 16 kDa for transthyretin and 14 kDa for SAA1 on uremic HDL (Figure III-1). The immunoblot reflected a similar enrichment for the respective proteins as observed by LC-MS/MS analysis (Table III-4A). In contrast to the LC-MS/MS analysis, immunoblot analysis was more sensitive and detected even small amounts of antitrypsin, transthyretin and apoA-IV on control HDL. Interestingly, RBP4 was only detected in uremic HDL, indicating a specific enrichment.

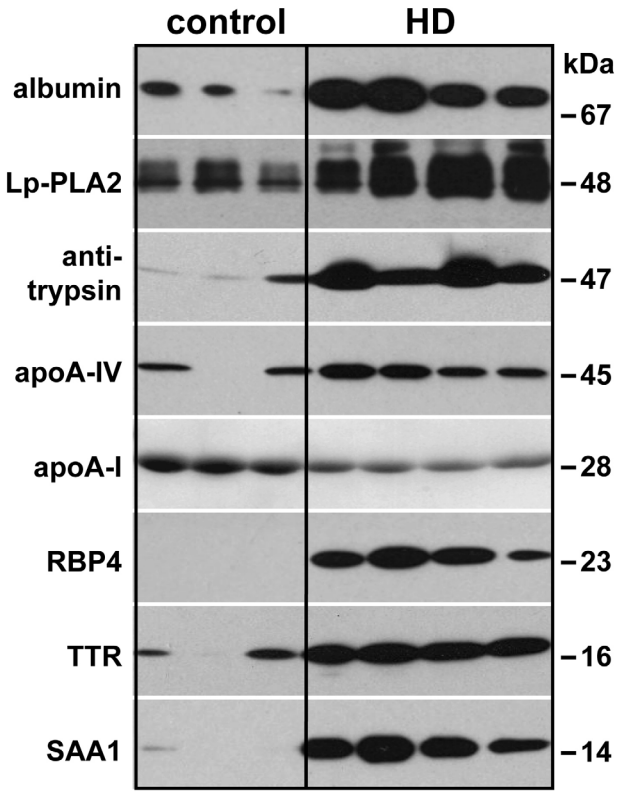

Figure III-1: Immunoblot detection of HDL-associated proteins. To confirm the results obtained by LC-MS/MS, HDL isolated from hemodialysis (HD) patients and control subjects were subjected to immunoblot analysis. HDL-associated proteins were separated by SDS-Page, transferred to PDVF membranes and probed using specific antibodies. Molecular weights are indicated on the right.

Chronic kidney disease is associated with an inflammatory response caused by the dialysis procedure, increased oxidative stress and dyslipidemia (167). The hemodialysis group exhibited a significant increase in the plasma inflammatory markers CRP and fibrinogen (Table III-2). As expected, the HDL-associated acute-phase protein SAA1 correlated with the plasma concentration of CRP and fibrinogen in hemodialysis patients (Table III-5). Interestingly, HDL-associated albumin did not correlate with plasma CRP or fibrinogen levels and did not correlate with HDL-associated SAA1 or plasma levels of albumin in hemodialysis patients (Table III-5). Moreover, apoC-III accumulation in HDL showed no correlation with HDL-associated albumin or SAA1 (Table III-6), but correlated with plasma apoC-III (not shown) and creatinine (Table III-6). Therefore, our data indicate different underlying mechanisms resulting in the enrichment of HDL with albumin, apoC-III or SAA1.

Table III-5: Correlations of HDL-associated proteins with plasma parameters of HD patients

	HDL albumin	HDL SAA1	HDL apoC-III	HDL Lp-PLA2	CREA	FIBRIN	CRP
HDL - albumin	1	-.043	-.181	-,005	-.180	-.038	-.125
HDL - SAA1	-.043	1	-.463	,074	-.101	**.673****	**.864****
HDL - apoC-III	-.181	-.463	1	-,189	**.510****	-.222	-.406
HDL - Lp-PLA2	-.005	.074	-.189	1	-.470	-.088	-.043
creatinine	-.180	-.101	**.510****	-,470	1	-.305	-.131
fibrinogen	-.038	**.673****	-.222	-,088	-.305	1	**.640****
CRP	-.125	**.864****	-.406	-,043	-.131	**.640****	1

Shown are Pearson's correlation coefficients (n = 27). Significances were accepted at the level of **p<0.01. CREA, creatinine; FIBRIN, fibrinogen.

However, further data analysis revealed a strong positive correlation between HDL-associated albumin and apoA-VI, antitrypsin, and RBP4 (Table III-6). In line with this observation, a recent study observed that plasma albumin binds several plasma proteins including apoA-VI, antitrypsin and RBP4 (168) raising the possibility that albumin carries proteins onto HDL.

Table III-6: Correlation of HDL-associated proteins

	albumin	SAA1	apoC-III
antitrypsin	**0.626****	0.214	0.025
apoA-IV	**0.773****	0.175	0.309
RBP4	**0.791****	0.249	0.158
transthyretin	**0.626****	0.192	0.133

Presented are Pearson's correlation coefficients (n = 46).
Significances were accepted at the level of **P<0.01.

4.3. Cholesterol acceptor capability of uremic HDL is decreased

Cholesterol efflux capacity from macrophages has a strong inverse association with the likelihood of coronary artery disease, independently of the HDL cholesterol level (41). We observed that the capability of uremic HDL to promote cholesterol efflux from lipid-laden macrophages was significantly reduced at 2 hours (Figure III-2A) and after longtime exposure of 20 hours (Figure III-2B) in comparison to control HDL. Importantly, neither diabetes nor lipid-lowering therapy significantly altered cholesterol acceptor capacity (Figure III-2G, H) or proteomic composition of uremic HDL (Table III-7).

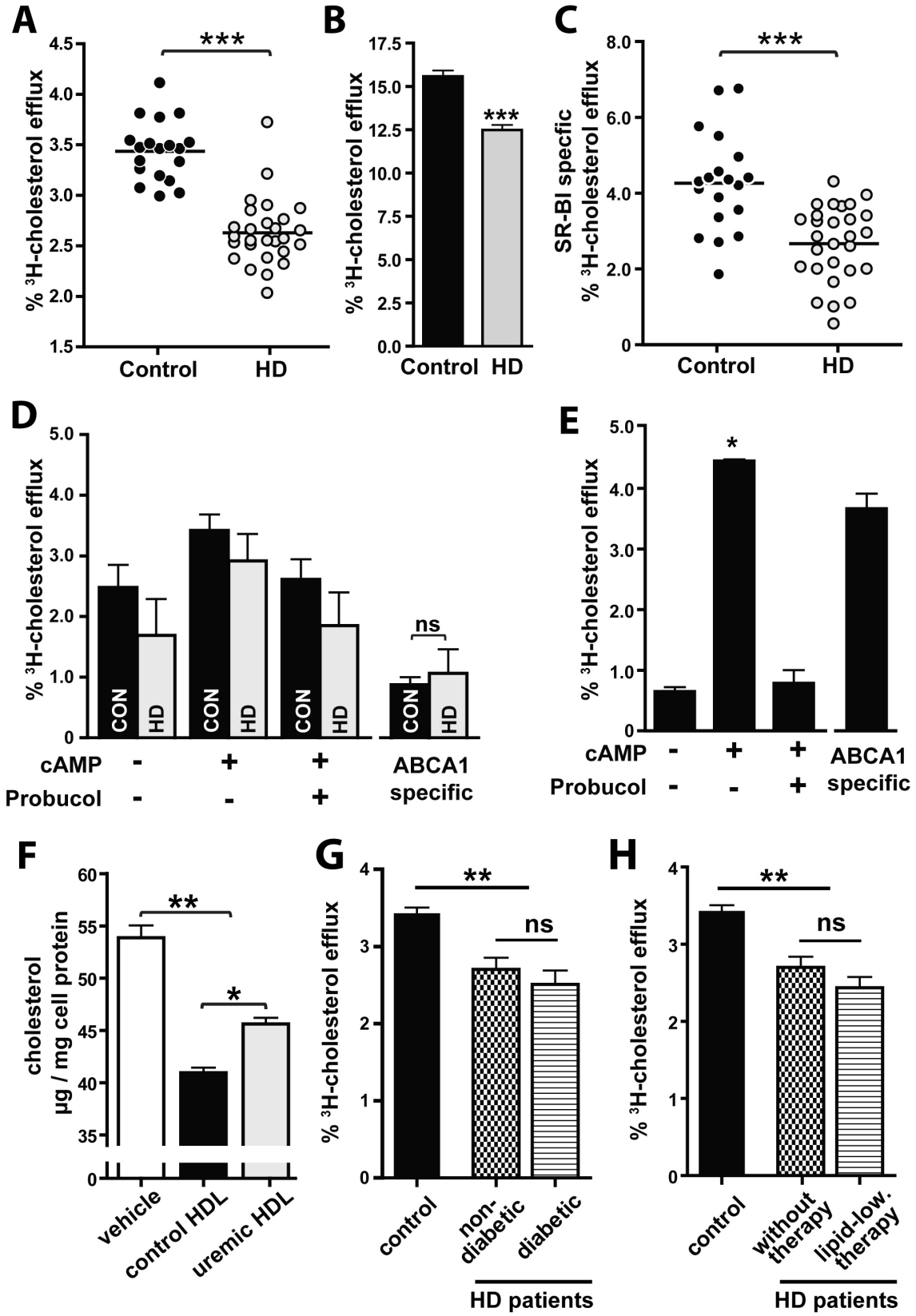

Figure III-2: HDL from hemodialysis patients possess decreased cholesterol efflux potentials. HDL from 27 hemodialysis patients (HD) and 19 control subjects (control) were examined for their ability efflux cholesterol. (A) HDL-mediated efflux (50 µg/ml) of [^{3}H]cholesterol from TO-901317 stimulated, lipid-loaded RAW264.7 macrophages for 2 hours (A) or 20 hours (B) at 37°C. Cholesterol efflux is expressed as the radioactivity in the medium relative to total radioactivity in medium and cells. Values shown represent means of three individual experiments

performed in duplicates. (C) To determine SR-BI mediated efflux, SR-BI expressing CHO cells were labeled with [^{3}H]-cholesterol and cholesterol efflux was determined in response to 100 µg/ml HDL for 2 hours at 37°C. Values shown represent means of two individual experiments performed in triplicate. (D) RAW264.7 macrophages were labeled with [^{3}H]-cholesterol and stimulated with 0.3 mmol/L cAMP. ABCA1 was inhibited with 20 µmol/L probucol to determine ABCA1-specific efflux - in response to 20 µg/ml HDL for 3 hours - by subtracting [^{3}H]cholesterol efflux in presence of probucol from [^{3}H]cholesterol efflux in absence of probucol. (E) The induction of ABCA1 expression by 0.3 mmol/L cAMP in RAW264.7 cells was confirmed by a high increase in [^{3}H]cholesterol efflux to lipid-free apoA-I for 3 hours at 37°C. Specific efflux was again calculated by subtracting efflux in presence of probucol form efflux in absence of probucol. (F) To assess net cholesterol flux, RAW264.7 macrophages were enriched in cholesterol by incubation with aggregated LDL (200 µg/ml) for 48 hours.. Cellular cholesterol flux was initiated by exposure of cells to serum free media with or without 100 µg/ml HDL from HD patients or control subjects for 14 hours. Afterwards cellular lipids were extracted and total cholesterol mass per mg cell protein determined. For ABCA1-specific efflux (D) and net cholesterol flux (F), pooled fractions of HDL from HD patients and controls were analyzed in triplicate in two independent experiments. The impact of (G) diabetes or (H) lipid-lowering therapy on the capacity of HDL from HD patients (n = 27) to promote cholesterol efflux was analyzed. Cholesterol efflux measure of (A) were used for comparision. No difference was observed for HD patients with diabetes or without, as well no difference was observed for HD patients with or without lipid lowering therapy. Statistical analysis was performed by Student's t-test for 2 groups and with ANOVA more than 2 groups. Significances were accepted at the level of **p<0.05, **p<0.01, ***p<0.001*

Table III-7: Impact of diabetes and lipid lowering therapy on the HDL proteome of HD patients (n=27)

	non-diabetic n = 17	diabetic n = 10	without lipid therapy n = 20	lipid lowering therapy n = 7
apoA-I	**47.29 ± 7.71**	**47.89 ± 7.55**	**47.68 ± 8.03**	**47.04 ± 6.32**
apoA-II	**8.84 ± 1.17**	**8.52 ± 0.61**	**8.72 ± 1.13**	**8.72 ± 0.52**
apoC-III	**6.77 ± 1.35**	**6.49 ± 0.97**	**6.62 ± 1.29**	**6.79 ± 1.02**
SAA1	**6.64 ± 6.29**	**6.13 ± 5.70**	**6.66 ± 6.50**	**5.87 ± 5.80**
SAA4	**6.36 ± 1.00**	**6.52 ± 1.07**	**6.22 ± 0.89**	**7.00 ± 1.18**
apoE	**6.22 ± 2.33**	**5.72 ± 2.00**	**5.76 ± 2.26**	**6.82 ± 1.86**
albumin	**6.10 ± 4.30**	**5.07 ± 3.98**	**5.95 ± 4.64**	**5.06 ± 2.31**
apoC-I	**3.87 ± 0.85**	**3.23 ± 0.59**	**3.70 ± 0.89**	**3.45 ± 0.54**
apoD	**2.49 ± 0.47**	**2.43 ± 0.52**	**2.43 ± 0.42**	**2.57 ± 0.65**
apoC-II	**2.00 ± 0.73**	**1.92 ± 0.80**	**1.97 ± 0.71**	**1.94 ± 0.87**
apoM	**1.37 ± 0.28**	**0.74 ± 0.46***	**1.21 ± 0.58**	**0.94 ± 0.61**
apoA-IV	**0.42 ± 0.28**	**0.41 ± 0.39**	**0.42 ± 0.34**	**0.38 ± 0.24**
antitrypsin	**0.45 ± 0.38**	**0.33 ± 0.25**	**0.41 ± 0.39**	**0.37 ± 0.35**
RBP4	**0.30 ± 0.30**	**0.23 ± 0.21**	**0.30 ± 0.25**	**0.22 ± 0.20**
transthyretin	**0.16 ± 0.15**	**0.12 ± 0.11**	**0.17 ± 0.15**	**0.07 ± 0.12**
α-2 catenin	**0.14 ± 0.17**	**0.13 ± 0.16**	**0.16 ± 0.16**	**0.08 ± 0.15**
paraoxonase 1	**0.07 ± 0.13**	**0.19 ± 0.30**	**0.09 ± 0.16**	**0.18 ± 0.31**
Ig alpha	**0.04 ± 0.10**	**0.23 ± 0.61**	**0.14 ± 0.44**	**0.02 ± 0.06**

Data shown represent the mean peptide count per subject ± SD. Statistical analysis was performed by two-way ANOVA. *p<0.05; diabetic vs. non-diabetic

Cholesterol efflux is predominantly mediated by SR-BI and ABCA1 in human monocyte-derived macrophages (169).

Therefore, we investigated whether SR-BI and/or ABCA1 mediated cholesterol efflux to uremic HDL is impaired. For that purpose, we used SR-BI overexpressing CHO cells and cAMP stimulated macrophages to specifically up-regulate ABCA1. The induction of ABCA1 was confirmed by cholesterol efflux studies with lipid-free apoA-I (Figure III-2E). The difference in efflux between control and SR-BI - overexpressing cells was taken as a measure of SR-BI-mediated efflux. ABCA1-specific efflux was determined by subtracting cholesterol efflux in presence of probucol (ABCA1 inhibitor) from efflux in absence of the inhibitor. We observed that SR-BI mediated cholesterol efflux to uremic HDL was significantly reduced compared with control HDL (Figure III-2C), but ABCA1 induced efflux to uremic and control HDL did not differ significantly (Figure III-2D).

Cholesterol efflux is bi-directional and measurement of cholesterol efflux alone does not indicate net cholesterol flux from cells. Therefore, we measured the cholesterol content of lipid-laden macrophages after a 20 hour exposure to control and uremic HDL. We observed that control HDL reduced intracellular cholesterol about ~20%, whereas uremic HDL was significantly less potent in mediating net cholesterol flux (Figure III-2F).

4.4. SAA1, albumin, apoC-III and triglyceride content of HDL correlate with impaired cholesterol efflux potential

Prompted by the observation that the cholesterol efflux capability of uremic HDL was significantly reduced, we assessed whether the relative concentration of major proteins and lipids in uremic HDL correlates with the impaired ability to efflux cholesterol.

As expected, a strong positive correlation of HDL-associated apoA-I, apoA-II (Figure III-3A) and phospholipids (Figure III-3C) with the cholesterol efflux potential of uremic and control HDL was observed. Notably, apoA-I and apoA-II are also positively correlated with the phospholipid content of HDL, which is in agreement with the high phospholipid binding capability of apoA-I/A-II (Figure III-4). In contrast, the HDL proteins SAA1, albumin, apoC-III (Figure III-3B) and the HDL triglyceride content (Figure III-3C) negatively correlated with the cholesterol efflux capability of HDL.

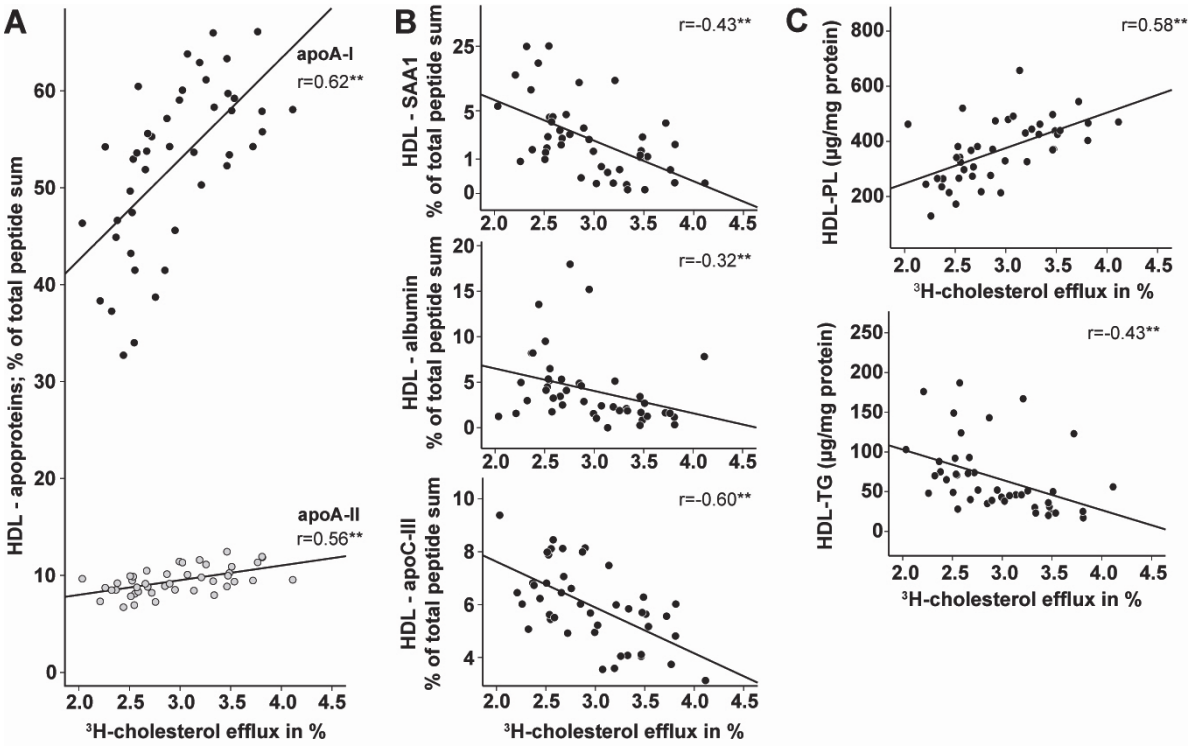

Figure III-3: Determinants of cholesterol efflux potential of HDL. To determine factors influencing HDL cholesterol efflux potential, the proteomic data were correlated with the [^{3}H]-cholesterol-efflux capability (see Figure III-2A) of HDL preparations from HD patients and controls. (A) Positive correlation of apoA-I and apoA-II with [^{3}H]-cholesterol-efflux. (B) Negative correlation of HDL-SAA1, HDL-albumin and HDL-apoC-III with [^{3}H]-cholesterol-efflux. (C) Correlations of phospholipid and triglyceride content of HDL with the [^{3}H]-cholesterol-efflux. The Pearson's correlation coefficients are noted for each plot; ***p<0.01*

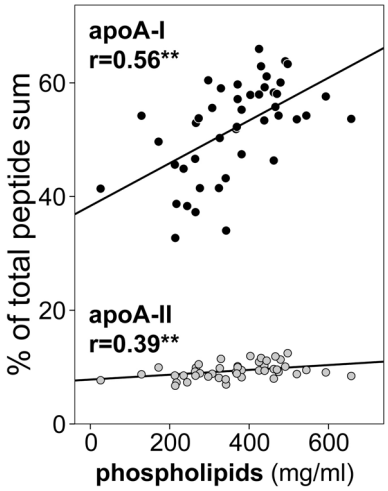

Figure III-4: HDL-phospholipid content correlates with its apoA-I and apoA-II content. The Pearson's correlation coefficient is noted; ***p<0.01*.

4.5. SAA1, albumin and apoC-III replace apolipoproteins A-I and A-II

It is well known that in the circulation SAA associates with HDL particles, causing HDL remodeling with displacement of apo-A-I (170-172). To gain further insight into the relationship between protein composition and cholesterol efflux potential of HDL, we performed a detailed correlation analysis. An inverse correlation of HDL-associated apoproteins A-I and A-II with SAA1 was observed (Figure III-5A). Interestingly, also albumin and apoC-III inversely correlated with apoA-I and apoA-II content of HDL (Figure III-5B, C).

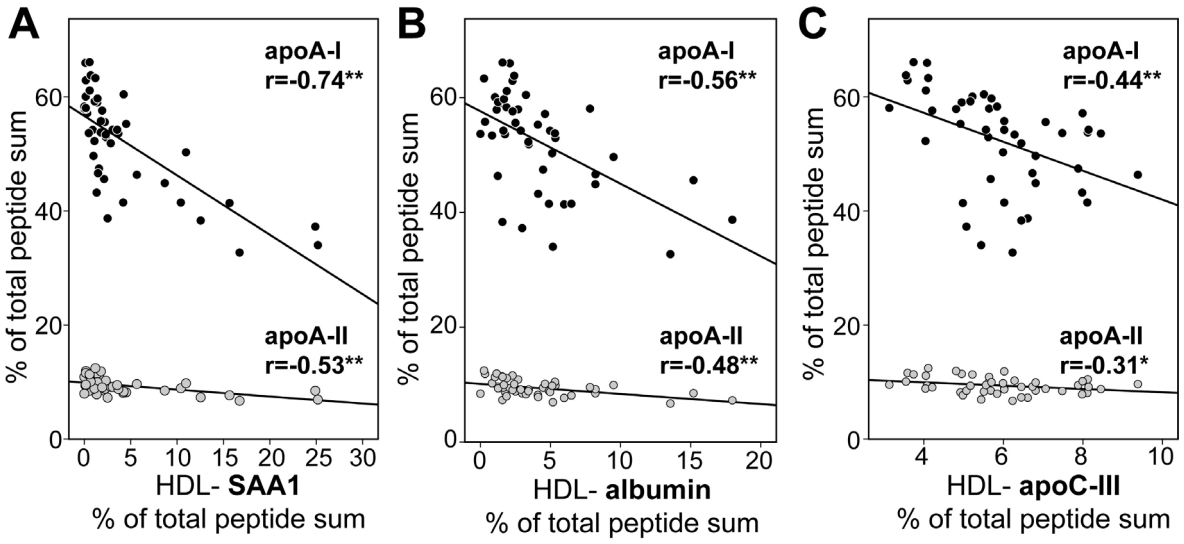

Figure III-5: SAA1, albumin and apoC-III replace the HDL proteins apoA-I and apoA-II. ApoA-I and apoA-II content of HDL from patients and controls was correlated with (A) HDL-SAA1, (B) HDL-albumin and (C) HDL-apoC-III content. The Pearson's correlation coefficients are noted for each plot*; **p<0.01; *p<0.05*

4.6. ApoC-III is linked to a high triglyceride content whereas Lp-PLA2 negatively correlates with HDL-associated phospholipids

Changes in the lipid composition of HDL directly influence the ability of the lipoprotein to bind and retain cholesterol (45,173). Cholesterol efflux was shown to be directly proportional to the amount of phospholipids in reconstituted HDL particles (173). In line with these observations, we found a strong correlation between the phospholipid content of HDL and its cholesterol efflux capability (Figure III-3C). We next assessed whether the Lp-PLA2 content of HDL correlates with the phospholipid content of HDL. HDL Lp-PLA2 mass showed a negative correlation with HDL phospholipids (Figure III-6A) and cholesterol efflux capability (Figure III-6B). Quantification of HDL-associated Lp-PLA2 activity revealed a

strong correlation with HDL-Lp-PLA2 mass (Figure III-6C). We also measured lyso-phospholipid content of HDL and observed that Lp-PLA2 activity significantly correlates with lyso-phospholipid content of HDL, indicating that Lp-PLA2 hydrolyses phospholipids in HDL (Figure III-6D). The levels of apoC-III, a known inhibitor of lipoprotein lipase and an important regulator of triglyceride metabolism (174) were reported to be altered in renal disease (175). In good agreement, we observed an increased apoC-III and triglyceride content in uremic HDL (Table III-2) correlating with each other (Figure III-6E). Therefore, the known risk factors apoC-III and Lp-PLA2 may be directly involved in rendering HDL dysfunctional.

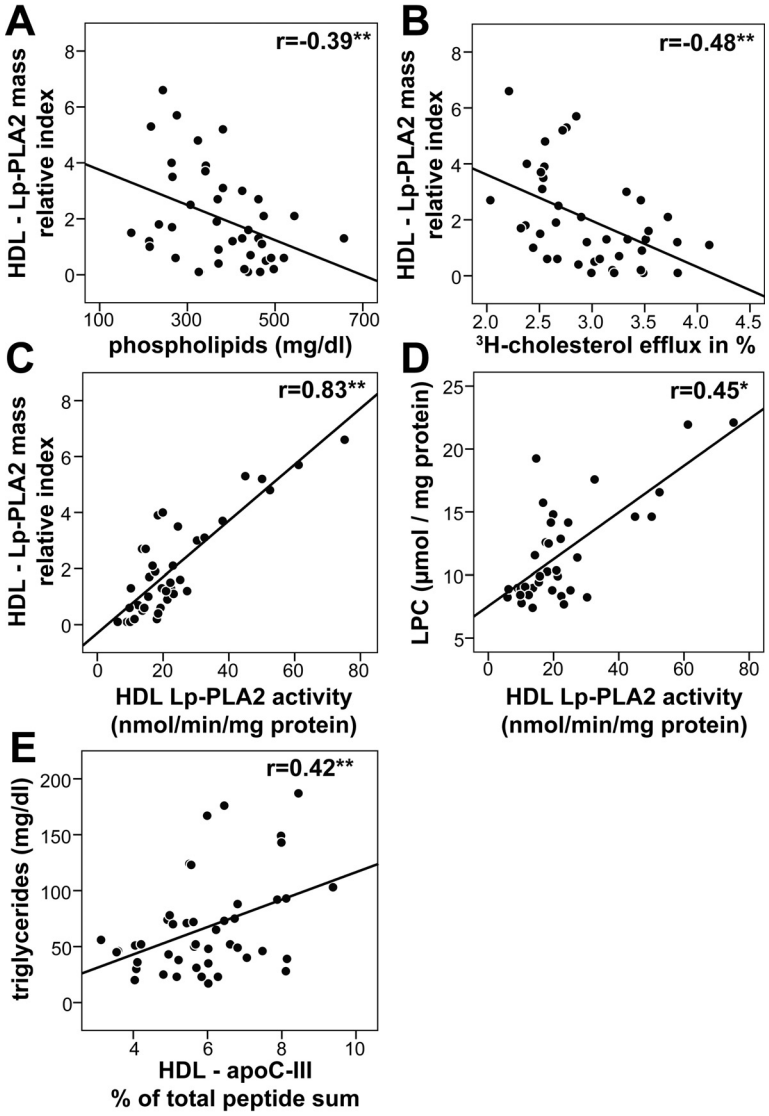

Figure III-6: Lp-PLA2 content of HDL negatively correlates with HDL-phospholipids and cholesterol efflux capability. (A) Negative correlation between the HDL – Lp-PLA2 mass and HDL-phospholipids. (B) Negative correlation between HDL-Lp-PLA2 mass and HDL mediated [3H]-cholesterol-efflux capability. (C) Strong positive correlation between HDL-Lp-PLA2 mass and HDL-Lp-PLA2 activity. (D) Positive correlation of HDL-Lp-PLA2 activity and lyso-PC content of HDL. (E) Positive correlation of HDL-apoC-III with HDL-triglycerides. The Pearson's correlation coefficients are noted for each plot*; *p<0.05, **p<0.01*.

4.7. Loss of HDL associated phospholipids impair cholesterol efflux capacity

Next, we tested whether reducing phospholipids to levels observed in uremic HDL reduce cholesterol efflux capacity. Phospholipase treatment effectively reduced the phospholipid content of HDL (Figure III-7A) paralleled by an increased lyso-phospholipid content (Figure III-7B). To assess the impact of lyso-phospholipid on cholesterol efflux capacity, control HDL was enriched with lyso-phospholipid (Figure III-7C). Importantly, phospholipase mediated hydrolysis of phospholipids reduced cholesterol efflux capacity whereas lyso-phospholipid enrichment did not (Figure III-7C).

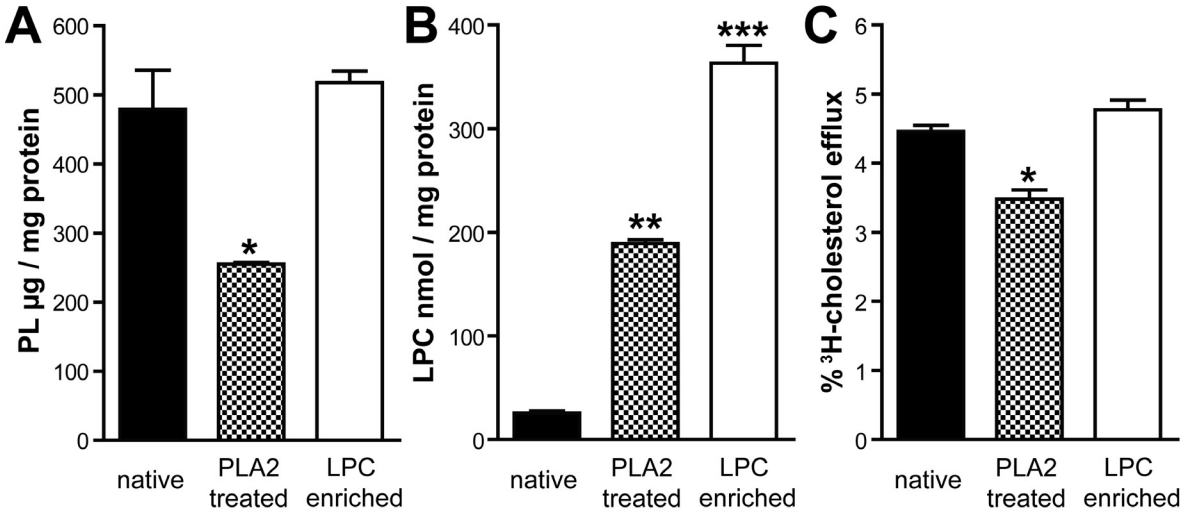

Figure III-7: PLA2 induced reduction of HDL-mediated cholesterol efflux is caused by reduced phospholipids. Native HDL, PLA2 treated HDL, and lyso-PC-enriched HDL were analyzed for their (A) phospholipid content, (B) lyso-PC content and (C) [^{3}H]-cholesterol efflux capability. Statistical analysis was performed by ANOVA. Significances were accepted at the level of **p<0.05, **p<0.01, ***p<0.001*

The current study provides evidence that HDL of patients suffering from renal disease carries a unique proteome and lipid composition linked to an impaired cholesterol efflux capacity (Figure III-8). Our findings raise the possibility that dysfunctional HDL contributes to accelerated atherosclerosis in end-stage renal patients. We applied LC-MS/MS and immunoblot technique, lipid analysis to determine alterations of the HDL proteome and lipid composition in end stage renal disease patients on regular hemodialysis. Several proteins, including high-abundant proteins like SAA1, albumin, apoC-III and low-abundant proteins like antitrypsin, apoA-VI, RBP4, transthyretin and Lp-PLA2 were identified to be

significantly enriched in uremic HDL (Table III-2). The SAA1 and albumin content of uremic HDL was 8- and 3 fold increased, making them major HDL-associated proteins. Notably, SAA1 accumulation correlated with the plasma inflammatory markers CRP and fibrinogen whereas albumin, apoC-III and Lp-PLA2 did not (Table III-5). Moreover, HDL associated apoC-III significantly correlated with plasma creatinine, but not SAA1, albumin or Lp-PLA2 suggesting that different mechanisms mediate their association to HDL (Table III-5). However, further data analysis revealed a strong positive correlation between HDL-associated albumin and apoA-VI, antitrypsin, transthyretin and RBP4 (Table III-6). These data indicate that similar mechanisms trigger HDL enrichment with these proteins or that albumin itself carries proteins onto HDL. In line with that finding, a recent study observed that plasma albumin binds several plasma proteins including apoA-VI, antitrypsin and RBP4 (168).

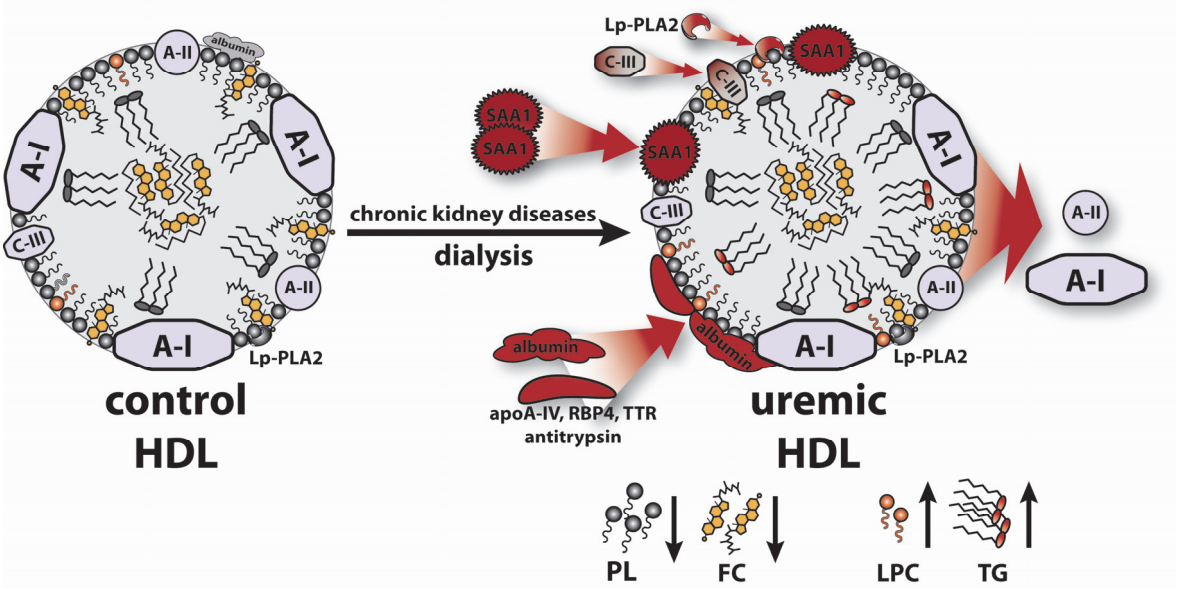

Figure III-8: Schematic illustration of HDL remodeling in uremic patients. HDL from uremic hemodialysis patient's exhibit significant changes in proteome and lipid composition linked to impaired cholesterol acceptor capability. Proteomic analysis revealed increased levels of SAA1, albumin, apoC-III as well as increased levels of the low-abundant HDL-associated proteins apoA-IV, RBP4, transthyretin (TTR), antitrypsin and Lp-PLA2 in uremic HDL. These proteomic alterations were accompanied by the loss of apoA-I and apoA-II. In addition, uremia and dialysis lead to profound alterations in HDL-lipid composition reflected as a decrease in phospholipids (PL) and free cholesterol (FC) and in an increase in triglyceride (TG) and lyso-PC (LPC) content

5. Discussion:

A major finding of the present study is that the enrichment of HDL with SAA1, albumin, apoC-III and Lp-PLA2 correlated with altered metabolic properties of HDL. We observed that the reduced cellular cholesterol efflux capability of uremic HDL is linked to a depletion of HDL-associated apoA-I, apoA-II and phopholipids (Figure III-3), all factors known to increase cholesterol acceptor capability of HDL (45). The shedding of predominantly apoA-I is not surprising as apoA-I is the least lipophilic of the HDL apolipoproteins. Our data indicate that in addition to SAA1, which is known to displace apoA-I from HDL (171,172), albumin and apoC-III are capable to replace apolipoproteins on HDL. The substitution of apoA-I and apoA-II negatively correlated with the phospholipid content of HDL, in agreement with the high phospholipid binding capacity of apoA-I and apoA-II. We conclude that the reduced phospholipid content of uremic HDL mainly contributes to the low cholesterol efflux capacity, since phospholipase treatment of control HDL (resulting in a HDL-phospholipid content similar to uremic HDL) decreased efflux capacity to about the same extend as observed with uremic HDL (Figure III-7). In line with our observation, it was recently demonstrated that alterations in phospholipid content, and not the presence of SAA in human HDL, impaired the ability of acute phase HDL to promote cholesterol efflux (176). In plasma, HDL undergoes a series of changes that are mediated by CETP and PLTP. CETP mediates the exchange of HDL associated cholesteryl esters with triglycerides from apoB-containing lipoproteins, while PLTP transfers phospholipids and free cholesterol from triglyceride rich lipoproteins to HDL. However, most studies have shown no significant change in plasma CETP or PLTP concentrations or activities in patients with end-stage renal disease on hemodialysis (159), ruling out a major impact of these enzymes on lipid alterations observed in uremic HDL.

A recent study demonstrated that chronic kidney disease patients of stages 3 and 4 are characterized by an increase in plasma Lp-PLA2 activity (177). A novel finding in our present study was that Lp-PLA2, a novel risk factor that is involved in the development of atherosclerosis, was 2.8-fold increased in uremic HDL (Table III-4B). Interestingly, Lp-PLA2 content of HDL negatively correlated with phospholipid levels of HDL, indicating that Lp-PLA2 might hydrolyze (oxidized) phospholipids in HDL (Figure III-6A). In line with that observation, we found that

HDL associated Lp-PLA2 activity and lyso-PC content significantly correlated with HDL associated Lp-PLA2 mass (Figure III-6C, D). In the circulation, Lp-PLA2 normally resides on LDL, but about 20% is associated with HDL (178). It has to be noted that HDL isolation methods based on prolonged ultracentrifugation may result in the dissociation and re-distribution of Lp-PLA2 among lipoproteins. In particular, Lp-PLA2 associated with small dense LDL appears to shift by ultracentrifugation (179). We isolated HDL in a one step rapid ultracentrifugation protocol and did not detect apoB-100 (major apolipoprotein of LDL) (Table III-4A). Therefore, we can exclude a major contribution of small, dense LDL associated Lp-PLA2 in our HDL fraction. A recent meta-analysis reported that Lp-PLA2 levels are positively correlated with an increased risk of developing coronary heart disease and stroke (138) and therefore therapies targeting Lp-PLA2 in plasma and atherosclerotic plaque are now being developed. The observed increased content of Lp-PLA2 in uremic HDL raises the possibility that HDL-associated Lp-PLA2 might also contribute to increased atherosclerosis in renal patients.

A further notable finding in the current study was that increased apoC-III content of uremic HDL was coupled to an increased content of HDL associated triglycerides (Figure III-6E), which correlated with plasma creatinine levels. This indicates that apoC-III metabolism is altered in renal disease. Most importantly, both HDL associated apoC-III and triglyceride content correlated negatively with cholesterol efflux potential of HDL. ApoC-III is a small apolipoprotein that is synthesized mainly in the liver and circulates in plasma in association with apoB containing lipoproteins and HDL. ApoC-III inhibits lipoprotein lipase and hepatic lipase and is thought to inhibit hepatic uptake of triglyceride-rich particles as well (180). In case-control studies, plasma concentrations of apoC-III containing lipoproteins were reported to be strong independent risk factors for cardiovascular disease (181). Moreover, recent experimental studies have also shown that apoC-III may be a crucial link between renal dyslipidemia and increased atherosclerosis (182).

Recent advances in proteomic analysis due to use of high-throughput and high-content analysis has paved the way for clinical proteomics. The proteomic alterations in uremic HDL identified in our present study could therefore provide the basis for the assessment of (i) HDL functionality and (ii) identify humans at increased risk of cardiovascular disease. In summary, we here report that renal disease impairs the cholesterol acceptor potential of HDL. The functional

impairment is linked to a unique protein cargo in uremic HDL accompanied by a decreased phospholipid and increased triglyceride content (Figure III-8).

IV. Chapter:

References

(1) Nicholls SJ, Zheng L, Hazen SL. Formation of dysfunctional high-density lipoprotein by myeloperoxidase. Trends Cardiovasc Med 2005 08;15(1050-1738; 1050-1738; 6):212-219.

(2) Navab M, Reddy ST, Van Lenten BJ, Anantharamaiah GM, Fogelman AM. The role of dysfunctional HDL in atherosclerosis. J Lipid Res 2009 04;50 Suppl(0022-2275):S145-S149.

(3) Smith JD. Dysfunctional HDL as a diagnostic and therapeutic target. Arterioscler Thromb Vasc Biol 2010 Feb;30(2):151-155.

(4) WHO 2011. Cardiovascular diseases (Factsheet N° 317). 2011; Available at: http://www.who.int/mediacentre/factsheets/fs317/en/index.html.

(5) Murray CJ, Lopez AD. Global mortality, disability, and the contribution of risk factors: Global Burden of Disease Study. The Lancet 1997 5/17;349(9063):1436-1442.

(6) Leal J, Luengo-Fernández R, Gray A, Petersen S, Rayner M. Economic burden of cardiovascular diseases in the enlarged European Union. European Heart Journal 2006 July 01;27(13):1610-1619.

(7) Libby P. Vascular biology of atherosclerosis: overview and state of the art. Am J Cardiol 2003 Feb 6;91(3A):3A-6A.

(8) Stary HC, Chandler AB, Dinsmore RE, Fuster V, Glagov S, Insull W, et al. A Definition of Advanced Types of Atherosclerotic Lesions and a Histological Classification of Atherosclerosis : A Report From the Committee on Vascular Lesions of the Council on Arteriosclerosis, American Heart Association. Circulation 1995 September 01;92(5):1355-1374.

(9) Stary H, Chandler A, Glagov S, Guyton J, Insull W, Rosenfeld M, et al. A definition of initial, fatty streak, and intermediate lesions of atherosclerosis. A report from the Committee on Vascular Lesions of the Council on Arteriosclerosis, American Heart Association. Circulation 1994 May 01;89(5):2462-2478.

(10) Munro JM, Cotran RS. The pathogenesis of atherosclerosis: atherogenesis and inflammation. Lab Invest 1988 Mar;58(3):249-261.

(11) Dai GH, Kaazempur-Mofrad MR, Natarajan S, Zhang YZ, Vaughn S, Blackman BR, et al. Distinct endothelial phenotypes evoked by arterial waveforms derived from atherosclerosis-susceptible and -resistant regions of human vasculature. Proc Natl Acad Sci U S A 2004 OCT 12 2004;101(41):14871-14876.

(12) Skalen K, Gustafsson M, Rydberg EK, Hulten LM, Wiklund O, Innerarity TL, et al. Subendothelial retention of atherogenic lipoproteins in early atherosclerosis. Nature 2002 Jun 13;417(6890):750-754.

(13) Boren J, Gustafsson M, Skalen K, Flood C, Innerarity TL. Role of extracellular retention of low density lipoproteins in atherosclerosis. Curr Opin Lipidol 2000 Oct;11(5):451-456.

(14) Lutters BCH, Leeuwenburgh MA, Appeldoorn CCM, Molenaar TJM, Van Berkel TJC, Biessen EAL. Blocking endothelial adhesion molecules: a potential therapeutic strategy to combat atherogenesis. Curr Opin Lipidol 2004 OCT 2004;15(5):545-552.

(15) Libby P, Ridker PM, Hansson GK. Progress and challenges in translating the biology of atherosclerosis. Nature 2011 May 19;473(7347):317-325.

(16) Paulson KE, Zhu SN, Chen M, Nurmohamed S, Jongstra-Bilen J, Cybulsky MI. Resident intimal dendritic cells accumulate lipid and contribute to the initiation of atherosclerosis. Circ Res 2010 Feb 5;106(2):383-390.

(17) Johnson JL, Newby AC. Macrophage heterogeneity in atherosclerotic plaques. Curr Opin Lipidol 2009 Oct;20(5):370-378.

(18) Becker S, Warren M, Haskill S. Colony-stimulating factor-induced monocyte survival and differentiation into macrophages in serum-free cultures. The Journal of Immunology 1987 December 01;139(11):3703-3709.

(19) de Villiers WJS, Smart EJ. Macrophage scavenger receptors and foam cell formation. J Leukoc Biol 1999 NOV 1999;66(5):740-746.

(20) Moore KJ, Freeman MW. Scavenger receptors in atherosclerosis: Beyond lipid uptake. Arteriosclerosis Thrombosis and Vascular Biology 2006 AUG 2006;26(8):1702-1711.

(21) Feng B, Yao PM, Li Y, Devlin CM, Zhang D, Harding HP, et al. The endoplasmic reticulum is the site of cholesterol-induced cytotoxicity in macrophages. Nat Cell Biol 2003 Sep;5(9):781-792.

(22) Tabas I. Macrophage death and defective inflammation resolution in atherosclerosis. Nat Rev Immunol 2010 Jan;10(1):36-46.

(23) Gordon T, Castelli WP, Hjortland MC, Kannel WB, Dawber TR. High density lipoprotein as a protective factor against coronary heart disease. The Framingham Study. Am J Med 1977 05;62(0002-9343; 0002-9343; 5):707-714.

(24) Sever PS, Dahlof B, Poulter NR, Wedel H, Beevers G, Caulfield M, et al. Prevention of coronary and stroke events with atorvastatin in hypertensive patients who have average or lower-than-average cholesterol concentrations, in the Anglo-Scandinavian Cardiac Outcomes Trial--Lipid Lowering Arm (ASCOT-LLA): a multicentre randomised controlled trial. Drugs 2004;64 Suppl 2(0012-6667; 0012-6667):43-60.

(25) Ridker PM, Danielson E, Fonseca FA, Genest J, Gotto AM,Jr., Kastelein JJ, et al. Rosuvastatin to prevent vascular events in men and women with elevated C-reactive protein. N Engl J Med 2008 11/20;359(1533-4406; 0028-4793; 21):2195-2207.

(26) Baigent C, Keech A, Kearney PM, Blackwell L, Buck G, Pollicino C, et al. Efficacy and safety of cholesterol-lowering treatment: prospective meta-analysis of data from 90,056 participants in 14 randomised trials of statins. Lancet 2005 10/08;366(1474-547; 0140-6736; 9493):1267-1278.

(27) Feig JE, Rong JX, Shamir R, Sanson M, Vengrenyuk Y, Liu J, et al. HDL promotes rapid atherosclerosis regression in mice and alters inflammatory properties of plaque monocyte-derived cells. Proc Natl Acad Sci U S A 2011 Apr 26;108(17):7166-7171.

(28) Vergeer M, Holleboom AG, Kastelein JJP, Kuivenhoven JA. The HDL hypothesis: does high-density lipoprotein protect from atherosclerosis? Journal of Lipid Research 2010 August 01;51(8):2058-2073.

(29) Johnsen SH, Mathiesen EB, Fosse E, Joakimsen O, Stensland-Bugge E, Njolstad I, et al. Elevated high-density lipoprotein cholesterol levels are protective against plaque progression: a follow-up study of 1952 persons with carotid atherosclerosis the Tromso study. Circulation 2005 Jul 26;112(4):498-504.

(30) Nissen SE, Tardif JC, Nicholls SJ, Revkin JH, Shear CL, Duggan WT, et al. Effect of torcetrapib on the progression of coronary atherosclerosis. N Engl J Med 2007 Mar 29;356(13):1304-1316.

(31) Barter PJ, Caulfield M, Eriksson M, Grundy SM, Kastelein JJ, Komajda M, et al. Effects of torcetrapib in patients at high risk for coronary events. N Engl J Med 2007 Nov 22;357(21):2109-2122.

(32) Yvan-Charvet L, Kling J, Pagler T, Li H, Hubbard B, Fisher T, et al. Cholesterol efflux potential and antiinflammatory properties of high-density lipoprotein after treatment with niacin or anacetrapib. Arterioscler Thromb Vasc Biol 2010 Jul;30(7):1430-1438.

(33) Cannon CP, Shah S, Dansky HM, Davidson M, Brinton EA, Gotto AM, et al. Safety of Anacetrapib in Patients with or at High Risk for Coronary Heart Disease. N Engl J Med 2010 12/16;363(25):2406-2415.

(34) Stein EA, Roth EM, Rhyne JM, Burgess T, Kallend D, Robinson JG. Safety and tolerability of dalcetrapib (RO4607381/JTT-705): results from a 48-week trial. European Heart Journal 2010 February 01;31(4):480-488.

(35) Schwartz GG, Olsson AG, Ballantyne CM, Barter PJ, Holme IM, Kallend D, et al. Rationale and design of the dal-OUTCOMES trial: efficacy and safety of dalcetrapib in patients with recent acute coronary syndrome. Am Heart J 2009 Dec;158(6):896-901.e3.

(36) Asztalos BF, Collins D, Cupples LA, Demissie S, Horvath KV, Bloomfield HE, et al. Value of high-density lipoprotein (HDL) subpopulations in predicting recurrent cardiovascular events in the Veterans Affairs HDL Intervention Trial. Arterioscler Thromb Vasc Biol 2005 Oct;25(10):2185-2191.

(37) Asztalos BF, Cupples LA, Demissie S, Horvath KV, Cox CE, Batista MC, et al. High-density lipoprotein subpopulation profile and coronary heart disease prevalence in male participants of the Framingham Offspring Study. Arterioscler Thromb Vasc Biol 2004 Nov;24(11):2181-2187.

(38) Briel M, Ferreira-Gonzalez I, You JJ, Karanicolas PJ, Akl EA, Wu P, et al. Association between change in high density lipoprotein cholesterol and cardiovascular disease morbidity and mortality: systematic review and meta-regression analysis. BMJ 2009 Feb 16;338:b92.

(39) Roma P, Gregg RE, Meng MS, Ronan R, Zech LA, Franceschini G, et al. In vivo metabolism of a mutant form of apolipoprotein A-I, apo A-IMilano, associated with familial hypoalphalipoproteinemia. J Clin Invest 1993 Apr;91(4):1445-1452.

(40) Frikke-Schmidt R, Nordestgaard BG, Stene MC, Sethi AA, Remaley AT, Schnohr P, et al. Association of loss-of-function mutations in the ABCA1 gene with high-density lipoprotein cholesterol levels and risk of ischemic heart disease. JAMA 2008 Jun 4;299(21):2524-2532.

(41) Khera AV, Cuchel M, de la Llera-Moya M, Rodrigues A, Burke MF, Jafri K, et al. Cholesterol efflux capacity, high-density lipoprotein function, and atherosclerosis. N Engl J Med 2011 Jan 13;364(2):127-135.

(42) Wilson MD, Rudel LL. Review of cholesterol absorption with emphasis on dietary and biliary cholesterol. J Lipid Res 1994 Jun;35(6):943-955.

(43) Lu K, Lee MH, Patel SB. Dietary cholesterol absorption; more than just bile. Trends Endocrinol Metab 2001 Sep;12(7):314-320.

(44) Hegele RA. Plasma lipoproteins: genetic influences and clinical implications. Nat Rev Genet 2009 Feb;10(2):109-121.

(45) Rothblat GH, Phillips MC. High-density lipoprotein heterogeneity and function in reverse cholesterol transport. Curr Opin Lipidol 2010 JUN 2010;21(3):229-238.

(46) Vaisar T, Pennathur S, Green PS, Gharib SA, Hoofnagle AN, Cheung MC, et al. Shotgun proteomics implicates protease inhibition and complement activation in the antiinflammatory properties of HDL. J Clin Invest 2007 03;117(0021-9738; 0021-9738; 3):746-756.

(47) Rezaee F, Casetta B, Levels JH, Speijer D, Meijers JC. Proteomic analysis of high-density lipoprotein. Proteomics 2006 01;6(1615-9853; 1615-9853; 2):721-730.

(48) Karlsson H, Leanderson P, Tagesson C, Lindahl M. Lipoproteomics II: mapping of proteins in high-density lipoprotein using two-dimensional gel electrophoresis and mass spectrometry. Proteomics 2005 04;5(1615-9853; 1615-9853; 5):1431-1445.

(49) Rosenson RS, Brewer HB,Jr, Chapman MJ, Fazio S, Hussain MM, Kontush A, et al. HDL measures, particle heterogeneity, proposed nomenclature, and relation to atherosclerotic cardiovascular events. Clin Chem 2011 Mar;57(3):392-410.

(50) Kontush A, Chapman MJ. Antiatherogenic function of HDL particle subpopulations: focus on antioxidative activities. Curr Opin Lipidol 2010 Aug;21(4):312-318.

(51) Camont L, Chapman MJ, Kontush A. Biological activities of HDL subpopulations and their relevance to cardiovascular disease. Trends Mol Med 2011 Aug 10.

(52) Glomset JA. The plasma lecithins:cholesterol acyltransferase reaction. J Lipid Res 1968 Mar;9(2):155-167.

(53) Sankaranarayanan S, Oram JF, Asztalos BF, Vaughan AM, Lund-Katz S, Adorni MP, et al. Effects of acceptor composition and mechanism of ABCG1-

mediated cellular free cholesterol efflux. J Lipid Res 2009 02;50(0022-2275; 0022-2275; 2):275-284.

(54) de la Llera-Moya M, Rothblat GH, Connelly MA, Kellner-Weibel G, Sakr SW, Phillips MC, et al. Scavenger receptor BI (SR-BI) mediates free cholesterol flux independently of HDL tethering to the cell surface. J Lipid Res 1999 Mar;40(3):575-580.

(55) Acton S, Rigotti A, Landschulz KT, Xu S, Hobbs HH, Krieger M. Identification of scavenger receptor SR-BI as a high density lipoprotein receptor. Science 1996 01/26;271(0036-8075; 0036-8075; 5248):518-520.

(56) Chinetti G, Gbaguidi FG, Griglio S, Mallat Z, Antonucci M, Poulain P, et al. CLA-1/SR-BI is expressed in atherosclerotic lesion macrophages and regulated by activators of peroxisome proliferator-activated receptors. Circulation 2000 05/23;101(1524-4539; 0009-7322; 20):2411-2417.

(57) Hirano K, Yamashita S, Nakagawa Y, Ohya T, Matsuura F, Tsukamoto K, et al. Expression of human scavenger receptor class B type I in cultured human monocyte-derived macrophages and atherosclerotic lesions. Circ Res 1999 07/09;85(1524-4571; 0009-7330; 1):108-116.

(58) Rye KA, Bursill CA, Lambert G, Tabet F, Barter PJ. The metabolism and anti-atherogenic properties of HDL. J Lipid Res 2009 Apr;50 Suppl:S195-200.

(59) Kee P, Caiazza D, Rye KA, Barrett PH, Morehouse LA, Barter PJ. Effect of inhibiting cholesteryl ester transfer protein on the kinetics of high-density lipoprotein cholesteryl ester transport in plasma: in vivo studies in rabbits. Arterioscler Thromb Vasc Biol 2006 Apr;26(4):884-890.

(60) Yasuda T, Ishida T, Rader DJ. Update on the Role of Endothelial Lipase in High-Density Lipoprotein Metabolism, Reverse Cholesterol Transport, and Atherosclerosis. Circulation Journal 2010 NOV 2010;74(11):2263-2270.

(61) Kathiresan S, Melander O, Anevski D, Guiducci C, Burtt NP, Roos C, et al. Polymorphisms associated with cholesterol and risk of cardiovascular events. N Engl J Med 2008 Mar 20;358(12):1240-1249.

(62) Kathiresan S, Melander O, Guiducci C, Surti A, Burtt NP, Rieder MJ, et al. Six new loci associated with blood low-density lipoprotein cholesterol, high-density lipoprotein cholesterol or triglycerides in humans. Nat Genet 2008 Feb;40(2):189-197.

(63) Willer CJ, Sanna S, Jackson AU, Scuteri A, Bonnycastle LL, Clarke R, et al. Newly identified loci that influence lipid concentrations and risk of coronary artery disease. Nat Genet 2008 Feb;40(2):161-169.

(64) Temel RE, Brown JM. A new framework for reverse cholesterol transport: non-biliary contributions to reverse cholesterol transport. World J Gastroenterol 2010 Dec 21;16(47):5946-5952.

(65) Temel RE, Sawyer JK, Yu L, Lord C, Degirolamo C, McDaniel A, et al. Biliary sterol secretion is not required for macrophage reverse cholesterol transport. Cell Metab 2010 Jul 4;12(1):96-102.

(66) Feig JE, Shamir R, Fisher EA. Atheroprotective effects of HDL: Beyond reverse cholesterol transport. Curr Drug Targets 2008 MAR 2008;9(3):196-203.

(67) Assmann G, Nofer JR. Atheroprotective effects of high-density lipoproteins. Annu Rev Med 2003;54:321-341.

(68) Rye K, Bursill CA, Lambert G, Tabet F, Barter PJ. The metabolism and anti-atherogenic properties of HDL. J Lipid Res 2009 APR 2009;50:S195-S200.

(69) Parthasarathy S, Barnett J, Fong LG. High-density lipoprotein inhibits the oxidative modification of low-density lipoprotein. Biochimica et Biophysica Acta (BBA) - Lipids and Lipid Metabolism 1990 5/22;1044(2):275-283.

(70) Bowry VW, Stanley KK, Stocker R. High density lipoprotein is the major carrier of lipid hydroperoxides in human blood plasma from fasting donors. Proc Natl Acad Sci U S A 1992 11/01;89(0027-8424; 0027-8424; 21):10316-10320.

(71) Sattler W, Stocker R. Greater selective uptake by Hep G2 cells of high-density lipoprotein cholesteryl ester hydroperoxides than of unoxidized cholesteryl esters. Biochem J 1993 Sep 15;294 (Pt 3)(Pt 3):771-778.

(72) Goyal J, Wang K, Liu M, Subbaiah PV. Novel function of lecithin-cholesterol acyltransferase. Hydrolysis of oxidized polar phospholipids generated during lipoprotein oxidation. J Biol Chem 1997 Jun 27;272(26):16231-16239.

(73) Kriska T, Marathe GK, Schmidt JC, McIntyre TM, Girotti AW. Phospholipase action of platelet-activating factor acetylhydrolase, but not paraoxonase-1, on long fatty acyl chain phospholipid hydroperoxides. J Biol Chem 2007 Jan 5;282(1):100-108.

(74) Watson AD, Berliner JA, Hama SY, La Du BN, Faull KF, Fogelman AM, et al. Protective effect of high density lipoprotein associated paraoxonase. Inhibition of the biological activity of minimally oxidized low density lipoprotein. J Clin Invest 1995 Dec;96(6):2882-2891.

(75) Aviram M, Rosenblat M, Bisgaier CL, Newton RS, Primo-Parmo SL, La Du BN. Paraoxonase inhibits high-density lipoprotein oxidation and preserves its functions. A possible peroxidative role for paraoxonase. J Clin Invest 1998 Apr 15;101(8):1581-1590.

(76) Garner B, Waldeck AR, Witting PK, Rye KA, Stocker P. Oxidation of high density lipoproteins - II. Evidence for direct reduction of lipid hydroperoxides by methionine residues of apolipoproteins AI and AII. J Biol Chem 1998 MAR 13 1998;273(11):6088-6095.

(77) Barter PJ, Nicholls S, Rye KA, Anantharamaiah GM, Navab M, Fogelman AM. Antiinflammatory properties of HDL. Circ Res 2004 10/15;95(1524-4571; 8):764-772.

(78) Cockerill GW, Rye KA, Gamble JR, Vadas MA, Barter PJ. High-density lipoproteins inhibit cytokine-induced expression of endothelial cell adhesion molecules. Arterioscler Thromb Vasc Biol 1995 Nov;15(11):1987-1994.

(79) Calabresi L, Franceschini G, Sirtori CR, De Palma A, Saresella M, Ferrante P, et al. Inhibition of VCAM-1 expression in endothelial cells by reconstituted high density lipoproteins. Biochem Biophys Res Commun 1997 Sep 8;238(1):61-65.

(80) Zhang WJ, Stocker R, McCall MR, Forte TM, Frei B. Lack of inhibitory effect of HDL on TNFalpha-induced adhesion molecule expression in human aortic endothelial cells. Atherosclerosis 2002 Dec;165(2):241-249.

(81) Patel S, Di Bartolo BA, Nakhla S, Heather AK, Mitchell TW, Jessup W, et al. Anti-inflammatory effects of apolipoprotein A-I in the rabbit. Atherosclerosis 2010 Oct;212(2):392-397.

(82) Bursill CA, Castro ML, Beattie DT, Nakhla S, van der Vorst E, Heather AK, et al. High-density lipoproteins suppress chemokines and chemokine receptors in vitro and in vivo. Arterioscler Thromb Vasc Biol 2010 Sep;30(9):1773-1778.

(83) Van Lenten BJ, Wagner AC, Nayak DP, Hama S, Navab M, Fogelman AM. High-density lipoprotein loses its anti-inflammatory properties during acute influenza a infection. Circulation 2001 05/08;103(1524-4539; 0009-7322; 18):2283-2288.

(84) Van Lenten BJ, Hama SY, de Beer FC, Stafforini DM, McIntyre TM, Prescott SM, et al. Anti-inflammatory HDL becomes pro-inflammatory during the acute phase response. Loss of protective effect of HDL against LDL oxidation in aortic wall cell cocultures. J Clin Invest 1995 Dec;96(6):2758-2767.

(85) van der Westhuyzen DR, de Beer FC, Webb NR. HDL cholesterol transport during inflammation. Curr Opin Lipidol 2007 Apr;18(2):147-151.

(86) Ansell BJ, Navab M, Hama S, Kamranpour N, Fonarow G, Hough G, et al. Inflammatory/antiinflammatory properties of high-density lipoprotein distinguish patients from control subjects better than high-density lipoprotein cholesterol levels and are favorably affected by simvastatin treatment. Circulation 2003 12/02;108(1524-4539; 0009-7322; 22):2751-2756.

(87) Navab M, Hama SY, Hough GP, Subbanagounder G, Reddy ST, Fogelman AM. A cell-free assay for detecting HDL that is dysfunctional in preventing the formation of or inactivating oxidized phospholipids. J Lipid Res 2001 Aug;42(8):1308-1317.

(88) Vaisar T, Mayer P, Nilsson E, Zhao XQ, Knopp R, Prazen BJ. HDL in humans with cardiovascular disease exhibits a proteomic signature. Clin Chim Acta 2010 07/04;411(1873-3492; 0009-8981; 13-14):972-979.

(89) Green PS, Vaisar T, Pennathur S, Kulstad JJ, Moore AB, Marcovina S, et al. Combined statin and niacin therapy remodels the high-density lipoprotein proteome. Circulation 2008 09/16;118(1524-4539; 1524-4539; 12):1259-1267.

(90) Moradi H, Pahl MV, Elahimehr R, Vaziri ND. Impaired antioxidant activity of high-density lipoprotein in chronic kidney disease. Transl Res 2009 02;153(1931-5244; 2):77-85.

(91) Bhattacharyya T, Nicholls SJ, Topol EJ, Zhang R, Yang X, Schmitt D, et al. Relationship of paraoxonase 1 (PON1) gene polymorphisms and functional activity with systemic oxidative stress and cardiovascular risk. JAMA 2008 Mar 19;299(11):1265-1276.

(92) Klebanoff SJ. Oxygen metabolism and the toxic properties of phagocytes. Ann Intern Med 1980 Sep;93(3):480-489.

(93) Klebanoff SJ. Myeloperoxidase: friend and foe. J Leukoc Biol 2005 05;77(0741-5400; 0741-5400; 5):598-625.

(94) Hazen SL, Heinecke JW. 3-Chlorotyrosine, a specific marker of myeloperoxidase-catalyzed oxidation, is markedly elevated in low density lipoprotein isolated from human atherosclerotic intima. J Clin Invest 1997 05/01;99(0021-9738; 0021-9738; 9):2075-2081.

(95) Daugherty A, Dunn JL, Rateri DL, Heinecke JW. Myeloperoxidase, a catalyst for lipoprotein oxidation, is expressed in human atherosclerotic lesions. J Clin Invest 1994 Jul;94(1):437-444.

(96) Marsche G, Hammer A, Oskolkova O, Kozarsky KF, Sattler W, Malle E. Hypochlorite-modified high density lipoprotein, a high affinity ligand to scavenger receptor class B, type I, impairs high density lipoprotein-dependent selective lipid uptake and reverse cholesterol transport. J Biol Chem 2002 08/30;277(0021-9258; 0021-9258; 35):32172-32179.

(97) Zheng L, Nukuna B, Brennan ML, Sun M, Goormastic M, Settle M, et al. Apolipoprotein A-I is a selective target for myeloperoxidase-catalyzed oxidation and functional impairment in subjects with cardiovascular disease. J Clin Invest 2004 08;114(0021-9738; 0021-9738; 4):529-541.

(98) Bergt C, Pennathur S, Fu X, Byun J, O'Brien K, McDonald TO, et al. The myeloperoxidase product hypochlorous acid oxidizes HDL in the human artery wall and impairs ABCA1-dependent cholesterol transport. Proc Natl Acad Sci U S A 2004 08/31;101(0027-8424; 0027-8424; 35):13032-13037.

(99) Zheng L, Settle M, Brubaker G, Schmitt D, Hazen SL, Smith JD, et al. Localization of nitration and chlorination sites on apolipoprotein A-I catalyzed by myeloperoxidase in human atheroma and associated oxidative impairment in ABCA1-dependent cholesterol efflux from macrophages. J Biol Chem 2005 01/07;280(0021-9258; 0021-9258; 1):38-47.

(100) van Dalen CJ, Whitehouse MW, Winterbourn CC, Kettle AJ. Thiocyanate and chloride as competing substrates for myeloperoxidase. Biochem J 1997 10/15;327 (Pt 2)(0264-6021; 0264-6021):487-492.

(101) Lane AE, Tan JT, Hawkins CL, Heather AK, Davies MJ. The myeloperoxidase-derived oxidant HOSCN inhibits protein tyrosine phosphatases and modulates cell signalling via the mitogen-activated protein kinase (MAPK) pathway in macrophages. Biochem J 2010 Aug 15;430(1):161-169.

(102) Lloyd MM, van Reyk DM, Davies MJ, Hawkins CL. Hypothiocyanous acid is a more potent inducer of apoptosis and protein thiol depletion in murine macrophage cells than hypochlorous acid or hypobromous acid. Biochem J 2008 Sep 1;414(2):271-280.

(103) Wang Z, Nicholls SJ, Rodriguez ER, Kummu O, Horkko S, Barnard J, et al. Protein carbamylation links inflammation, smoking, uremia and atherogenesis. Nat Med 2007 Oct;13(10):1176-1184.

(104) Uchida K. Role of reactive aldehyde in cardiovascular diseases. Free Radic Biol Med 2000 06/15;28(0891-5849; 0891-5849; 12):1685-1696.

(105) Wang GW, Guo Y, Vondriska TM, Zhang J, Zhang S, Tsai LL, et al. Acrolein consumption exacerbates myocardial ischemic injury and blocks nitric oxide-induced PKCepsilon signaling and cardioprotection. J Mol Cell Cardiol 2008 06;44(1095-8584; 0022-2828; 6):1016-1022.

(106) Kraus LM, Elberger AJ, Handorf CR, Pabst MJ, Kraus AP,Jr. Urea-derived cyanate forms epsilon-amino-carbamoyl-lysine (homocitrulline) in leukocyte proteins in patients with end-stage renal disease on peritoneal dialysis. J Lab Clin Med 1994 06;123(0022-2143; 0022-2143; 6):882-891.

(107) Oimomi M, Nishimoto S, Matsumoto S, Hatanaka H, Ishikawa K, Kawasaki T, et al. Carbamylated plasma protein in renal failure. Nippon Jinzo Gakkai Shi 1986 03;28(0385-2385; 3):269-271.

(108) Apostolov EO, Shah SV, Ok E, Basnakian AG. Quantification of carbamylated LDL in human sera by a new sandwich ELISA. Clin Chem 2005 04;51(0009-9147; 0009-9147; 4):719-728.

(109) Apostolov EO, Ray D, Savenka AV, Shah SV, Basnakian AG. Chronic uremia stimulates LDL carbamylation and atherosclerosis. J Am Soc Nephrol 2010 11;21(1533-3450; 1046-6673; 11):1852-1857.

(110) Marsche G, Furtmuller PG, Obinger C, Sattler W, Malle E. Hypochlorite-modified high-density lipoprotein acts as a sink for myeloperoxidase in vitro. Cardiovasc Res 2008 07/01;79(0008-6363; 0008-6363; 1):187-194.

(111) Sattler W, Mohr D, Stocker R. Rapid isolation of lipoproteins and assessment of their peroxidation by high-performance liquid chromatography

postcolumn chemiluminescence. Methods Enzymol 1994;233(0076-6879; 0076-6879):469-489.

(112) Jonas A. Reconstitution of high-density lipoproteins. Methods Enzymol 1986;128:553-582.

(113) Friedewald WT, Levy RI, Fredrickson DS. Estimation of the concentration of low-density lipoprotein cholesterol in plasma, without use of the preparative ultracentrifuge. Clin Chem 1972 06;18(0009-9147; 0009-9147; 6):499-502.

(114) Matyash V, Liebisch G, Kurzchalia TV, Shevchenko A, Schwudke D. Lipid extraction by methyl-tert-butyl ether for high-throughput lipidomics. J Lipid Res 2008 05;49(0022-2275; 0022-2275; 5):1137-1146.

(115) Marsche G, Frank S, Raynes JG, Kozarsky KF, Sattler W, Malle E. The lipidation status of acute-phase protein serum amyloid A determines cholesterol mobilization via scavenger receptor class B, type I. Biochem J 2007 02/15;402(1470-8728; 0264-6021; 1):117-124.

(116) Wadsack C, Hrzenjak A, Hammer A, Hirschmugl B, Levak-Frank S, Desoye G, et al. Trophoblast-like human choriocarcinoma cells serve as a suitable in vitro model for selective cholesteryl ester uptake from high density lipoproteins. Eur J Biochem 2003 Feb;270(3):451-462.

(117) Marsche G, Frank S, Hrzenjak A, Holzer M, Dirnberger S, Wadsack C, et al. Plasma-advanced oxidation protein products are potent high-density lipoprotein receptor antagonists in vivo. Circ Res 2009 03/27;104(1524-4571; 0009-7330; 6):750-757.

(118) Takahashi Y, Miyata M, Zheng P, Imazato T, Horwitz A, Smith JD. Identification of cAMP analogue inducible genes in RAW264 macrophages. Biochim Biophys Acta 2000 07/24;1492(0006-3002; 2-3):385-394.

(119) Gan KN, Smolen A, Eckerson HW, La Du BN. Purification of human serum paraoxonase/arylesterase. Evidence for one esterase catalyzing both activities. Drug Metabolism and Disposition 1991 January 01;19(1):100-106.

(120) Kontush A, Chantepie S, Chapman MJ. Small, dense HDL particles exert potent protection of atherogenic LDL against oxidative stress. Arterioscler Thromb Vasc Biol 2003 10/01;23(1524-4636; 1079-5642; 10):1881-1888.

(121) Damm M, Holzer M, Radspieler G, Marsche G, Kappe CO. Microwave-assisted high-throughput acid hydrolysis in silicon carbide microtiter platforms-A rapid and low volume sample preparation technique for total amino acid analysis in proteins and peptides. J Chromatogr A 2010 10/21(1873-3778; 0021-9673).

(122) Heinecke JW. The role of myeloperoxidase in HDL oxidation and atherogenesis. Curr Atheroscler Rep 2007 10;9(1523-3804; 1523-3804; 4):249-251.

(123) Svensson PA, Englund MC, Snackestrand MS, Hagg DA, Ohlsson BG, Stemme V, et al. Regulation and splicing of scavenger receptor class B type I in human macrophages and atherosclerotic plaques. BMC Cardiovasc Disord 2005;5(1471-2261; 1471-2261):25.

(124) Fournier N, Paul JL, Atger V, Cogny A, Soni T, Llera-Moya M, et al. HDL phospholipid content and composition as a major factor determining cholesterol efflux capacity from Fu5AH cells to human serum. Arterioscler Thromb Vasc Biol 1997 11;17(1079-5642; 1079-5642; 11):2685-2691.

(125) Papahadjopoulos D, Weiss L. Amino groups at the surfaces of phospholipid vesicles. Biochim Biophys Acta 1969;183(0006-3002; 0006-3002; 3):417-426.

(126) Murao K, Terpstra V, Green SR, Kondratenko N, Steinberg D, Quehenberger O. Characterization of CLA-1, a human homologue of rodent scavenger receptor BI, as a receptor for high density lipoprotein and apoptotic thymocytes. J Biol Chem 1997 07/11;272(0021-9258; 0021-9258; 28):17551-17557.

(127) Liu T, Krieger M, Kan HY, Zannis VI. The effects of mutations in helices 4 and 6 of ApoA-I on scavenger receptor class B type I (SR-BI)-mediated cholesterol efflux suggest that formation of a productive complex between reconstituted high

density lipoprotein and SR-BI is required for efficient lipid transport. J Biol Chem 2002 06/14;277(0021-9258; 0021-9258; 24):21576-21584.

(128) Larrede S, Quinn CM, Jessup W, Frisdal E, Olivier M, Hsieh V, et al. Stimulation of cholesterol efflux by LXR agonists in cholesterol-loaded human macrophages is ABCA1-dependent but ABCG1-independent. Arterioscler Thromb Vasc Biol 2009 11;29(1524-4636; 1524-4636; 11):1930-1936.

(129) Shao B, Pennathur S, Pagani I, Oda MN, Witztum JL, Oram JF, et al. Modifying apolipoprotein A-I by malondialdehyde, but not by an array of other reactive carbonyls, blocks cholesterol efflux by the ABCA1 pathway. J Biol Chem 2010 06/11;285(1083-351; 0021-9258; 24):18473-18484.

(130) Sviridov D, Hoang A, Sawyer WH, Fidge NH. Identification of a sequence of apolipoprotein A-I associated with the activation of lecithin : cholesterol acyltransferase. J Biol Chem 2000 JUN 30 2000;275(26):19707-19712.

(131) Cavigiolio G, Shao B, Geier EG, Ren G, Heinecke JW, Oda MN. The interplay between size, morphology, stability, and functionality of high-density lipoprotein subclasses. Biochemistry (N Y) 2008 APR 22 2008;47(16):4770-4779.

(132) Sorci-Thomas M, Kearns MW, Lee JP. Apolipoprotein A-I domains involved in lecithin-cholesterol acyltransferase activation. Structure:function relationships. Journal of Biological Chemistry 1993 October 05;268(28):21403-21409.

(133) Mackness B, Hunt R, Durrington PN, Mackness MI. Increased immunolocalization of paraoxonase, clusterin, and apolipoprotein A-I in the human artery wall with the progression of atherosclerosis. Arterioscler Thromb Vasc Biol 1997 Jul;17(7):1233-1238.

(134) Besler C, Heinrich K, Rohrer L, Doerries C, Riwanto M, Shih DM, et al. Mechanisms underlying adverse effects of HDL on eNOS-activating pathways in patients with coronary artery disease. J Clin Invest 2011 Jul 1;121(7):2693-2708.

(135) Mackness M, Durrington P, Mackness B. Paraoxonase 1 activity, concentration and genotype in cardiovascular disease. Curr Opin Lipidol 2004 AUG 2004;15(4):399-404.

(136) James RW, Deakin SP. The importance of high-density lipoproteins for paraoxonase-1 secretion, stability, and activity. Free Radical Biology and Medicine 2004 DEC 15 2004;37(12):1986-1994.

(137) Stafforini DM, McIntyre TM, Carter ME, Prescott SM. Human plasma platelet-activating factor acetylhydrolase. Association with lipoprotein particles and role in the degradation of platelet-activating factor. Journal of Biological Chemistry 1987 March 25;262(9):4215-4222.

(138) Thompson A, Gao P, Orfei L, Watson S, Di AE, Kaptoge S, et al. Lipoprotein-associated phospholipase A(2) and risk of coronary disease, stroke, and mortality: collaborative analysis of 32 prospective studies. Lancet 2010 05/01;375(1474-547; 0140-6736; 9725):1536-1544.

(139) Bell JD, Lee JA, Lee HA, Sadler PJ, Wilkie DR, Woodham RH. Nuclear-Magnetic-Resonance Studies of Blood-Plasma and Urine from Subjects with Chronic-Renal-Failure - Identification of Trimethylamine-N-Oxide. Biochim Biophys Acta 1991 FEB 22 1991;1096(2):101-107.

(140) Krieger M. Scavenger receptor class B type I is a multiligand HDL receptor that influences diverse physiologic systems. J Clin Invest 2001 09;108(0021-9738; 0021-9738; 6):793-797.

(141) Van EM, Bos IS, Hildebrand RB, Van Rij BT, Van Berkel TJ. Dual role for scavenger receptor class B, type I on bone marrow-derived cells in atherosclerotic lesion development. Am J Pathol 2004 09;165(0002-9440; 0002-9440; 3):785-794.

(142) Marsche G, Levak-Frank S, Quehenberger O, Heller R, Sattler W, Malle E. Identification of the human analog of SR-BI and LOX-1 as receptors for hypochlorite-modified high density lipoprotein on human umbilical venous endothelial cells. FASEB J 2001 04;15(0892-6638; 0892-6638; 6):1095-1097.

(143) McLeod R, Reeve CE, Frohlich J. Plasma lipoproteins and lecithin:cholesterol acyltransferase distribution in patients on dialysis. Kidney Int 1984 Apr;25(4):683-688.

(144) Mekki K, Bouchenak M, Lamri M, Remaoun M, Belleville J. Changes in plasma lecithin: cholesterol acyltransferase activity, HDL2, HDL3 amounts and compositions in patients with chronic renal failure after different times of hemodialysis. Atherosclerosis 2002 6;162(2):409-417.

(145) Stark GR, Stein WH, Moore S. Reactions of Cyanate Present in Aqueous Urea with Amino Acids and Proteins. J Biol Chem 1960 1960;235(11):3177-3181.

(146) Rozenberg O, Aviram M. S-Glutathionylation regulates HDL-associated paraoxonase 1 (PON1) activity. Biochem Biophys Res Commun 2006 Dec 15;351(2):492-498.

(147) Wang K, Subbaiah PV. Importance of the free sulfhydryl groups of lecithin-cholesterol acyltransferase for its sensitivity to oxidative inactivation. Biochim Biophys Acta 2000 Nov 15;1488(3):268-277.

(148) Negre-Salvayre A, Dousset N, Ferretti G, Bacchetti T, Curatola G, Salvayre R. Antioxidant and cytoprotective properties of high-density lipoproteins in vascular cells. Free Radic Biol Med 2006 10/01;41(0891-5849; 7):1031-1040.

(149) Shih DM, Xia YR, Wang XP, Miller E, Castellani LW, Subbanagounder G, et al. Combined serum paraoxonase knockout/apolipoprotein E knockout mice exhibit increased lipoprotein oxidation and atherosclerosis. J Biol Chem 2000 06/09;275(0021-9258; 23):17527-17535.

(150) Shih DM, Gu L, Xia YR, Navab M, Li WF, Hama S, et al. Mice lacking serum paraoxonase are susceptible to organophosphate toxicity and atherosclerosis. Nature 1998 07/16;394(0028-0836; 6690):284-287.

(151) White H, Held C, Stewart R, Watson D, Harrington R, Budaj A, et al. Study design and rationale for the clinical outcomes of the STABILITY Trial (STabilization of Atherosclerotic plaque By Initiation of darapLadIb TherapY)

comparing darapladib versus placebo in patients with coronary heart disease. Am Heart J 2010 OCT 2010;160(4):655-U289.

(152) Serruys PW, García-García HM, Buszman P, Erne P, Verheye S, Aschermann M, et al. Effects of the Direct Lipoprotein-Associated Phospholipase A2 Inhibitor Darapladib on Human Coronary Atherosclerotic Plaque. Circulation 2008 September 09;118(11):1172-1182.

(153) Go AS, Chertow GM, Fan D, McCulloch CE, Hsu CY. Chronic kidney disease and the risks of death, cardiovascular events, and hospitalization. N Engl J Med 2004 09/23;351(1533-4406; 0028-4793; 13):1296-1305.

(154) Stenvinkel P. Chronic kidney disease: a public health priority and harbinger of premature cardiovascular disease. J Intern Med 2010 08/04;268(1365-2796; 0954-6820; 5):456-467.

(155) Stenvinkel P. Interactions between inflammation, oxidative stress, and endothelial dysfunction in end-stage renal disease. J Ren Nutr 2003 04;13(1051-2276; 1051-2276; 2):144-148.

(156) Himmelfarb J, Stenvinkel P, Ikizler TA, Hakim RM. The elephant in uremia: oxidant stress as a unifying concept of cardiovascular disease in uremia. Kidney Int 2002 11;62(0085-2538; 0085-2538; 5):1524-1538.

(157) Tall AR. Cholesterol efflux pathways and other potential mechanisms involved in the athero-protective effect of high density lipoproteins. J Intern Med 2008 03;263(1365-2796; 0954-6820; 3):256-273.

(158) Duffy D, Rader DJ. Update on strategies to increase HDL quantity and function. Nat Rev Cardiol 2009 07;6(1759-5010; 7):455-463.

(159) Vaziri ND, Navab M, Fogelman AM. HDL metabolism and activity in chronic kidney disease. Nat Rev Nephrol 2010 05;6(1759-507; 1759-5061; 5):287-296.

(160) Sviridov D, Mukhamedova N, Remaley AT, Chin-Dusting J, Nestel P. Antiatherogenic functionality of high density lipoprotein: how much versus how good. J Atheroscler Thromb 2008 04;15(1340-3478; 1340-3478; 2):52-62.

(161) McGillicuddy FC, de la Llera MM, Hinkle CC, Joshi MR, Chiquoine EH, Billheimer JT, et al. Inflammation impairs reverse cholesterol transport in vivo. Circulation 2009 03/03;119(1524-4539; 0009-7322; 8):1135-1145.

(162) Kalantar-Zadeh K, Kopple JD, Kamranpour N, Fogelman AM, Navab M. HDL-inflammatory index correlates with poor outcome in hemodialysis patients. Kidney Int 2007 11;72(0085-2538; 0085-2538; 9):1149-1156.

(163) Vaziri ND, Moradi H, Pahl MV, Fogelman AM, Navab M. In vitro stimulation of HDL anti-inflammatory activity and inhibition of LDL pro-inflammatory activity in the plasma of patients with end-stage renal disease by an apoA-1 mimetic peptide. Kidney Int 2009 08;76(1523-1755; 0085-2538; 4):437-444.

(164) Jurek A, Turyna B, Kubit P, Klein A. The ability of HDL to inhibit VCAM-1 expression and oxidized LDL uptake is impaired in renal patients. Clin Biochem 2008 Aug;41(12):1015-1018.

(165) Old WM, Meyer-Arendt K, Aveline-Wolf L, Pierce KG, Mendoza A, Sevinsky JR, et al. Comparison of label-free methods for quantifying human proteins by shotgun proteomics. Mol Cell Proteomics 2005 10;4(1535-9476; 1535-9476; 10):1487-1502.

(166) Washburn MP, Ulaszek RR, Yates JR,III. Reproducibility of quantitative proteomic analyses of complex biological mixtures by multidimensional protein identification technology. Anal Chem 2003 10/01;75(0003-2700; 0003-2700; 19):5054-5061.

(167) Saland JM, Ginsberg HN. Lipoprotein metabolism in chronic renal insufficiency. Pediatr Nephrol 2007 08;22(0931-041; 0931-041; 8):1095-1112.

(168) Gundry RL, Fu Q, Jelinek CA, Van Eyk JE, Cotter RJ. Investigation of an albumin-enriched fraction of human serum and its albuminome. Proteomics Clin Appl 2007 01/01;1(1862-8354; 1862-8346; 1):73-88.

(169) Zhao Y, Van Berkel TJ, Van Eck M. Relative roles of various efflux pathways in net cholesterol efflux from macrophage foam cells in atherosclerotic lesions. Curr Opin Lipidol 2010 Oct;21(5):441-453.

(170) Coetzee GA, Strachan AF, van der Westhuyzen DR, Hoppe HC, Jeenah MS, de Beer FC. Serum amyloid A-containing human high density lipoprotein 3. Density, size, and apolipoprotein composition. J Biol Chem 1986 07/25;261(0021-9258; 0021-9258; 21):9644-9651.

(171) Artl A, Marsche G, Lestavel S, Sattler W, Malle E. Role of serum amyloid A during metabolism of acute-phase HDL by macrophages. Arterioscler Thromb Vasc Biol 2000 03;20(1079-5642; 1079-5642; 3):763-772.

(172) Jahangiri A, de Beer MC, Noffsinger V, Tannock LR, Ramaiah C, Webb NR, et al. HDL remodeling during the acute phase response. Arterioscler Thromb Vasc Biol 2009 Feb;29(2):261-267.

(173) Zhao Y, Sparks DL, Marcel YL. Specific phospholipid association with apolipoprotein A-I stimulates cholesterol efflux from human fibroblasts. Studies with reconstituted sonicated lipoproteins. J Biol Chem 1996 10/11;271(0021-9258; 0021-9258; 41):25145-25151.

(174) Jong MC, Hofker MH, Havekes LM. Role of ApoCs in lipoprotein metabolism: functional differences between ApoC1, ApoC2, and ApoC3. Arterioscler Thromb Vasc Biol 1999 03;19(1079-5642; 1079-5642; 3):472-484.

(175) Hirano T, Sakaue T, Misaki A, Murayama S, Takahashi T, Okada K, et al. Very low-density lipoprotein-apoprotein CI is increased in diabetic nephropathy: comparison with apoprotein CIII. Kidney Int 2003 06;63(0085-2538; 0085-2538; 6):2171-2177.

(176) de Beer MC, Ji A, Jahangiri A, Vaughan AM, de Beer FC, van der Westhuyzen DR, et al. ATP binding cassette G1-dependent cholesterol efflux during inflammation. J Lipid Res 2011 Feb;52(2):345-353.

(177) Papavasiliou EC, Gouva C, Siamopoulos KC, Tselepis AD. PAF-acetylhydrolase activity in plasma of patients with chronic kidney disease. Effect of long-term therapy with erythropoietin. Nephrol Dial Transplant 2006 May;21(5):1270-1277.

(178) Zalewski A, Macphee C. Role of lipoprotein-associated phospholipase A2 in atherosclerosis: biology, epidemiology, and possible therapeutic target. Arterioscler Thromb Vasc Biol 2005 05;25(1524-4636; 1079-5642; 5):923-931.

(179) McCall MR, La Belle M, Forte TM, Krauss RM, Takanami Y, Tribble DL. Dissociable and nondissociable forms of platelet-activating factor acetylhydrolase in human plasma LDL: implications for LDL oxidative susceptibility. Biochim Biophys Acta 1999 Jan 29;1437(1):23-36.

(180) von EA, Holz H, Sandkamp M, Weng W, Funke H, Assmann G. Apolipoprotein C-III(Lys58----Glu). Identification of an apolipoprotein C-III variant in a family with hyperalphalipoproteinemia. J Clin Invest 1991 05;87(0021-9738; 0021-9738; 5):1724-1731.

(181) Ooi EM, Watts GF, Farvid MS, Chan DC, Allen MC, Zilko SR, et al. High-density lipoprotein apolipoprotein A-I kinetics: comparison of radioactive and stable isotope studies. Eur J Clin Invest 2006 09;36(0014-2972; 0014-2972; 9):626-632.

(182) Bobik A. Apolipoprotein CIII and atherosclerosis: beyond effects on lipid metabolism. Circulation 2008 08/12;118(1524-4539; 0009-7322; 7):702-704.

Michael Holzer

Mariatrosterstrasse 10 ▪ 8043 Graz, Austria ▪ Cell: +436503918281 ▪ Office: +433163804513 ▪ E-Mail: michael.holzer@medunigraz.at

Scientific Interests

lipid metabolism ▪ HDL function ▪ atherosclerosis ▪ cellular immunity ▪ macrophages ▪ inflammation ▪ vascular disease

Education

- 10/2002 – 06/2008 **Karl-Franzens University, Graz, Austria,** Candidate of Biochemistry
- 04/2007 – 03/2008 **ETH, Zürich, Switzerland, Institute of Biochemistry,** Completion of Master Thesis
  Supervisor: Prof. Dr. Ari Helenius
  Master Thesis: "Comparative analysis of HPV16 entry by large-scale drug screening"
- 06/2008 **Karl Franzens University, Graz, Austria,** Master degree in biochemistry
- **Since 10/2008** **Medical University of Graz, Graz, Austria,** PhD Candidate of Molecular Medicine
  Supervisor: Dr. Gunther Marsche
  PhD Thesis: "High-density lipoprotein functionality in inflammatory diseases"
- **11/2011** **PhD graduation**

Publications

- Michael Holzer, Ruth Birner-Gruenberger, Tatjana Stojakovic, Dalia El-Gamal, Veronika Binder, Christian Wadsack, Akos Heinemann, and Gunther Marsche. Uremia alters HDL composition and function. *J Am Soc Nephrol.* 2011 Sep;22(9):1631-41.
- Michael Holzer, Martin Gauster, Thomas Pfeifer, Christian Wadsack, Guenter Fauler, Philipp Stiegler, Eckhard Beubler, Rufina Schuligoi, Akos Heinemann, and Gunther Marsche. Cyanate transforms HDL into a pro-atherogenic lipoprotein in human atherosclerotic lesions. *Antioxid Redox Signal.* 2011 Jun 15;14(12):2337-46
- El-Gamal D, Holzer M, Gauster M, Schicho R, Binder V, Konya V, Wadsack C, Schuligoi R, Heinemann A, Marsche G. Cyanate is a novel inducer of endothelial ICAM-1 expression. *Antioxid Redox Signal.* 2011 Aug 12; [Epub ahead of print]
- Damm M, Holzer M, Radspieler G, Marsche G, Kappe CO. Microwave-assisted high-throughput acid hydrolysis in silicon carbide microtiter platforms--a rapid and low volume sample preparation technique for total amino acid analysis in proteins and peptides. *J Chromatogr A.* 2010 Dec 10;1217(50):7826-32.
- Marsche G, Frank S, Hrzenjak A, Holzer M, Dirnberger S, Wadsack C, Scharnagl H, Stojakovic T, Heinemann A, Oettl K. Plasma-advanced oxidation protein products are potent high-density lipoprotein receptor antagonists in vivo. *Circ Res.* 2009 March 27;104(6):750-7.

Academic Awards

- European Society of Cardiology Meeting, Stockholm, Sweden, 08/2010 ▪ Young Basic Scientists Travel Grant
- 16th APHAR Meeting, Vienna, Austria, 11/2010 ▪ Travel Grant
- Human Peroxidase Meeting, Brussels, Belgium, 05/2011 ▪ Basic Scientist Travel Grant

Reference

Dr. Gunther Marsche ▪ Medical University of Graz, Graz, Austria ▪ Office: +433163804513 ▪ E-Mail: gunther.marsche@medunigraz.at